Influence of Hydrological Processes on Phosphate Leaching in Tile Drained Sandy Soils

A Case Study in the Bollenstreek

M.W. Tiesma

Faculty of Civil Engineering

TU Delft

Influence of Hydrological Processes on Phosphate Leaching in Tile Drained Sandy Soils

A Case Study in the Bollenstreek

by

M.W. Tiesma

to obtain the degree of Master of Science

in Civil Engineering

at the Delft University of Technology

Student number: 4613570

Thesis committee:

dr. T. A. Bogaard,	TU Delft
dr. J. W. A. Foppen,	TU Delft
dr. B. M. van Breukelen,	TU Delft
dr. J. Rozemeijer,	Deltares
M. V. Barcala Paolillo MSc.,	Deltares & Utrecht University

TU Delft Delft University of Technology

Contents

List of Acronyms

B1 temporal single drain-water storage barrel one.

D1 tile-drain one.

drain head head in the tile drain which is equal to the water level in the west ditch.

GW Groundwater.

ICS iron-coated sand.

khkv permeability coefficient.

P Phosphate.

PSD Phosphorus saturation degree.

Pw soluble phosphorus.

rd regulated drainage [2].

TP Total Phosphorus.

WFD water framework directive.

Preface

In the Netherlands, eutrophication is a problem that attracts a lot of public attention. Farmers are often mentioned in this public debate, as they are responsible for a not insignificant part of eutrophication. However, as the second largest agricultural exporter in the world, they are also a very big business. Since studies show that agricultural land is likely to be an important source of nutrient leaching, it was interesting to study a specific agricultural area. Especially since the case study was conducted in the Bollenstreek, which focuses on floriculture, the largest agricultural exporter in the Netherlands with 8.3 billion euros. Higher than the export of meat (7.7 billion euros). However, this area is also known for high nutrient concentrations on soils with low retention capacity. As there is a large flora industry with a long history on these fields, it was interesting to support the Rijnland Water Board and the P-trap[1] group in finding effective mitigation measures. During the work, it was interesting to note how an increase in knowledge in the field and in the literature refined the aim of this study. At the beginning, a small area was available for experiments with a new particle tracer. After the first results, it turned out that this new particle tracer experiment would not be possible during my thesis in this field. A change of PHder was made and various other devices were needed for new measurements. Among them was an autosampler, which had to be installed quickly. It is satisfying to look back on this process and have the final result, this report, in front of me. To make this study possible, the company Gebr. Hogervorst allowed us to carry out the measurements on their field. Deltares and TU-delft helped with the installation and delivery of the necessary equipment. I would like to thank the thesis committee for the feedback on my thesis. In particular, I would like to thank M.V. Barcala and and dr. T.A. Bogaard as my weekly supervisors for coaching, fieldwork and discussions on the analysis and interpretation of the results.

M.W. Tiesma
Delft, The Netherlands
June 2022

[1] P-TRAP – as a H2020 MSCA-ITN European Training Network – is a consortium of 16 international participants and hosting 11 Early-Stage Researchers (ESRs). A characteristic of these networks is a combined focus not only on science but also on training of a new generation of creative, entrepreneurial and innovative ESRs.

Scientifically P-TRAP targets two interlinked global problems: I) the flux of phosphate (P) from agricultural areas to surface waters is wasting a resource which is becoming scarce, and II) on the other hand, an enhanced loading of surface water with P is the main cause for eutrophication. Both are in conflict with our understanding of circular economy and a key challenge in meeting the objectives of the EU Water Framework Directive. Within P-TRAP we will develop new methods and approaches to trap P in drained agricultural areas and in the sediments of eutrophic lakes, aiming on constraining the uncontrolled loss of P in one system and preventing the others from overloading. [3]

Abstract

Leaching of phosphorus (P) from agricultural land is an important source of eutrophication in the Bollenstreek in the Netherlands. This is because floriculture has led to high P concentrations in the sandy soils with low organic carbon content, which are characterised by a low retention capacity for P. In this study, P concentrations in groundwater from three plots in the Bollensteek were found to exceed the water framework directive (WFD) by a factor of 40. The case study on a single plot showed a phosphate load of 5.5 kg/ha/year leached through the tile drains, which is an order of magnitude higher than fields outside the Bollensteek. To understand where phosphate comes from and how hydrological processes influence leaching, hydraulic and chemical measurements of soil, groundwater and tile drain outflow were taken in a field with regulated tile drainage, and two hydrological models were created to simulate wet winter and dry summer conditions. The results showed the flow paths from this plot under wet and dry conditions and illustrated how hydrological processes can influence phosphate leaching through the soil and tile drains.

Summary

Phosphorus (P) leaching from agricultural fields is an important source of eutrophication in the Bollenstreek, the Netherlands. The floriculture in the area resulted in large P concentrations in the sandy soils with low organic carbon content, which are characterized by a low retention capacity. Hence, leaching of P occurs extensively. Therefore, the waterboard of Rijnland is very interested in finding effective mitigation measures. To find out where which measures should be taken, it is important to improve the existing measures and to understand the hydrological drivers behind P leaching. This study focuses on the second aspect. P can be leached into the ditch through the soil or via tile drains. The water source that drives P leaching can come from precipitation, the surface level in the ditches and/or seepage. On the other hand, the ditches and seepage can also be a source of P. It is important to assess these sources to understand the role that fertilisation plays in P leaching from the field. Other studies on this topic have measured discharges and concentrations leaching from agricultural land or measured the chemical properties of the soil and groundwater on agricultural land. However, no studies were found that measured both on the same field. In order to assess the influence of the hydrological and chemical properties of the field on P leaching and to explain why certain concentrations and discharges were found at the outflow this case study focused on both the field and the runoff at Hogervorst. This allowed a better understanding of the influence of the hydrological system on P leaching. To do so, high-frequency measurements of the groundwater level, tile drain discharge and water quality at the tile drain outlet were carried out. In addition, soil content and groundwater quality was measured down to a depth of 4 m at several locations in the field. Moreover, two steady-state hydrological groundwater models were created and calibrated against the measured groundwater levels and discharges, representing wet winter and dry summer conditions. This model gave a better insight into the groundwater level distribution of the field and quantified different flow paths (e.g. tile drain, soil transport).

The results showed groundwater concentrations, tile drain outflow concentrations and a P load (5.5 kg/ha/year) through the tile drains, which were an order of magnitude higher compared to field studies outside the Bollenstreek. At other locations in the Bollenstreek, similar concentrations were found in the field and at the tile drain outlet. The soil at three measured locations in the Bollenstreek had a relative low amount of P at the top and a high P concentration at 0.7 m below the surface compared to non-calcareous sandy soils in the Netherlands. Since the depth of the tile drain is at 0.8 m below the surface, there is an increased risk of leaching high P concentrations at Hogervorst. At 1.5 m below the surface a 1.5 m thick layer was found which contained debris and clay. The clay contained P concentrations ten times higher than the concentrations found in the sandy soil at the top. Also the iron concentration was much higher which resulted in a similar Phosphorus saturation degree (PSD) value as the sandy soil. Two groundwater profile measurements before and after a large precipitation event showed similar P concentrations. Which indicates that the soil can function as a buffer. The period of time the soil can function as a buffer is unknown.

At Hogervorst, the contribution of seepage to P leaching was low and the two main water sources were ditch water from the west ditch and precipitation. The models showed that the water source depends on wet or dry conditions. In dry summers, water from the west ditch is transported east through the soil and tile drains. This flow was caused by another water level area east of Hogervorst, which has a water level that is 0.5 m lower. The model showed that transport to the neighbouring field was stopped when the difference in water level between east and west was reduced to 30 cm by raising the weirs in the neighbouring farm 20 cm. In wet winter conditions, precipitation raises the groundwater level and, according to the model, 66 % of the precipitation is transported to the east and 34 % to the west. Of the 34 % flowing towards the west, 70 % was transported through the drains. The ratio between the discharge of the tile drains and the total precipitation is 23.8 %, which is very close to the observations of 25 %. This shows that the model agrees well with the average distribution of flow paths in winter. Due to the regulated tile drains, a faster transport time was determined, which can be less than the measured oxidation time in Hogervorst of 14 to 21 days. Therefore, less P could precipitate or adsorb the iron hydroxides, which could play a role in the high P concentrations found at the tile drain outlet. The tracer experiment, field measurements and hydrological modelling showed that a rise in the water level due to rainfall increases the area that drains to the west via the tile drains. This could play a role in leaching concentrations from agricultural fields. At Hogervorst, higher P concentrations were found at the end of the field, which explains the increase in P concentrations measured at the tile drain outlet during discharge.

1

Introduction

Phosphate is a nutrient which is considered to decrease biodiversity and cause algae blooms when present in high concentrations [4–7]. Many agriculture-dominated lowland water systems worldwide suffer from eutrophication caused by high nutrient loads in surface waters. In the Netherlands, nutrient surpluses and leaching are higher than elsewhere in Europe [8] and the world [9], which is due to a highly concentrated and productive agricultural sector [10]. In the 'bollensteek' in the west of the Netherlands, floriculture led to high phosphate concentrations in the sandy soils, which are characterised by a low retention capacity [11]. This creates a high risk of phosphate leaching from the flower fields into surface waters [12]. Therefore, leaching of phosphate into surface waters is considered the greatest threat to eutrophication in the area [1]. Since the measured parcels had a phosphorus concentration 40 times above the WFD [1] norm and a nitrate concentration two times above the standard, the Rijnland water board, which manages the Bollenstreek, is very interested in minimising phosphate losses and establishing a framework to assess which measures are most effective for specific fields or areas.

Various retention measures are being developed to mitigate phosphate leaching [1, 13]. Two current options for mitigation are buffer zones (space between the ditch and the agricultural plot) and iron-coated sand (ICS) Filters at the tile drain outlet or around the drains of an agricultural field. The effectiveness of these methods depends on the hydrochemical processes in the field. However, the concentration-discharge relation driven by the hydrochemical processes are poorly understood [14–16]. This relationship is difficult to establish, as many different factors influence phosphate leaching, e.g. soil type, weather conditions, drain levels, plowing and crop types [1, 17–19]. In addition, high-frequency data to analyse the hydrological and chemical situation from the field to the ditch is limited [10, 17]. On two fields in the 'bollenstreek' various measurements were carried out to study the effect of iron-coated sand to mitigate phosphate leaching [1, 20]. However, no studies were found in the Bollenstreek investigating how field conditions affect the relationship between phosphate concentration and discharge through tile drains. The origin of phosphate in the fields and the contribution of the different flow paths into the ditch could be useful for understanding the discharge and phosphate concentrations leaching from the field and help to implement effective mitigation measures. Other case studies in various fields took concentration and discharge measurements at the outflow [19, 21] or took measurements of the chemical situation in the field [22, 23] but not measured both the outflow and the condition in the fields. In a region with intensive agricultural use (Noord-Brabant, the Netherlands), it was found that the poor chemical status of upper and near-surface groundwater leads to exceedance of quality standards in receiving surface waters, especially during periods of quick flow [12]. When certain flows were activated and to what extent it contributed to nutrient leaching was not known, as this depends on the local hydrological situation. However, in order to take effective mitigation action, it is important to understand these different drainage pathways. In particular, the hydrological functioning of the regulated drainage [2] (rd), which has the ability to drain, retain and recharge, is of interest to the Neterlands. Because in recent decades, the draining of Dutch agricultural land, land consolidation and urbanisation have led to a drop in the groundwater level. And climate change is causing increasingly extreme conditions that require new water management systems [24].

In general, there are two known sources of phosphorus in a field: 1) organic matter added to the topsoil, and 2) seepage water in deep seepage polders [1, 25–27]. However, the iron concentration in the field influences the retention of phosphorus (P) in the subsurface [28]. During oxidation, phosphorus is co-precipitated or

[1] EU directive which commits European Union member states to achieve good qualitative and quantitative status of all water bodies

adsorbed by iron hydroxides [29]. The precipitation of iron oxides has longer reaction times in the presence of phosphate and calcium [30]. These oxidation/reduction processes of iron and its interaction with phosphate are being studied by the P-TRAP consortium. Furthermore, the water transport dynamics of rain infiltration, seepage, drain transport, and ditch water infiltration affect the phosphate and iron concentrations through dilution and oxidation/reduction processes [11, 12, 31, 32]. Therefore, to understand phosphate leaching from agricultural fields, both the chemical and hydrological processes which drive phosphate leaching should be studied.

The objective of this research is to gain insights into field-scale water transport dynamics in order to determine the hydrological influence on P leaching and implement effective mitigation measures.
Therefore, a case study was conducted on a tile drained plot (100 by 125 metres) in Noordwijkerhout in the 'bollenstreek'. On this plot, the groundwater levels, drain discharge, soil characteristics, and (ground)water quality were monitored in space and time using high-frequency measurements. In this way, both the hydrological and chemical situation in the field and tile drain outlet were measured. By analysing the hydraulic data using a hydrological Modlfow 6 model in combination with the phosphate concentrations in the field and at the tile drain outlet, a step is taken towards understanding the hydrochemical transport of phosphate from the field to the ditch.

The hydrological model was constructed to show the difference in groundwater level distribution and mass balance under wet winter and dry summer conditions in the field. In doing so, the model separated discharge through the tile drains and the soil. To investigate infiltration, different heads were used at the boundaries of the field in deeper groundwater layers. In addition, the amount of recharge was changed, simulating precipitation that provided information about the dynamic behaviour of the system. Together with the tracer experiment and the hydraulic and chemical measurements, a conceptual model of this system was created. Based on the mass balance, the transport time was determined to see if oxidation takes place in the soil. The P-TRAP consortium studied the iron oxidation time in the case study in Noordwijkerhout. Precipitation with a high oxygen concentration can start the oxidation process. However, if the transport time is much shorter than the iron oxidation time, the phosphate has no time to precipitate. Iron oxidation is a fast process, but in the presence of phosphate it is slower. Comparing this time with the reaction times of P-Fe oxides can help us understand whether oxidation is taking place in the soil.

2

Methodology

This methodology chapter describes the executed field study, field work, lab work and modelling. The field study at Hogervorst found different water level areas which had an effect on the hydrological situation in the field which is explained in section 2.1 Management of the drainage system at Hogervorst. The hydraulic measurements section 2.2 shows how the groundwater level and the tile drain discharge was monitored at a high frequency (5 to 10 minute interval) and a salt tracer experiment was executed. A hydrological model was build to analyse the data and calculate a mass balance (see section 2.3). section 2.4 chemical measurements describes the soil content and water quality measurements in the field and at the tile drain outlet.

2.1. Management of the Drainage System of Hogervorst

The tile drained pilot field is owned by the Gebr. Hogervorst and is located in Noordwijkerhout, a village in the so-called 'Bollenstreek'. The field is mainly used for the cultivation of daffodils and has a sandy soil with a high phosphorus concentration, which is characteristic for the Bollenstreek, as explained in chapter 1. The pilot plot is mainly anthropogenic. According to the owner, the field is built on a 1.5 m thick debris/clay layer consisting of local remnants of building materials such as bricks and mixed with clay. On top of this is a 1.5 m thick layer of sand. According to the farmer, this was put in place 30 years ago to increase the surface area of the field, which is currently +0.3 m NAP.

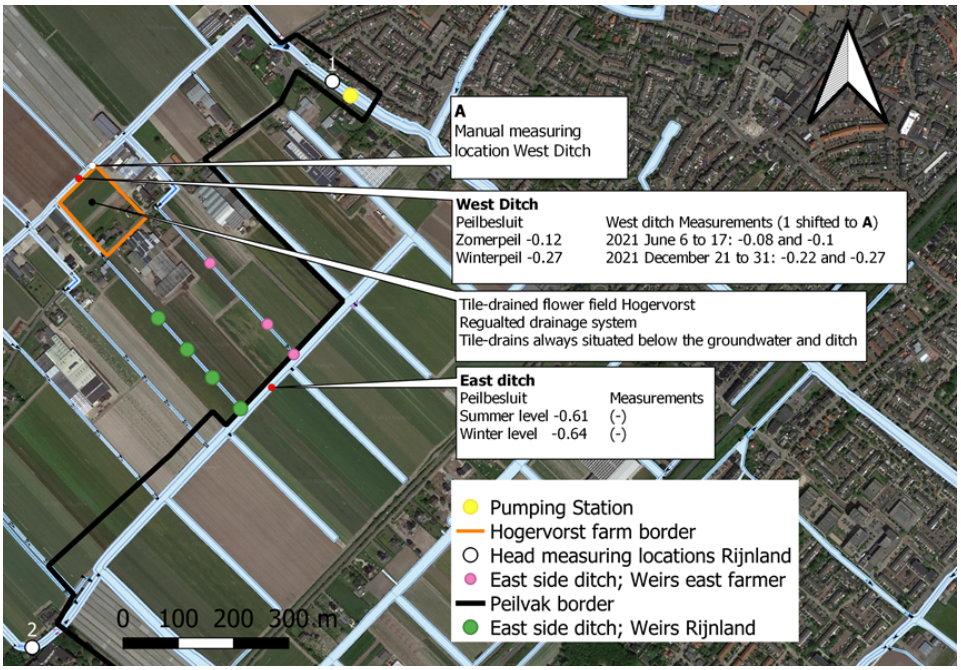

Figure 2.1: Overview of Water management on the farm field from Gebr. Hogervorst in Noordwijkerhout.

An overview of the water management situation in the area is visualised in Figure 2.1. The field boundaries are marked with orange lines, measuring 125 by 100 metres. The field contains 10 tile drains, which are spaced 10 metres apart, and 80 cm below the surface. The drains are always below the groundwater level and the

water level of the ditch. Therefore, this system is also called rd. The ditch water can infiltrate into the drain when the ditch level is above the groundwater level and discharge groundwater when the ditch level is lower. The drains are 90 metres long and each has an open connection to the western ditch. The water level of the ditch is regulated with weirs and has a summer and winter level (zomerpeil and winterpeil). The water level is raised in summer to support the infiltration of the ditch into the field and to prevent a low groundwater level during the dry summer months. In winter, the water level is lowered so that the field can drain into the ditch when it gets wet. The tile- drains were installed to infiltrate and drain larger amounts of water so that the water level is more stable [2]. There are no tile drains on the east side of the field. On the east, the field ends at a road. On the other side of the road is another field cultivated by another farmer. This field contains two side ditches on each side of the field, which are in open communication with the eastern ditch in winter. Note that the water level in the eastern ditch is half a metre lower than in the western ditch. In dry summers, the small weirs in the two side ditches are often closed to maintain a higher water level.

2.2. Hydraulic Measurements

This section explains the hydraulic measurements at Hogervorst. The discharge of a tile drain was measured with a single drain storage barrel (see subsection 2.2.1). A second barrel was installed, but it had numerous malfunctions and was therefore not operational during most of the field measurements (see Appendix D). The groundwater level was measured at 1 and 60 metres from the ditch. In June it was also possible to take groundwater measurements at 15 and 30 metres from the western ditch. An overview of the equipment, measurement locations and measurement time can be found in subsection 2.2.2. subsection 3.1.2 shows the manual data measurements at the west ditch during the fieldwork and the high frequency measurements from Waterboard Rijnland at sites 1 and 2 in Figure 2.1. subsection 2.2.3 explains the salt tracer experiment in which a tile drain response was artificially generated.

2.2.1. Tile Drain Measurements

Figure 2.2 schematically visualized how the temporal single drain-water storage barrel one (B1) collected and discharged groundwater from the tile drain. Figure 2.3 shows pictures from the outside and inside of B1. B1 is used to measure both the water quality at the drain outflow, and the drain discharge.

The barrel is connected to the drain via an extension tube as shown in Figure 2.3a. Therefore, under infiltration conditions, the water cannot flow directly from the ditch into the tile drain. However, the ditch water can still infiltrate into the soil. To maintain natural drainage, the drain extension tube floated above the water level in the ditch as shown in Figure 2.3a. When the water level in the field exceeds the level of the ditch extension tube water starts to flow into the barrel. However, there were undesirable factors that could have affected the level of the ditch extension tube by 2 to 3 cm (see Appendix A for more details).

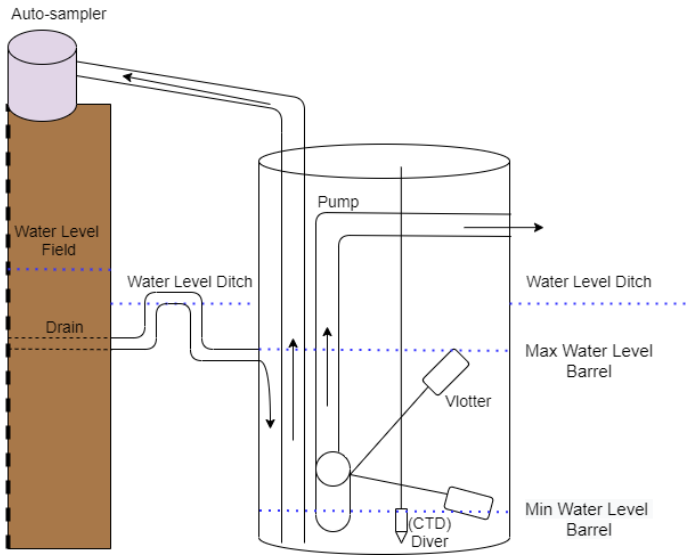

Figure 2.2: Temporary single drain water storage tank B1. This schematic overview shows how water enters the barrel from the drain extension tube connecting tile-drain one (D1) to the barrel. The pump is activated when the float switch reaches the maximum water level and is deactivated when a minimum water level is reached. The pressure sensor of the CTD multisensor monitors the water level in B1 to calculate the drain discharge. The automatic sampler takes water samples from the bottom of the barrel at a set interval.

(a) View of B1 from the outside. The drain is connected to B1 with a drain extension tube that floats on the water level of the ditch. Therefore D1 has to overcome the water pressure of the ditch before it can flow into B1. In this way, the water level in the ditch is simulated to create a natural drain response.

(b) View inside B1. The stones are installed to push the barrel down. The black hole shows the exit of the drain extension tube that enters the barrel. The pump is on the bottom of the barrel. The float switch is attached to the pump with a cable. The level at which the pump starts is set by the cable ties, which adjust the length of the cable. The transparent hose at the bottom of the barrel is connected to the automatic sampler. The small iron cable connected to the iron rod holds the pressure sensor (CTD multisensor) at the bottom of the barrel.

Figure 2.3: Outside and inside view of B1.

The discharge was calculated from the volume of water in the barrel divided by the duration between two pump activations. The activation of the pump is controlled by a float switch that automatically activates the pump when a certain water level is reached. During installation, this maximum level in the barrel was set below the minimum water level in the ditch. In other words, the water level in the barrel had no influence on the discharge into the barrel. The difference in the volume of water in the barrel before and after the pump was activated was estimated by a calibration test. This was done by filling the barrel until the pump was switched on and reading the pump number (the total volume registered by the pump). After this was done 5 to 8 times, an average volume difference was determined. As it happened a few times that the set-up had to be adjusted, a new calibration was made. This calibration data can be found in Appendix D

The duration between two activations of the pump was determined using data from a CTD multisensor (conductivity, water pressure and temperature), which registered the pressure differences in the barrel every five minutes. The specification of the CTD multisensor can be found at Table A.1. Using the date and time marking the minimum and maximum water level, the duration between two pump activations was determined. Using the calibrated volume and the measured time needed to fill the barrel, the discharge was calculated. To check the discharge calculations, the calculated total discharge volume was compared with the actual registered pump numbers.

2.2.2. Monitoring Wells to Monitor the Groundwater Level in the Field

To measure the groundwater level and to take water samples from the field, 12 monitoring wells were installed. The wells were constructed using a PVC-tube with a filter about 50 centimetres long. The locations of these monitoring wells are shown in Figure 2.4 and an overview of the monitoring dates and sensors can be found in Table A.1. A more detailed overview of the locations for P1 to P12 can be found in Appendix A.

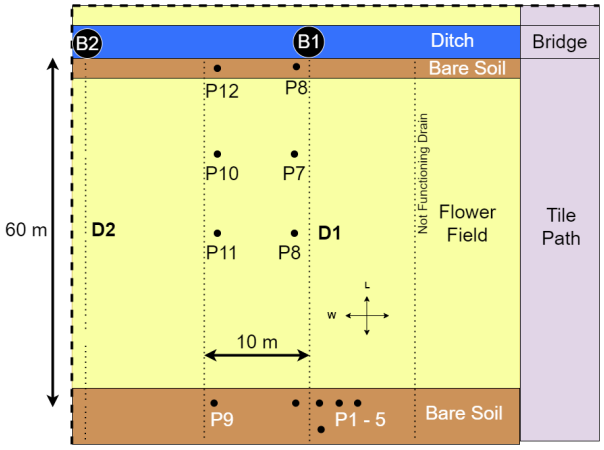

Figure 2.4: Schematic overview of the location of barrels one and two, drain one and two and monitoring tubes P1 to P12. The exact locations of the monitoring tubes can be found in appendix A Table A.2.

Two different types of measurements were carried out to measure the groundwater level at the monitoring wells. 1) Divers (automatic pressure measuring device) inside the monitoring wells which are in combination with a baro-meter installed at the surface of the field. 2) Manual measurements using a measuring tape with an additional weight during field visits. By performing levelling, the groundwater levels were expressed with respect to the average field surface level and NAP. The calculations can be found in Appendix A.

2.2.3. Tracer Experiments

Five tracer tests were conducted as part of two tracer experiments. The first experiment (test 1 and 2) was conducted in winter using an infiltration pond with tap/ditch water at 60 m from the western ditch. The second experiment (test 3, 4 and 5) was conducted in summer using a salt solution at 15 m (test 3 and 5) and 30 m (test 4) from the western ditch. Since the 3^{th} and 4^{th} test gave usable results, they are explained in the report.
Figure 2.5 provides a visualisation of the salt tracer experiment (test 3, 4 and 5). Since it was difficult to design an experiment when the groundwater level exceeded the water level in the ditch, the drain extension tube was lowered to create a drain response. To inject the salt tracer, a PVC injection tube was placed in the shell bed directly above the drain. To detect the injected salt tracer at the drain outlet, two EC meters (CTD multisensor, Greinsinger GMH343) were installed in the outlet of drain extension tube.

Note that the conditions in this artificial response are somewhat different compared to a natural response, which could affect the results. First, the level of the ditch was kept the same while the level of the drain was lowered. Secondly, the groundwater level distribution in the field was different from a drain response caused by an increased water level due to precipitation.

Table 2.1: Salt tracer test 3 , 4 and 5

test	day	drain lowered	salt (g)	EC (µS/cm)	amount (L)	injection	duration after injection (hr)	Qavg (L/hr)	volume (L)
3	9-Sep	12:00	32	4000	10	12:00	4.0	112	451
4	10-Sep	9:54	88	8000	10	11:00	5.2	151	880
5	13-Sep	9:10	88	8000	10	9:22	1.3	64	80

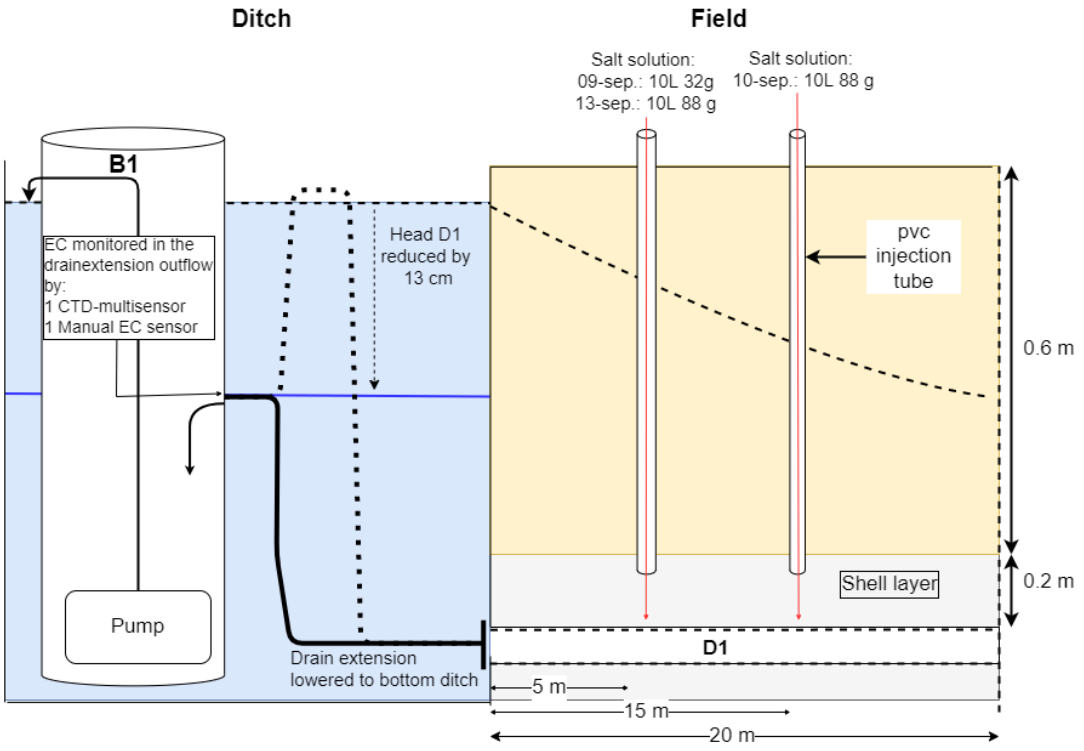

Figure 2.5: Set-up of the third and fourth tracer test. The dashed lines show the natural situation for the water level and the drain extension tube. The blue line shows the situation after the drain extension has been lowered. Note that the level of drain D1 has dropped to the inlet level of B1, which means a drop of 13 cm. A CTD-multisensor and a munual EC sensor were installed in the inlet of B1 to measure the EC level directly at the outlet of the drain extension tube. At 20 metres from the ditch the groundwater level was estimated to be equal to the reduced head of D1 based on the monitored groundwater levels.

2.3. Hydraulic Model Build- Up

MODFLOW 6 was used in combination with FloPy to create two steady-state models (wet winter and dry summer) with a grid size of 1 x 1 metre and 11 layers. To build the wet winter and dry summer model, several boundary conditions were set as explained in subsection 2.3.1. These boundary conditions were fixed, semi-fixed and calibrated. The semi-fixed and calibrated values were studied with a sensitivity analysis as explained in subsection 2.3.2. With the final boundary conditions, a mass balance was created and used to estimate the transport times, as explained in subsection 3.2.5.

2.3.1. Boundary Conditions (CHD, GHB and RCH)

The model makes use of three packages whose specifications can be found in Hughes [33]. Figure 2.1 shows the boundaries of the model (orange rectangle) and the situation outside the model boundaries. The boundary conditions are summarised in Table 2.2.

The boundary condition in the east represents the groundwater level on the neighbouring field. A CHD package was set for this boundary, which requires a head parameter. This simplification made it easier to study the effects of changing the head in the east. This is because it depends on a single variable, whereas constructing a model with side ditches requires the depth of the ditch, the conductivity of the ditch and the levels of the weirs. The disadvantage of this simplification is that there is no difference in groundwater level between the middle of the field and the side ditches, which also affects the mass balance. According to the owner, no weirs were set in winter, therefore the head in the east was set to the actual water level of the eastern ditch in the wet winter model. In summer, conditions were more complicated. In dry weather, the weirs were adjusted to increase the (ground)water level. Therefore, three different heads were used in the summer model to investigate the effects of the weirs. The western ditch is also simulated with a CHD boundary condition. The head was obtained from the manual ditch water level measurements and high frequency data from Rijnland as explained in subsection 3.1.2. For the actual head, the average value for summer or winter water level of

Table 2.2: Modflow 6 packages and parameters used to set the model boundary conditions. [1] the side ditches at the east field contain weirs which are sometimes set in dry summer conditions to increase the groundwater level. Therefore in the wet winter model the boundary was set to the east ditch and in the dry summer model three different heads were set to indicate the effect of the weirs. [2] effective rainfall = precipitation - evaporation set over an selected average wet winter or dry summer time frame.

Boundary condition	Location	Package	Parameter(s)	Parameter values
east ditch	125 meter east from the west ditch	CHD	Head	East ditch water level [1]
West ditch	West ditch	CHD	Head	West ditch water level [1]
Drains	Perpendicular to West ditch. Length: 90 m Number 10, Distance between drains: 10 m	GHB	Head	West ditch water level
			Conductance	Calibration parameter
North, south	End of the field (width between North – South 100 meter)	-	-	impermeable
Bottom	18 meter	-	-	impermeable
Groundwater recharge	Top of the saturated zone	RCH	Recharge	Effective precipitation [2]
Hydraulic conductivity	Field	NPF	K_h, K_v	see Figure 2.6

the west ditch was used. The north, the south and the bottom were impermeable boundaries in the model. According to DINOloket (Appendix E), the soil at a depth of 17 metres probably contains a clay layer, which is why this level was used as an impermeable layer. At the northern and southern impermeable boundary, the ditches are insignificant because the 10 tile drains on the field regulate the groundwater level. Therefore, the amount of groundwater percolating into the side ditches was considered insignificant. The groundwater recharge was modelled using the RCH (recharge package), with the entire surface of the field gaining water in the wet winter model and losing water in the dry summer model. The values were calculated by taking the average value over a selected time frame as explained in the subsection subsection 2.3.2. The evaporation and precipitation data for the calculation of the effective precipitation were obtained from the KNMI at the weather station in Voorschoten.

The 10 tile drains at Hogervorst are simulated with a GHB that simulates both infiltration and discharge. The head of the GHB is equal to the water level in the west ditch, as they are in open connection and the drain is always below the level of the west ditch. The conductance of the tile drain is unknown and is used as a calibration parameter. Its value was not limited by a range.

The soil profile of the field and the calibration limits for k_h and k_v are shown in Figure 2.6. For the sand layers, k_v is assumed to be between 0.1 and 3 and k_h between 1 and 30 m/d [34]. Around the drains is a shell bed, which has a greater conductivity than sand [34]. Therefore, a three times larger conductance was applied for the shell bed than for sand. The clay/debris layer was between NAP -1.2 and -2.7 m. For this layer it was assumed that the k_h, k_v values were smaller by a factor of 100 compared to the sandy soil. Below the clay/debris layer, a thick sand layer was found which extents to NAP -17 m. To simplify the calibration, the anisotrophy of the soil was assumed to be 10. Furthermore, the entire profile was multiplied to increase or decrease the k_h and k_v value. Since k_h and k_v always differ by a factor of 10, they were combined in this study as one calibration parameter to $k_h k_v$. This parameter was called the permeability coefficient (khkv) in the report.

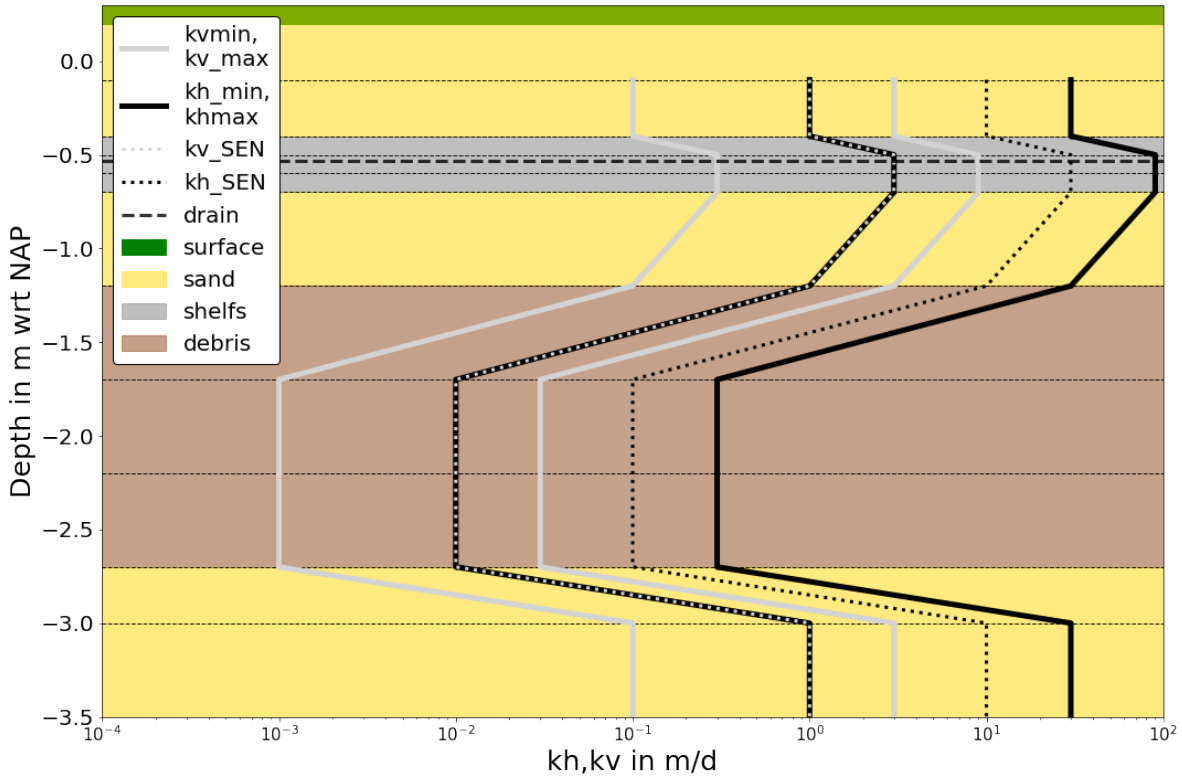

Figure 2.6: Soil profile from the top 3.5 meter, including k_h and k_v calibration boundaries. Note that the bottom of the model is situated at NAP -18 m.

2.3.2. Calibration and Validation

Figure 2.7 shows the flow diagram for the calibration and validation of the winter and summer model. First, the wet winter model was calibrated to the measured tile drain discharge and the measured groundwater level 60 metres from the western ditch. The permeability coefficient (khkv) and the drain conductance were used as calibration parameters. The final permeability coefficient obtained from the wet winter calibration was used in the dry summer model. With the permeability coefficient set, the drain conductance was used as the only calibration parameter to fit the measured groundwater level at 15, 30 and 60 m from the western ditch in dry summer conditions.

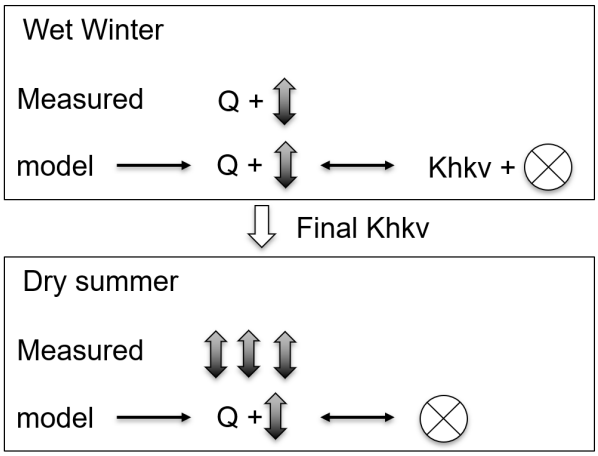

Figure 2.7: Calibration and Validation wet winter and dry summer model. Where the measured tile drain discharge and groundwater level observations were used to calibrate the model with the drain conductance and the permeability coefficient ($k_h k_v$).

To calibrate the "wet winter" and "dry summer" conditions, a specific time frame was defined for each model with measured precipitation, tile drain discharge, ditch water level and groundwater levels. Since discharge from the tile drains indicates wet conditions, the longest measured period with persistent drainage of the tile drain in winter was used. For the dry summer, a time frame was chosen where the groundwater level was measured at the three sites, no precipitation was present and the ditch was at summer level (Zomerpeil).

In order to study the different variables in depth, a sensitivity analysis was performed. The sensitivity analysis was executed with parameters before the completed calibration (START calibration) and with the completed calibration (END calibration) for winter and summer conditions.

2.3.3. Transport Times

An estimate of the transport times from the field to the eastern and western ditches was made from the model under wet winter conditions using the formula Equation 2.1. Where Q is the discharge determined from the model under wet winter conditions. And V_{max} is the maximum volume before 'new' water from precipitation leaves the system.

$$\frac{V_{max}}{Q} = \frac{l \cdot b \cdot h \cdot n}{Q} = t \tag{2.1}$$

Where l is the distance from the point with the highest groundwater level to the western ditch or the eastern boundary. l was determined using the measured groundwater levels during relative dry conditions in winter. Effective width b is the expected width to flow to the drain. The height h is the distance between the drain and the groundwater level. For this distance, the position of the maximum head from the wet winter model was used. n is the porosity.

2.4. Chemical Measurements

Chemical measurements were carried out in the field and in the tile drain outlet. First, in subsection 2.4.1 the laboratory analysis of soil samples and groundwater extraction methods are explained. Second, subsection 2.4.2 shows the collection of water quality samples with an auto-sampler at the tile drain outlet. Third, in subsection 2.4.3 the laboratory analysis of the water samples taken in the field and at the tile drain outlet are explained.

2.4.1. Soil and Groundwater Samples From the Field

In the subsurface of the field, samples were taken from both the soil and the groundwater. Six depth profiles were established in the field up to 3.8 metres below the surface. The location of these six depth profiles is shown in Table A.2. For each of these six profiles, the first 60 cm to the groundwater level were analysed using soil samples. For these six profiles, a sample was taken just below the surface and at the groundwater level (about 60 cm below the surface). In addition to these six profiles, several additional soil samples were taken in the field down to the top of the clay/debris layer about 150 cm below the surface.

The soil samples were prepared at TU Delft and measured at the ICP at Deltares. Table 2.3 shows the preparation for analysing a sample with three different reagents. To limit the total amount of samples for the ICP, not every extracted soil sample was analysed. And not every sample was analysed with three reagents. The extractions with HCL and ammonium oxalate were used for all six profiles and for extracted clay at 150 cm depth. The water extraction reagent was only used for the topsoil in the six profiles.

Table 2.3: Three different soil sample preparations used to measure the chemical soil characteristics.

Reagent	Soil (gram)	Concentration	Volume (ml)	Bottle (ml)
HCL	2.5	3 M	25	50
Ammonium Oxalate	2.5	0.2 M ammonium oxalate acidified to PH = 3 with 0.2 M oxalic acid	50	125
Demi Water	0.5	-	30	50

The soil samples used for the HCL extractions were oven dried and the ammonium oxalate and demi-water extractions were air dried. The samples were placed in a shaker at 100 rpm at room temperature for different periods of time.

- HCL: 70 hr
- Ammonium Oxalate: 2 hr in the dark
- Demi Water: 1 hr

After shaking, the samples were collected after being filtered with a 0.45 μm filter. Then the demi-water samples were acidified with 100 μl of concentrated nitric acid. After preparation, the samples were analysed by ICP-OES at Deltares in Utrecht.

Groundwater was sampled using two methods: 1) from the observation wells and 2) from the GVP. Water was collected from six observation wells (P1 to P6) using a vacuum pump. Samples were collected during site

visits. Eight water samples from P1, P2, P3, P4 and P5 and four from P6 were collected from the same monitoring wells during the period 11-03-2021 to 21-5-2021. The location of these monitoring wells is shown in Figure 2.4. The disadvantage of monitoring wells is the large filter length of 50 cm. Therefore, the groundwater can enter the tube in a wide area and mix inside the tube. The second method uses a hollow iron tube with a retractable tip at the end of the tube. This tip had a filter with a length of about 5 cm from where the groundwater could enter the tube. A small plastic tube inside the hollow iron tube connected the filter to the vacuum pump at the surface. Since the length of the filter was only about 5 cm, the groundwater was sampled at a very specific depth. The soil probe was used to create 10 depth profiles, six of which were created on the field at Hogervorst. The location of the six profiles is shown in Table A.2. The other four profiles were taken from other fields in the 'bollenstreek' and are not discussed in this report. With the GVP it was tried to reach a maximum depth of 3.8 meter and extract a groundwater sample every 30 centimeter. However, due to sampling problems, measurements could not be taken at some depths. There were several reasons for this: a clogged filter, a broken filter, a clogged tube, a clay layer or impenetrable debris. Due to these problems, the creation of the depth profiles was very time-consuming and therefore took 5 days to extract the 10 profiles.

In addition to the extracted samples, which were analysed in the laboratory, the EC, PH and redox values of the groundwater extracted with the GVP were measured with a manual redox, EC and PH device. To continuously refresh the groundwater samples, the measuring devices were placed in Greiner tubes from which the GVP continuously pumped fresh groundwater into the tubes (see Figure 2.8).

Figure 2.8: Overview of groundwater sampling with the GVP. The iron tube on the right is the GVP from which the water is taken with the peristaltic pump. On the left are the Greiner tubes with the EC, Ph and redox devices.

2.4.2. Extracting Water Quality Samples at the Drain Outflow

From 18 March to the third of June, an autosampler was installed in B1 to collect water samples from the tile drain outflow. The autosampler consists of 24 bottles with a capacity of 1L each. The autosampler collects the water from B1 at a preset frequency. In Figure H.6b it is shown how a hose has been placed in B1 from which water can be pumped into a sample of the autosampler. The frequency was normally set to one sample every eight hours. This way, it takes eight days to collect all 24 samples. If the weather forecast predicted rain, an attempt was made to record this event and increase the frequency. The exact frequency differs from each of the three rain events recorded. As the automatic sampler had to be set manually and the samples were taken to Utrecht, this was labour intensive. During the fieldwork from 8 to 12 May 2021, there were three responses (period of time when water flows out of the drain) recorded with a lowered drain extension tube. The outflow extension was lowered from 16 April to 14 May to increase the possibility of a response in summer. For a complete overview of the adjustments to the tile drain extension tube, see Appendix D. In addition, two samples were taken from the western ditch near the tile drain outlet of D1 on 25.5.2021 and 21.5.2021.

2.4.3. Lab Analysis Water Samples

For all extracted water samples the following procedures were used to measure phosphorus, iron and manganese concentrations.

Phosphate measurement: The samples were previously acidified with HCl. The samples were filtered with a 0.45 µm filter. Phosphorus was measured photometrically at 880 nm. The sample is incubated for 30 minutes and previously reacted with an ammonium heptamolybdate solution acidified with sulphuric acid and freshly added ascorbic acid. The photometric measurement is compared to the calibration line (R2>0.99).

Iron (II) and total iron measurement: The samples were previously acidified with nitric acid to fix the iron (II) and avoid precipitation. All samples were filtered with a 0.45 µm filter. Iron was determined photometrically with a acetate buffered phenanthroline solution at 510 nm. For total iron the samples were previously reduced with hydroxylammonium chloride. Both iron (II) and total iron were incubated for 20 minutes before taking the measurement. The photometric measurement is compared to the calibration line (R2>0.99).

Manganese measurement: The samples were previously acidified with nitric acid to avoid precipitation. All samples were filtered with a 0.45 μm filter. The sample was made to react with hydroxylamine, formaldehyde, and ammonium hydroxide, incubated for 30 minutes and the photometric measurement was taken at 450 nm. The photometric measurement is compared to the calibration line (R2>0.99).

Anions and Cations - Ion Chromatography (Dionex): background anions and cations were measured by ion chromatography as soon as possible after the samples reached the laboratory. Including: nitrate, nitrate, bromide, sulfate, phosphate, sodium, ammonium, potassium, magnesium, and calcium. The results are expressed in mg/L of the molecules (i.e 0.23 mg PO4/L = 2.4 μM/L). The samples were previously filtered at 0.45 μm and they were not acidified because of the Dionex equipment requirements. Not acidifying the samples may cause precipitation of calcium phosphates or iron oxides and iron phosphates as the samples oxidize. This is why, although the IC measured phosphate the photometric method is more reliable. Ammonium and nitrate, and sulfate concentrations can indicate how reducing the conditions of the water are. Differences in calcium, manganese, chloride, bromide, and potassium can indicate that the water is from a different source.

3

Results

First, in section 2.2 an overview of the hydraulic measurements and the analysis of them is given. Secondly, in section 3.2 the calibration of the model and its results are presented. Thirdly, the results of the P concentrations found are presented in section 2.4.

3.1. Hydraulic Measurements

This chapter shows the results of the measurements of rainfall, tile drain discharge, groundwater levels and ditch water levels. First, an overview of the data is given in subsection 3.1.1. Then the validation of the ditch measurements is explained in subsection 3.1.2. These ditch measurements were used to study the activation of the measured tile drain response as shown in subsection 3.1.3. In subsection 3.1.4 the relative amount of rainfall transported by the tile drainage is explained. In subsection 3.1.5 the results of the salt tracer experiment are described.

3.1.1. Effective Rainfall, Tile Drain Discharge, Groundwater Level and Ditch Water Level Observations Overview

Figure 3.1 shows the precipitation intensity, cumulative precipitation volume (orange line) and the cumulative effective precipitation volume (blue line). The cumulative precipitation volume [m^3] is the discharge area of a single drain [1] multiplied by the measured (effective) precipitation [2] in Voorschoten. The effective precipitation corresponds to the precipitation in winter. In summer, however, the effective precipitation and the precipitation differ due to the higher evaporation in summer.

Figure 3.1 shows the drain discharge measured at D1 (blue line) and the cumulative drain discharge (yellow line). From the graph, it can be seen that there were large fluctuations in tile drain discharge in winter and summer, ranging from 0 to 0.3 m^3/h. Furthermore, the graph showed that there was less drain response in summer. Between 8-12-2020 and 1-3-2021, nearly 80 m^3 water was discharged. From April to August, there was only about 5 m^3 Water flowed out of the drain. Note that from 2021-05-20 to 2021-07-20, no measurements of the discharge were available because the barrel was disconnected. Since there was a large rainstorm during this period that raised the groundwater level well above the water level of the ditch, the response between April and August is likely to be higher. However, it is noticeable that the amount of rainfall up to April was 200 m3, while the amount of rainfall between April and August (excluding the rainfall between 2021-05-20 and 2021-07-20) was 353 m^3. Thus, although the amount of rainfall was higher, less water was transported by the drain. This relationship between tile drain response and rainfall volumes was further analysed by dividing the data into eight parts (see subsection 3.1.4)

The bottom graph shows the water level in the western ditch compared to the groundwater level at P1 and P2 60 metres from the ditch. As the field has a rd system, the tile drain is activated when the groundwater level in the field exceeds the ditch water level, as explained in section 2.1. To check whether this was the case, the time of the drain response was compared with the time when the groundwater level in the field exceeds the

[1] Groundwater from half the length between two drains is assumed to flow to a single drain. Therefore, a total effective width of 10 metres is used. The length at which the modelled groundwater level was above the western ditch water level during the wet winter is used as the effective length (60 metres). Therefore, 60*10 = 600m^2 is taken as the effective area.

[2] The KNMI weather station in Voorschoten provides hourly precipitation data and daily evaporation values. The average hourly precipitation minus the daily evaporation thus gives the effective precipitation.

water level of the western ditch. The results can be found in subsection 3.1.3 after validating the water level in the west ditch subsection 3.1.2.

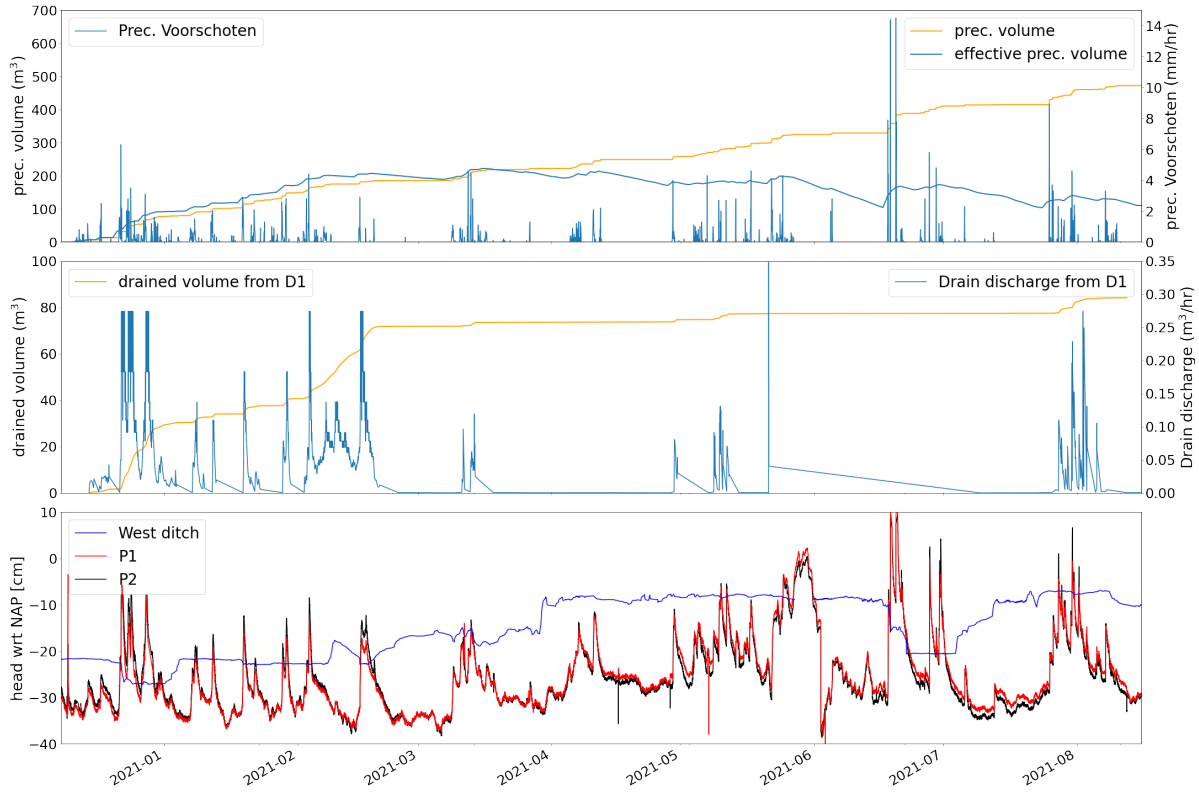

Figure 3.1: Complete data set of measured hydraulic responses. The upper graph shows the precipitation and the (effective) cumulative rainfall for the effective area between 2 drains (10 * 60 metres). The middle graph shows the measured tile drain discharge and drained volume at D1. The bottom graph shows the measured western ditch and the groundwater level at P1 and P2 60 metres from the western ditch. The figure provides an overview of the dynamic behaviour and rapid changes in groundwater level ; discharges over the measured period from 2020-12-08 to 2021-07-21.

3.1.2. Water Level in the West Ditch

The Rijnland Water Board controls the water level with weirs to a winter and a summer level. These water levels were measured at an interval of 10 to 30 minutes at two monitoring sites, as shown in Figure 2.1.

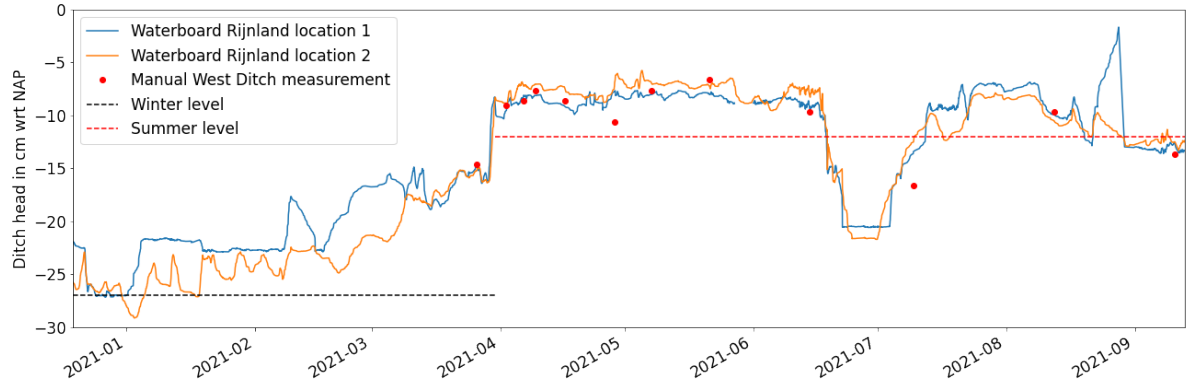

Figure 3.2: The monitored water levels of site 1 and 2, as shown in Figure 2.1, have shifted towards the manually measured ditch level at Hogervorst (red dots).

To check whether these measurements agree with the west ditch at Hogervorst, they were compared with manual measurements at the bridge given as **A** in Figure 2.1. The measurements agreed well with the manual measurements (see Figure 3.2).

3.1.3. Drain Response After High Groundwater Events

Using the measured groundwater level at 60 metres from the western ditch (P1 and P2), the water level in the ditch and the measured drain response, the relationship between the drain response and the groundwater level in the field was further studied. For this purpose, the drain response time was compared to the time when the water level in the field exceeded the western ditch. For ease of reading, a response is when water flows out of the tile drain and an event is when the water level in the field is higher than the water level in the western ditch.

For calculating the response and event time two restrictions were made:

- Response: The duration between two pump activations by the float switch when the maximum water level in the barrel was reached was greater than 0 and less than 24 hours.
- Event: water level in P1, P1+5 pr P1+10 is larger than the water level in the ditch.

The events and responses to these constraints are visualised in Figure 3.3. The top graph shows the groundwater level 60 metres from the ditch and the western ditch level. The middle graph shows the responses and events calculated with a Python script. The bottom graph shows the tile drain discharge from D1. The figure shows that the calculated event took place when the groundwater level exceeds the ditch. Furthermore, a calculated drain response is found when there was an outflow. So the calculated events and responses agree with the measured data.

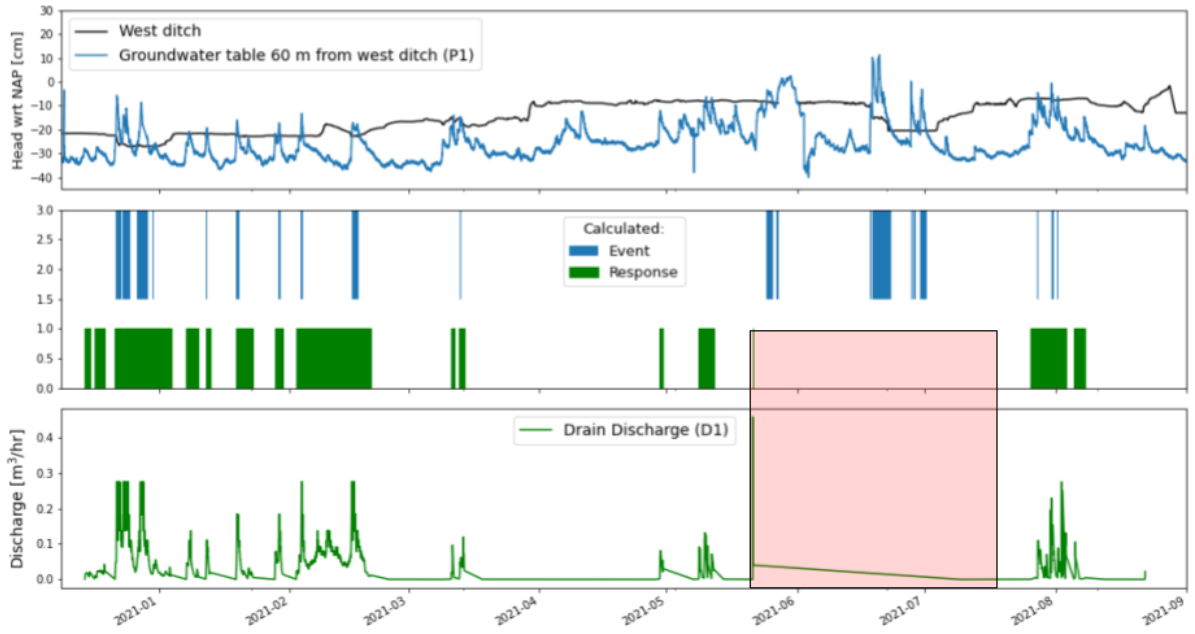

Figure 3.3: Calculated events (blue) and drain responses (green) as defined in subsection 3.1.3 based on the measurements: West ditch ; water level at the end of the field (60 metres from the west ditch); tile drain discharge from B1. Note: 2021-05-20 to 2021-07-20 no response was measured as B1 was disconnected.

Furthermore, the figure shows that the responses are longer than the events (measured at 60 metres from the western ditch at P1 and P2), whereas it was expected that a response would occur when an event occurs. However, the events in the figure were calculated with the groundwater level at the end of the field. It was expected that the event time near the ditch would be longer and correspond to the measured response. This expectation was based on the measured groundwater levels near the ditch (P6, P7, P8), which had higher groundwater levels than 60 metres from the ditch (P1 and P2). Therefore, it was expected that the groundwater level near the ditch would be above the ditch for longer than at the end of the field and would therefore cause a longer response. However, the groundwater level near the ditch was only measured in June.

To test this expectation, the measured groundwater level at the end of the field was shifted by +5, +10 and +20 cm and the new events were calculated, the results of which can be found in Table 3.1. As already seen in Figure 3.3, responses occurred when there was no event at 60 metres from the western ditch. Of the 61 days (1464 hours) where a response was measured, only 12 days occurred during an event 60 metres from

the western ditch. The upward shift of the groundwater level led to an extension of the event time, which confirms the expectation. However, after an elevation of 20 cm, there were still 13 days where a response occurred without an event, while a in % decreased to 23 %. a in % indicates whether there was a response without an event. If a in % is 100 %, it means that there is never a response when there is no event. a in % shows that at 60 metres from the western ditch there was always a response when there was an event, which should be the case. However, when 5, 10 and 20 cm are added, a in% decreases, while there are still responses when there is no event. Since the drain can only respond when an event occurs, the fluctuation of the water level must be less near the ditch than at the end of the field. This also corresponds to the modelled water distribution during a wet winter response Figure 3.5.

Table 3.1: Relation between the measured drain response and the total event time between 2020/12/12 and 2021/9/9, which is 271 days.
Index: additional level in centimetres above the measured water level 60 metres from the ditch.
a = (∑ (response time during event time) / total event time) *100
b = (total event time / total response time) * 100

Index	total Response	response when event	response when no event	Event	a in %	b in %
+0	61 days	12 days	49 days	12 days	100	20
+5	61 days	28 days	33 days	30 days	95	51
+10	61 days	43 days	19 days	64 days	67	110
+20	61 days	48 days	13 days	204 days	23	332

3.1.4. Rainfall Volume Compared to Drain Response Volume

To study the amount of rainfall compared to the drain response volume the measured data is divided into 8 parts. The rain and tile drain discharge volume for part 1 to 8 were calculated and presented in Table 3.2. Note that precipitation is used and not effective precipitation so evaporation is not subtracted. An overview of the data was given in Figure 3.1. However, a detailed graphical overview for all eight parts can be found in Appendix B. The table shows that during winter the tile drain discharge volume in relation to precipitation volume was larger compared to summer. It was highly likely that the much higher evaporation values in summer caused the lower tile drain response. The effective evaporation in part 7 and 8 (Appendix B.) was negative meaning a larger evaporation than precipitation while part 1 to 6 the effective evaporation was equal to the actual rainfall. Since, there was almost no evaporation in part 1 to 6 it was found that 32 % of the water leaching from the entire field was discharged through the tile drains. However, subsection 3.1.3 indicated that the area close to the ditch was more active causing a smaller drain response area.

Table 3.2: Drain response volume compared to rainfall volume into drain 1.

part	date start	date stop	tot response (m3)	tot rain (m3)	drain / rain ratio (%)
1	2020-12-08	2020-12-21	2	28	8
2	2020-12-21	2021-01-05	29	67	43
3	2021-01-06	2021-01-15	3	22	17
4	2021-01-18	2021-02-01	7	47	14
5	2021-02-01	2021-03-01	31	37	83
6	2021-03-10	2021-03-16	2	28	6
7	2021-04-10	2021-05-21	4	64	6
8	2021-07-20	2021-08-16	7	59	11
Barrel disconnected	2021-05-20	2021-07-20	-	120	0
Winter (1 to 6)	2020-12-08	2021-03-16	73	229	32
Summer (7 to 8)	2021-04-10	2021-08-16	11	123	9

3.1.5. Tracer Experiment

During this study, two tracer experiments were conducted consisting of 5 tests as explained in subsection 2.2.3. The analysis of the first experiment (test 1 and 2) is not covered in this report, but led to improvements for the second tracer experiment. The results of test 3 and 4 are visualised in Figure 3.4. In test 5, the CTD-multisenor measuring the EC did not work properly and therefore did not collect reliable information.

Test 3 (5 metres from the ditch) showed an increase in EC at the outflow of the drain extension 35 minutes after injection. Within this time frame (after injection and before the increase in EC), a total of 65 litres passed the drain outflow. The drain storage in the first 5 metres should be about 39 litres with an approximate drain diameter of 10 centimetres. So at least 39 litres of water had to be discharged before salt could be detected at the outlet of the drain. So 65 - 39 = 26 additional litres were discharged before an increase in the EC value was detected. Therefore, 26 litres infiltrated the first 5 metres of the drain before the injected saline solution reached the drain outlet. Furthermore, the EC continued to rise and was still rising when the experiment was stopped after 3 hours. A mixing calculation showed that 51% of the salt was recovered before the end of test 3. Test 4 (15 metres from the ditch) showed a very slight gradual increase in EC compared to test 3. After six hours, 880 litres of water had passed the drain, while EC only increased by 20 µS/cm.

Note that tests 3 and 4 show some short peaks in the EC. These peaks occurred when the water in B1 reached the level of the drain extension tube where the EC device (CTD diver) was located. In test 3, only part of these peaks were measured because the pump was manually activated before the level of the drain extension tube was reached.

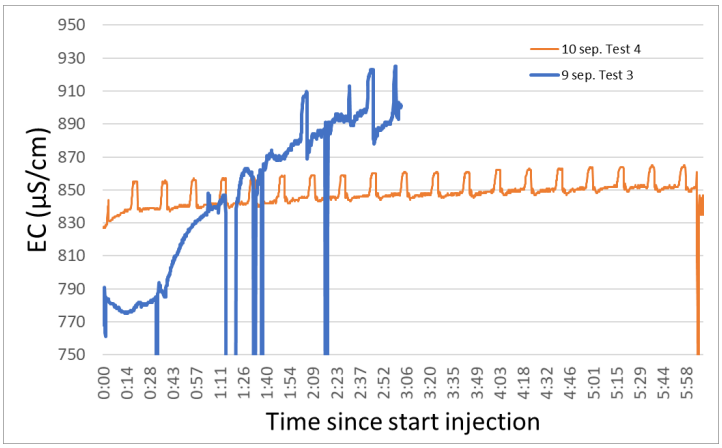

Figure 3.4: EC measurements at 5 (blue line) and 15 (orange line) metres from the ditch (test 3 and 4 respectively). In test 3, an increase in EC was measured 35 minutes after injection and 65 litres were discharged from D1, whereupon EC continued to increase. The results of test 4 showed a slow, gradual increase in EC of 20 µS/cm.

3.2. Hydraulic Steady State MF6 Model

First, the calibration to the final models is shown in subsection 3.2.1. Then the results of a nationwide model and the effects that tile drainage and head below the clay/debris layer may have on infiltration in Hogervorst are presented in subsection 3.2.2. Based on the two models, a wet and dry condition in summer and winter was modeled (see subsection 3.2.3). The mass balances are shown in subsection 3.2.4 and the transport times in subsection 3.2.5.

3.2.1. Wet Winter and Dry Summer Calibration

An overview of the values used at the start of the calibration and the final values after calibration are shown in Table 3.3.

The observed (ground)water levels and drain discharge for the wettest month and the 10 wettest winter days are shown by boxplots in Figure Figure 3.5. It was decided to use 10 days as this was the longest period in the measured dataset during which tile drainage continued. The modelled groundwater levels and discharges of the final wet winter model are shown in green, blue, orange and yellow. The green line represents the situation with the START values and the yellow line the final wet winter model. The continues black line shows the location of the drain. The head in the tile drain which is equal to the water level in the west ditch (drain head) is presented with black dotted lines.

Table 3.3: Overview of the calibration values before and after calibration for the wet winter and dry summer model.

Parameter		**K_v (m/d)**	**K_h (m/d)**	**Drain conductance (m2/d)**	**Effective precipitation (m/d)**	
Package		Node Property Flow (NPF)		General head boundary (GHB)	Recharge (RCH)	
START calibration	description	Value as indicated in figure 2.7		Arbitrary number	Winter Summer	Avg. eff. prec. in Jan. 2021 Avg. eff. evap. in Jun. 2021
	value	K_v_SEN	K_h_SEN	0.2	Winter Summer	0.0025 -0.465
END Calibration	Description	Calibrated with the Winter Model.		Winter and summer calibration	Winter Summer	Avg. eff. prec. Dec. 21 to 31 Avg. evap. Jun. 6 to 17
	value	K_v_SEN × 2	K_h_SEN × 2	Winter Summer	2 0.2	7.8 -3.4

The data showed that large rain showers were required to generate a drain response. The distribution of the groundwater level in January (green boxplot) showed that only the outlines exceeded the drain head (black dashed line). Even on the 10 wettest days of the winter, from 21 to 31 December (yellow boxplot), groundwater levels were observed below the ditch level. However, the groundwater level was within the 75 th percentile of the observed ditch water level. Furthermore, the tile drain response was continuous (see Appendix B). The wet winter model with START calibration values showed a groundwater level just above the drain head and a low discharge comparable to the observed discharge. Using the 10 wettest days and a higher drain conductance value increased the groundwater level above the 75th percentile (blue lines). Increasing the k_h and k_v values by a factor of 2 decreased the groundwater level and discharge within the 75th and 25th percentile limits (orange line). Finally, increasing the drain conductance by a factor of 10 instead of a factor of 5, the discharge corresponds to the median of the observed discharge (yellow line). The modelled groundwater level lies between the 75th and 25th percentile, but above the median. Since an attempt was made to simulate a wet winter situation, this was considered an acceptable groundwater level corresponding to actual wet conditions.

For summer conditions the average evaporation measurements from 6 to 17 June were used, multiplied by the crop factor of tubers in June of 0.7 [35]. During this time frame there was no precipitation and the ditch level was not changed as shown in Figure 3.2. Using the same drain conductance as the final wet winter model gave a groundwater level exceeding the groundwater level observation (see Figure 3.7. Using the lower START calibration value of the drain conductance showed a better fit. This value was than used in the final dry summer model. To understand the possible mitigation measures in the east the groundwater level was increased by 20 and 40 cm (see Figure 3.7). The effect of increasing the east ditch water level on the water balance is further explained in subsection 3.2.4.

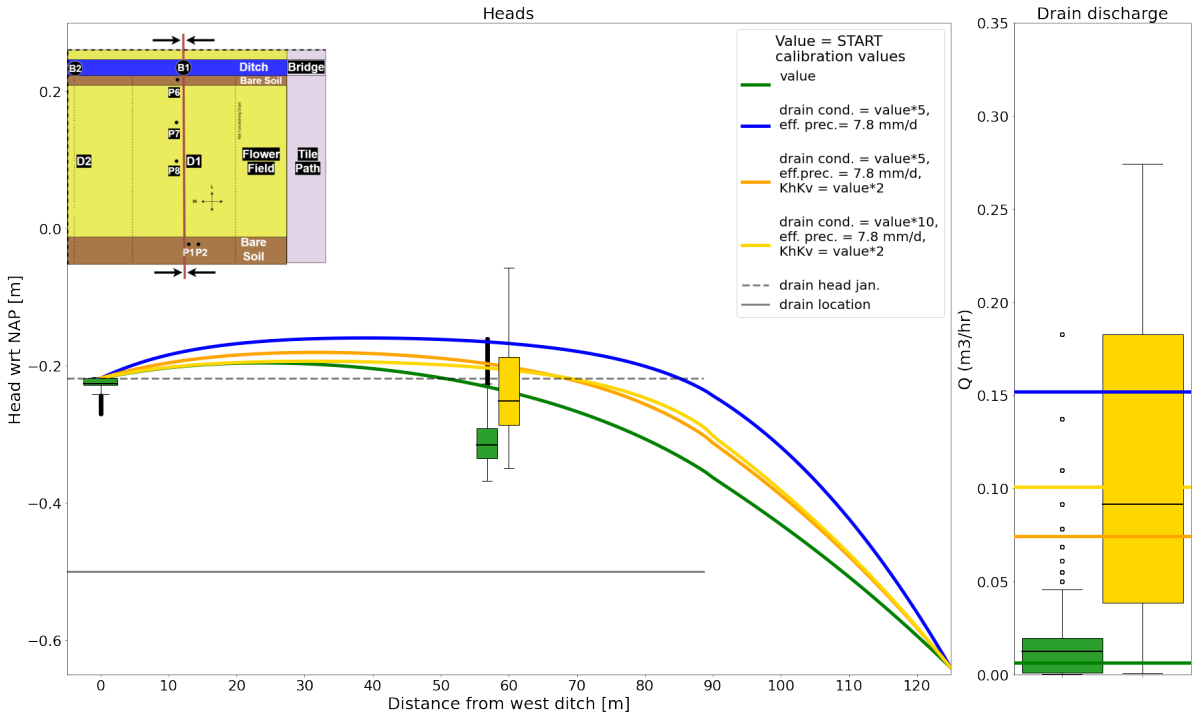

Figure 3.5: Final calibration of the steady-state wet winter model. The boxplots represent the (ground)water level and discharge of the wettest month, January (green boxplot) and the 10 wettest days, 21 to 31 December (yellow boxplots). The green, blue and orange lines summarise the calibration of the final model (yellow line) based on the sensitivity analysis and the observed (ground)water levels and discharges. The values of the START calibration can be found in Table 3.3.

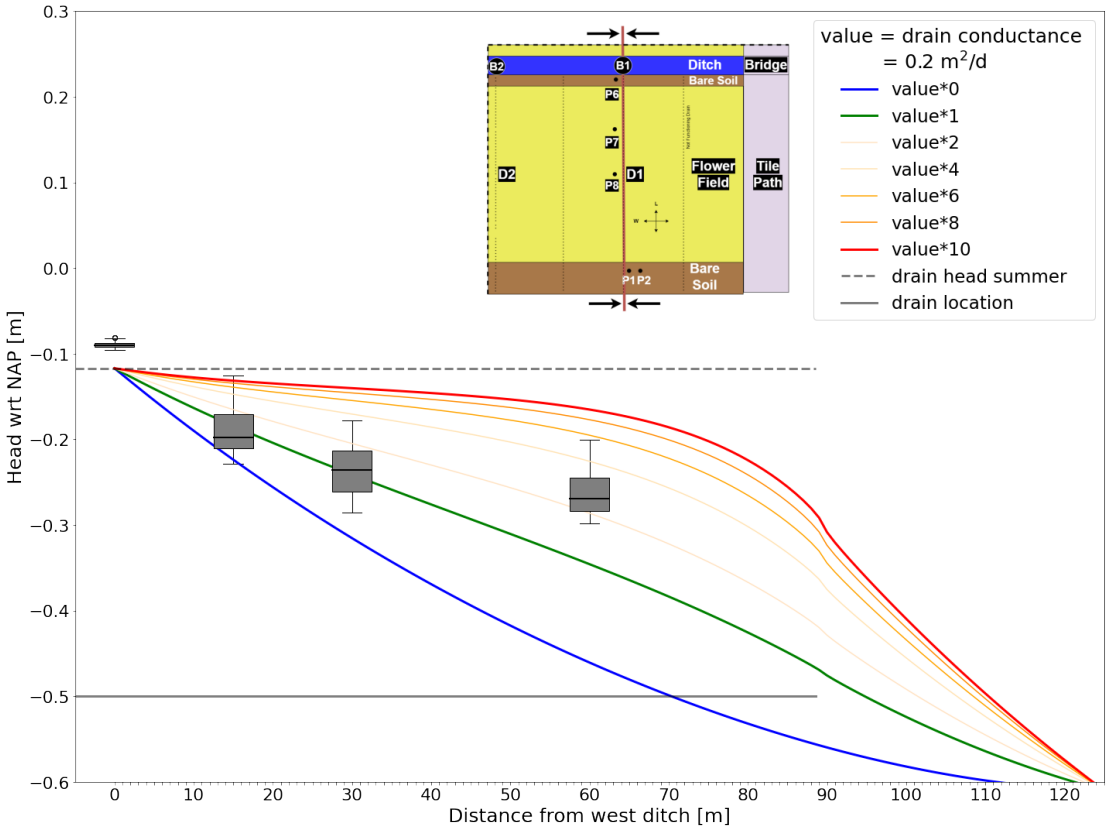

Figure 3.6: Final calibration of the steady-state dry summer model. The START value (green line) is used for the final summer model. Note that a GHB of 2 (used in the wet winter model) exceeds the observed groundwater tables in summer.

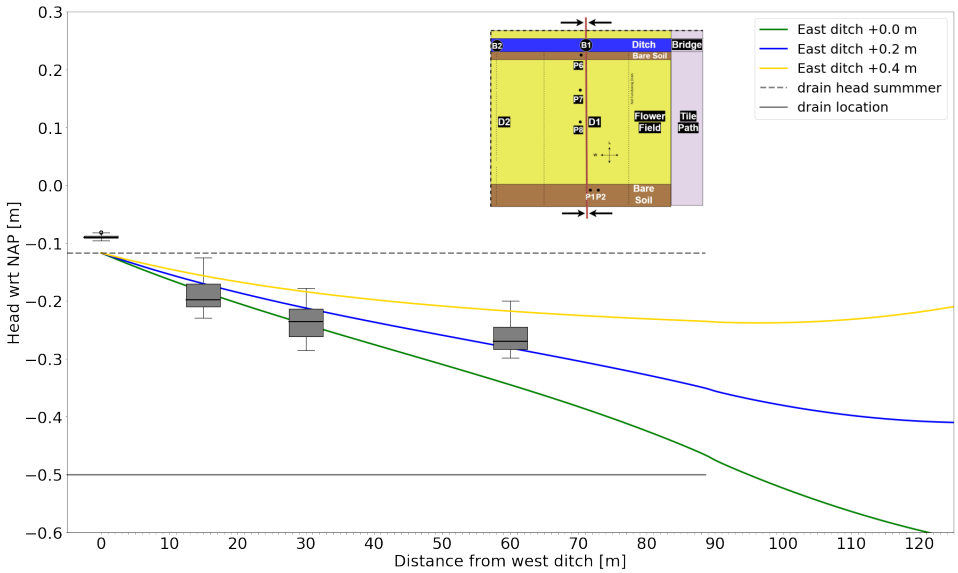

Figure 3.7: Final steady-state dry summer model with groundwater level observations from 6 to 17 June. $K_h k_v$, equal to the winter model. The drain conductance was set to its START value of 0.2. The blue and yellow lines show the effects of raising the eastern ditch by 0.2 and 0.4 metres, respectively.

3.2.2. Seepage

A first indication of whether the seepage at Hogervorst is significant was found with the LHM 4.1 model. [36]. Figure 3.8 shows the infiltration modelled by LHM4.1 on and around the field of Hogervorst. The outline of the field has been marked with a black line. Note that the grid size of the LHM 4.1 model was larger than the field. The LHM 4.1 model shows a low seepage of -0.25 mm/day, indicating that there was little leakage.

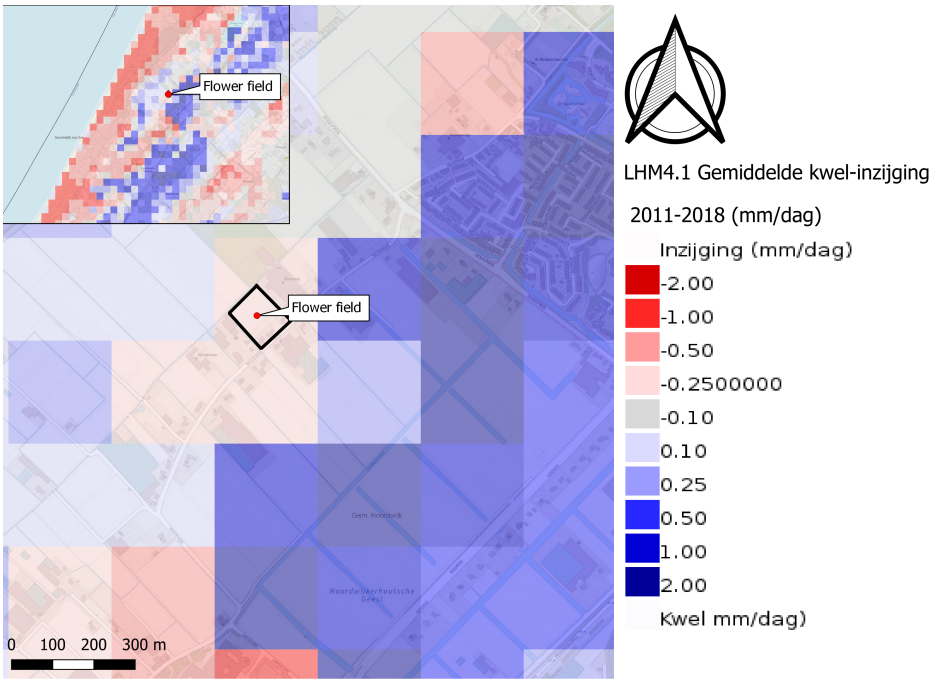

Figure 3.8: National Hydrological Model (LHM) 4.1 seepage model in (mm/day) [36]. The flower field at Hogervorst has been marked with a red dot. The outline of the field is marked with a black box. The LHM 4.1 model shows negligible seepage at Hogervorst.

The Wet winter model and dry summer model show that the tile drains do not cause a large upward flow (see Figure 3.9 and Figure 3.10).

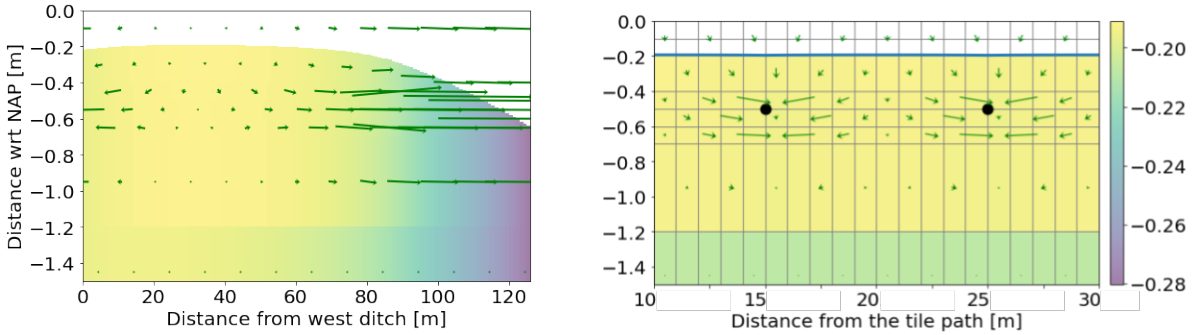

(a) Wet winter cross section at D1

(b) Wet winter cross-section at 20 metres from the west ditch.

Figure 3.9: The model for the wet summer shows that the discharge of the tile drains does not cause a large upward flow.

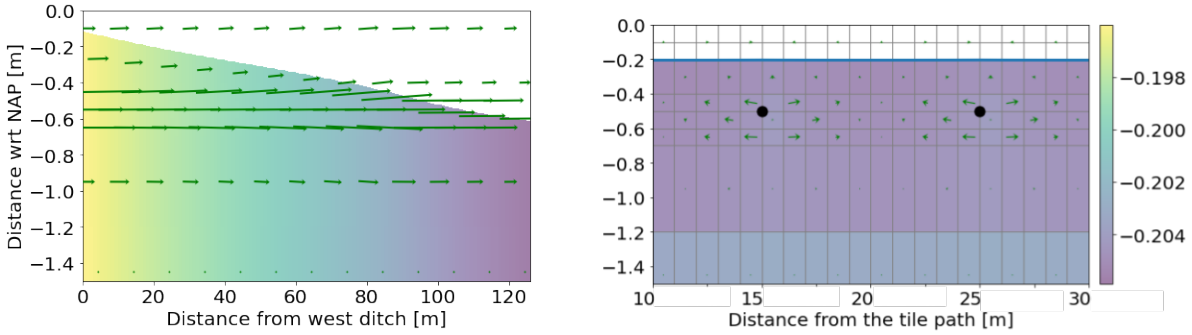

(a) Dry summer cross section at D1

(b) Dry summer cross section at 20 metres from the west ditch

Figure 3.10: The model for the dry summer shows that the irrigation of the tile drains does not cause a large upward flow.

The possible effects of infiltration in wet winter are shown in Figure 3.11. Found by increasing the head below the clay/debris layer. The green line shows the model output with the END calibration values. The yellow line shows the situation where the head below the debris/clay layer was increased from -0.22 m NAP in the west and -0.64 m NAP in the east to 0 m NAP. This raises the groundwater level about 3 cm 60 metres from the ditch. The discharge from the effective surface area of D1 was also increased from 0.1 to 0.22 m^3/hr.

The possible effects of infiltration in summer are shown in Figure 3.7. The figure shows that the groundwater level in this situation increased by 10 cm 60 metres from the ditch, when the head below the debris/clay layer was increased from -0.22 m NAP in the west and -0.64 m NAP in the east to 0 m NAP.

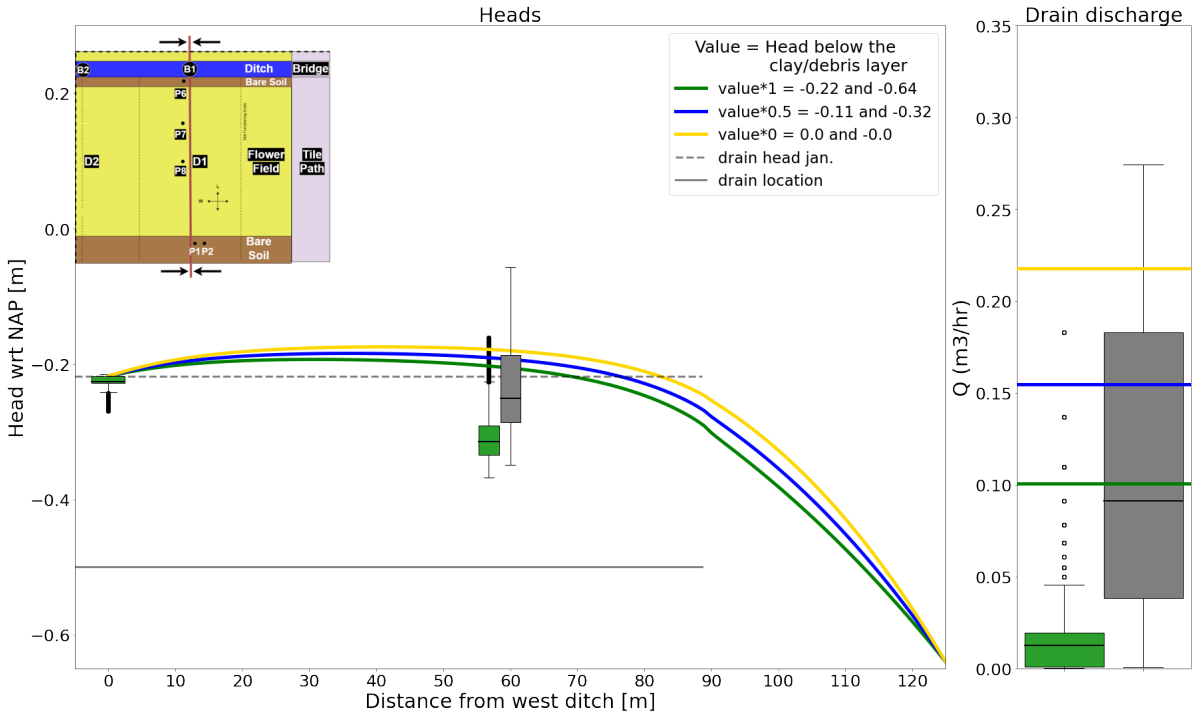

Figure 3.11: Sensitivity analysis of the CHD parameter under the clay/debris layer for seepage in the wet-winter model. The END calibration parameters are used for the model input. The boxplots represent the (ground)water level and discharge of the wettest month January (green boxplots) and the 10 wettest days, 21 to 31 December (grey boxplots). The CHD value below the debris layer is increased from -0.22 m NAP in the west and -0.64 m NAP in the east (green line) to 0 (yellow line).

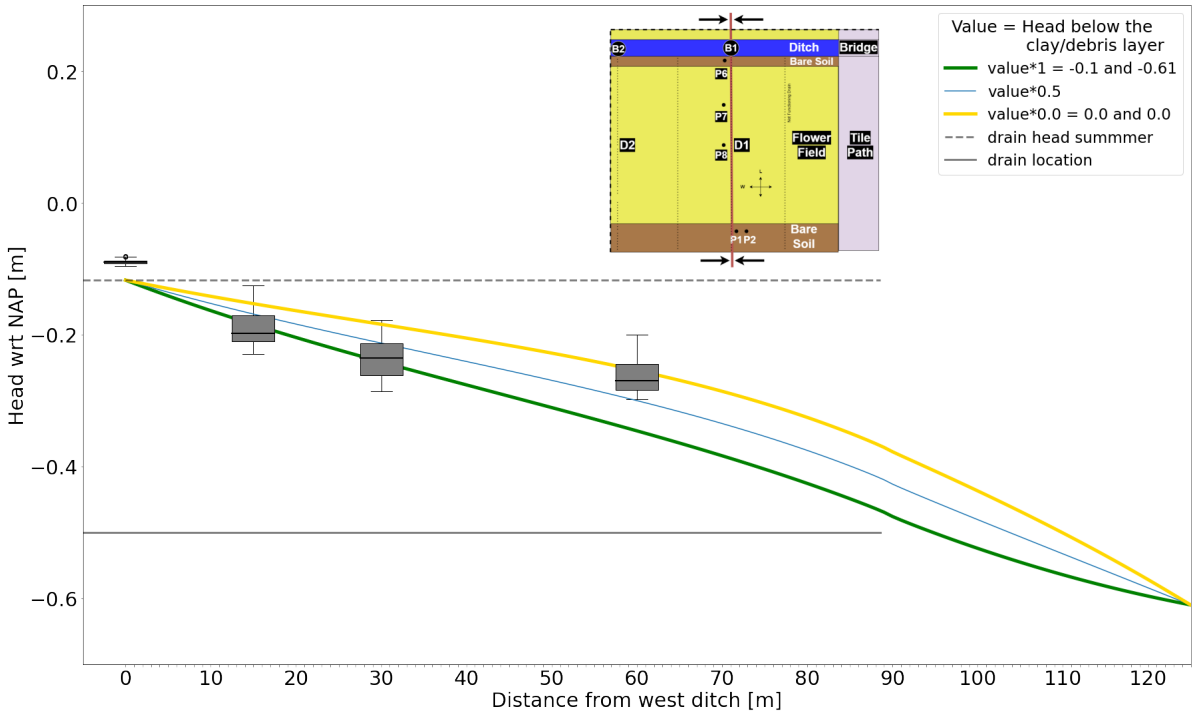

Figure 3.12: Sensitivity analysis of the CHD parameter under the clay/debris layer for seepage in the dry-summer model. The boxplots show the (ground)water level from 6 to 17 June. The END calibration values are used for the model input. The CHD value below the debris layer is increased from -0.2 m NAP in the west and -0.64 m NAP (blue line in the east) to 0 (green line) in two steps.

3.2.3. Wet and Dry Conditions in Summer and Winter

Figure 3.13 shows two things. It gives an overview of the observations of the ditch, groundwater level and tile drain discharge during winter and summer. And it gives an overview of the model results for both wet and dry conditions in summer (dotted lines) and winter (solid lines). The green and yellow lines show the modelled results with effective precipitation of 3.9 and 7.9 mm/d, respectively, with the solid yellow line representing the wet winter model. The blue lines show the situation without precipitation. For this situation, where the ditch water infiltrates into the field, a drain conductance of 0.2 was used. This was the value used for dry summer conditions. As this represented infiltrating conditions, the same value was used here. The red dotted line represents the calibrated dry summer model.

The model showed that when the effective precipitation was increased from 3.9 mm/d to 7.8 mm/d, the groundwater level shifted about 20 m to the east for both the winter and summer models. A larger area thus discharges groundwater via the tile drains into the western ditch.

In addition, the figure shows the difference in groundwater level between dry and wet conditions in summer and winter. Without effective precipitation, the summer and winter models are close to the mean observed value, which is below the tile drain head. When summer recharge is further reduced to -3.4 mm/d, the groundwater level drops further. The observations of the groundwater level show that even lower values were found in summer. Moreover, the groundwater observations show a larger difference between the mean groundwater level and the drain head. In summer the difference is 14 cm and in winter 8 cm. This indicates that the storage capacity is often greater in summer. This seems logical, as evaporation values are higher in summer.

The figure also shows the dispersion in the ditch level, groundwater level and tile drain discharge during summer (orange) and winter (light blue). The groundwater level and tile drain discharge show many outliers. This means that these values were only reached for a short period of time. Figure 3.1 shows how groundwater levels change rapidly during rain showers. Appendix B shows an overview of eight time spans, showing the rise and fall of the groundwater level in more detail. Based on the groundwater level observations, it was also noted that precipitation events exceeded the drain head during summer, although the storage capacity was higher. The observed tile drain outflow also showed discharge during summer although it was lower compared to the winter observations.

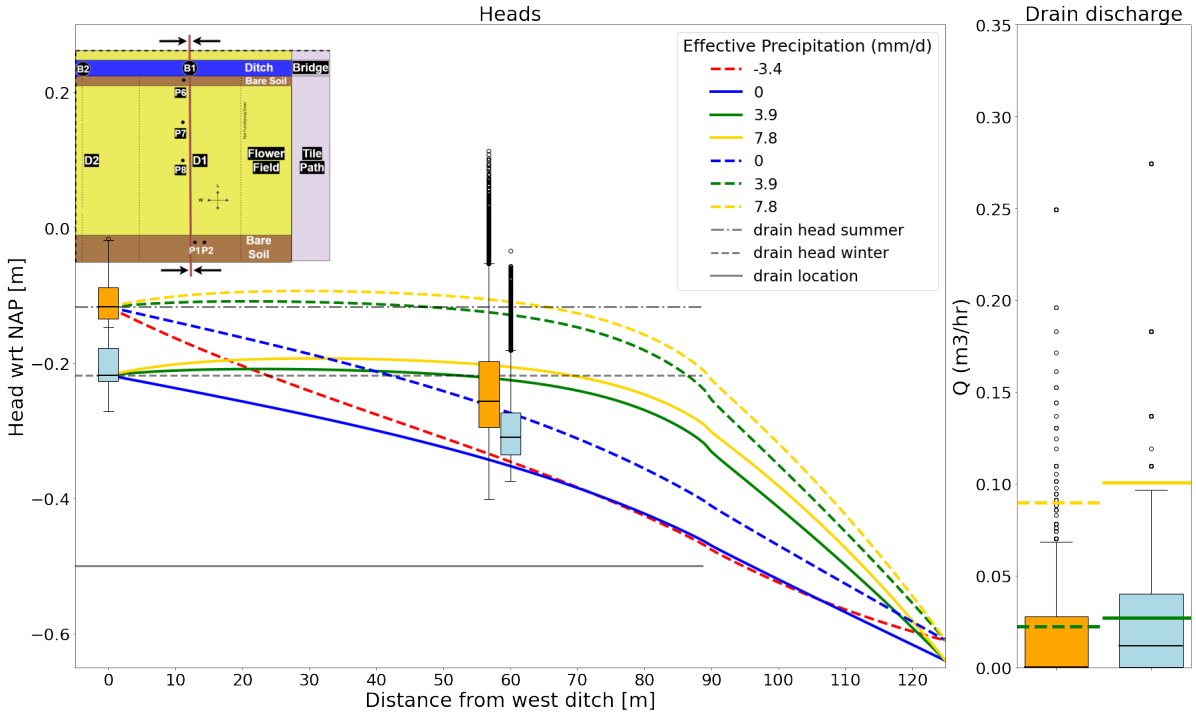

Figure 3.13: Wet and dry conditions in summer and winter. Orange boxplots = observations during summer (27-03-2021 to 12-9-2021). light-blue boxplots = observations during winter (30-10-2020 to 27-03-2021).

3.2.4. Steady State Mass Balance

Using the final wet winter steady-state model, a water balance was created and is shown in Figure 3.15. The water balance showed that during wet conditions, when the groundwater level exceeds the water level in the drain, groundwater above the debris/clay layer is transported to the east and west. In this case, 34 m^3/day is transported towards the west and 64 m^3/day towards the east. Of the groundwater leaving the field to the west, 24 m^3/day is transported by the drain and 10 m^3/day is discharged from the soil into the ditch. The model thus indicates that a larger part of the groundwater discharges through the tile drain on the west side of the field. However, looking at the overall water balance, it is clear that the difference in the groundwater level between east and west has a significant impact and ensures that most of the water leaves the field in the east. The groundwater below the clay/debris layer is also responsible for much of the groundwater flowing from west to east. Note, however, that the area above the clay/debris layer is only 1.5 metres and the entire model is 18 metres deep. Furthermore, the same head is assumed as above the debris/clay layer.

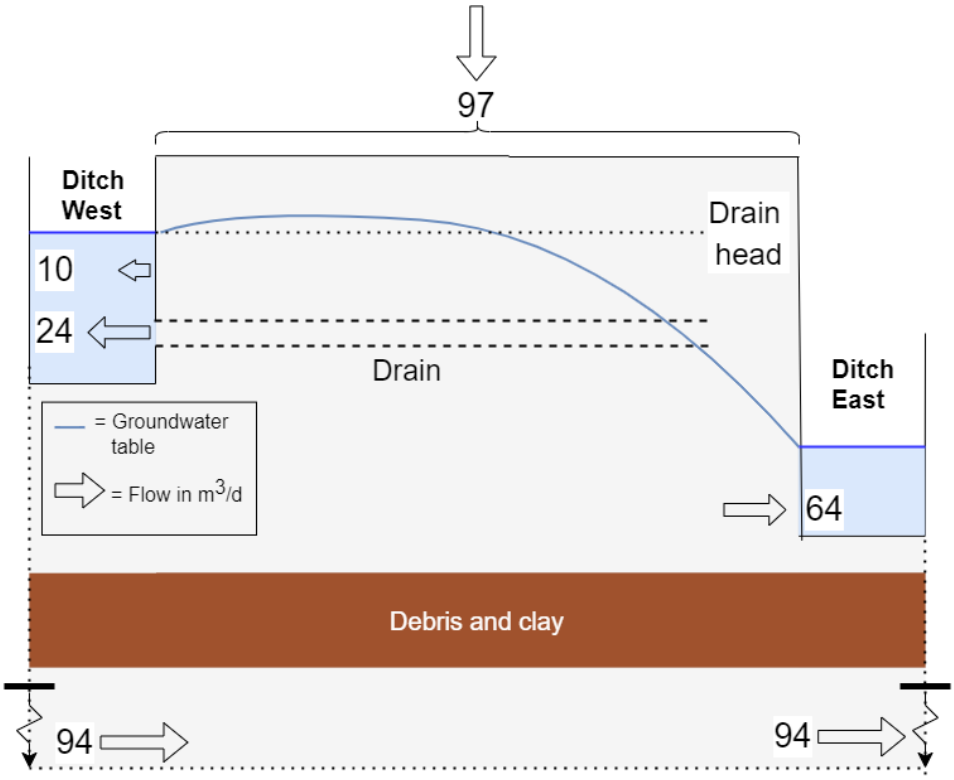

Figure 3.14: Mass balance of the entire field (100 * 125 m) under wet winter conditions. The drain head is the water level of the western ditch. Note that the drains itself are only 90 metres long. Note that the area above the debris layer is only 1.5 m and the whole model is 18 m deep.

Figure 3.15 shows the modelled situation under dry summer conditions. The three different colours represent the effects on the groundwater level and the discharge at Hogervorst when the head in the East Field is increased representing increased weir heights in the east ditch. The exact locations of the weirs and the simplifications are explained in subsection 2.3.1. The result shows that there is no flow to the west in all 3 situations during dry summer weather. Since the threshold of the (ditch/til drain level) is not exceeded. The flow to the east is 11 m^3/hr when the eastern head boundary is set to summer level. This corresponds to a situation where the side ditches are in open connection with the main ditch. However, if the CHD head boundary in the east is raised by 0.2 metres, the inflow to the east boundary stops and all the water flowing into the field from the west evaporates. Below the debris layer, a larger flow is found, which also decreases when the water level in the east is raised. Note, however, that the same head is assumed as above the debris/clay layer.

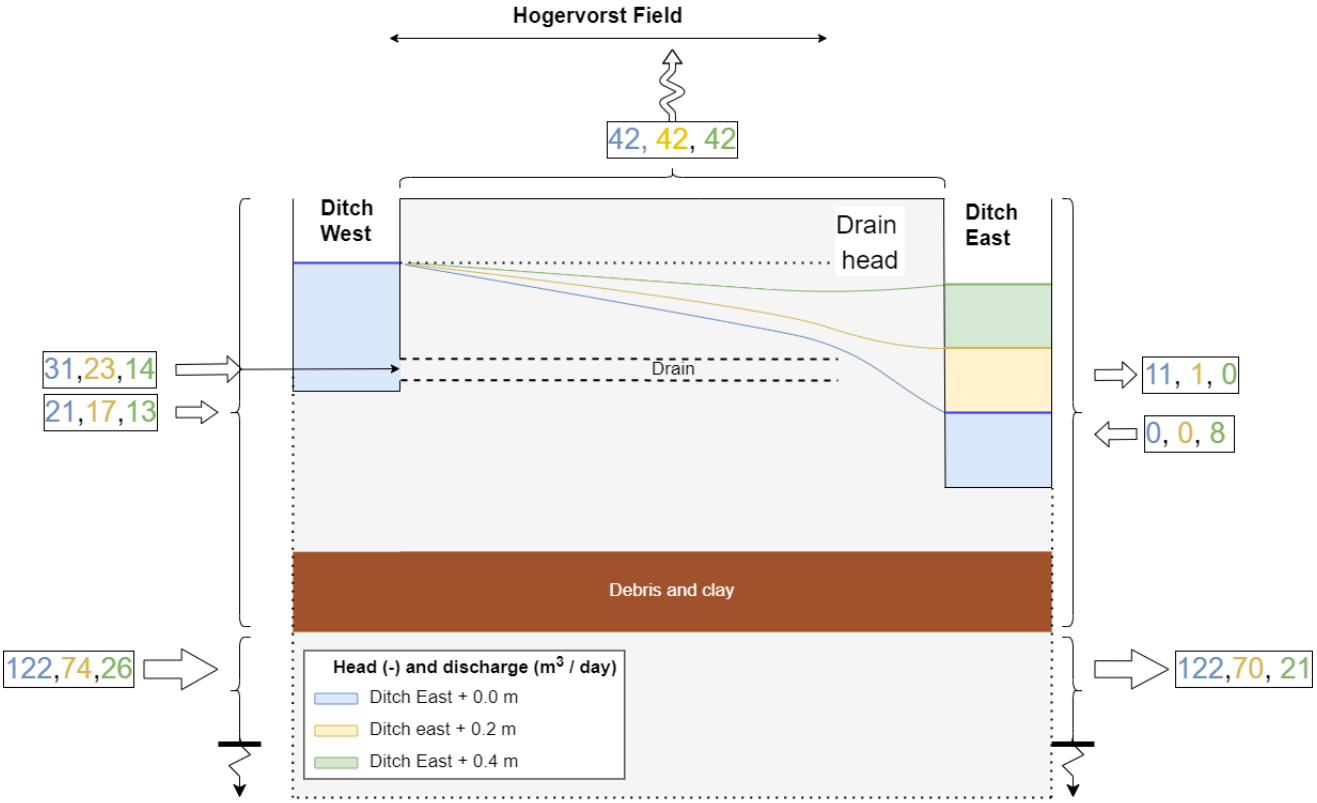

Figure 3.15: Mass balance of dry summer conditions of the entire field (100 * 125 m). The drain head is the water level of the west ditch. Note that the drain itself is only 90 metres long. Note that the area below the clay/debris layer is in reality 16.5 m and above the debris only 1.5 m.

3.2.5. Transport Times

The transport time parameters and the calculated results are displayed in Table 3.4. The discharge (Q) and length (L) were determined with the wet-winter model. The highest water level in the wet-winter model was found 60 metres from the western ditch. As explained in subsection 3.2.5, this location was used to determine the length L. The minimum distance H is the distance between the location of the tile drain and the threshold (groundwater level of the west ditch). This is because this is the minimum groundwater level required to create a drain response. Since the tile drain is at NAP - 0.5 m and the level of the western ditch in summer is NAP - 0.2 m, the minimum height (H) is 0.3 m. To find the shortest transport time, this distance was used as H for the calculation of the transport time to the west. As there were no drains in the east, the distance between the groundwater level under dry winter conditions and the clay/debris layer was used, which was 1 metre. A value of 0.3 was determined for the porosity of the sand [34]. The width (B) was calculated using half the distance between the drains (5 m), giving a total width of 10 metres. The transport time found to the east exceeds the oxidation time of 14 to 21 days, indicating a lower risk of P leaching. The transport time to the west also exceeds the oxidation time at 60 metres from the western ditch. Note, however, that the transport time is less than 14 days when the distance to the ditch (L) and the drain (B) is reduced, indicating an increased risk of P leaching. Since the tile drain is relatively far below the water level in the west ditch, 0.3 m of water must first be discharged before new water can enter the drain.

Table 3.4: Transport time to the western and eastern ditch, from 60 metres from the western ditch. The transport times ditch east and ditch west show the maximum transport times. Shorter transport times are found near the drain and ditch, as shown by the West B ditch, where the width was reduced from 10 m to 2.5 m. *Q is the discharge from the wet winter model.

Transport Direction (-)	Input					Output
	Q* (m3/day)	H (m)	B (m)	L (m)	n (-)	Transport time (days)
Ditch East	6.4	1	10	65	0.3	30
Ditch West A	2.4	0.3	10	60	0.3	23
Ditch West B	2.4	0.3	2.5	30	0.3	3

3.3. Chemical Measurements

This section shows the observed Phosphate (P) concentrations in the field and tile drain discharge. Additional measurements of PH, Redox potential, EC, Temperature, Iron, Manganese and Calcium are shown in Appendix G.

3.3.1. P concentrations in the field

Soil samples and water quality samples were taken from the field and analysed. The ICP at Deltares analysed the concentration of many different substances. However, to analyse where the phosphorus comes from, only phosphorus measurements were used, which are shown in this section. Table 3.5 shows the results of the soil samples and Figure 3.16 shows the water quality data. The other chemical characteristics of the soil and water quality samples can be found in Appendix G.

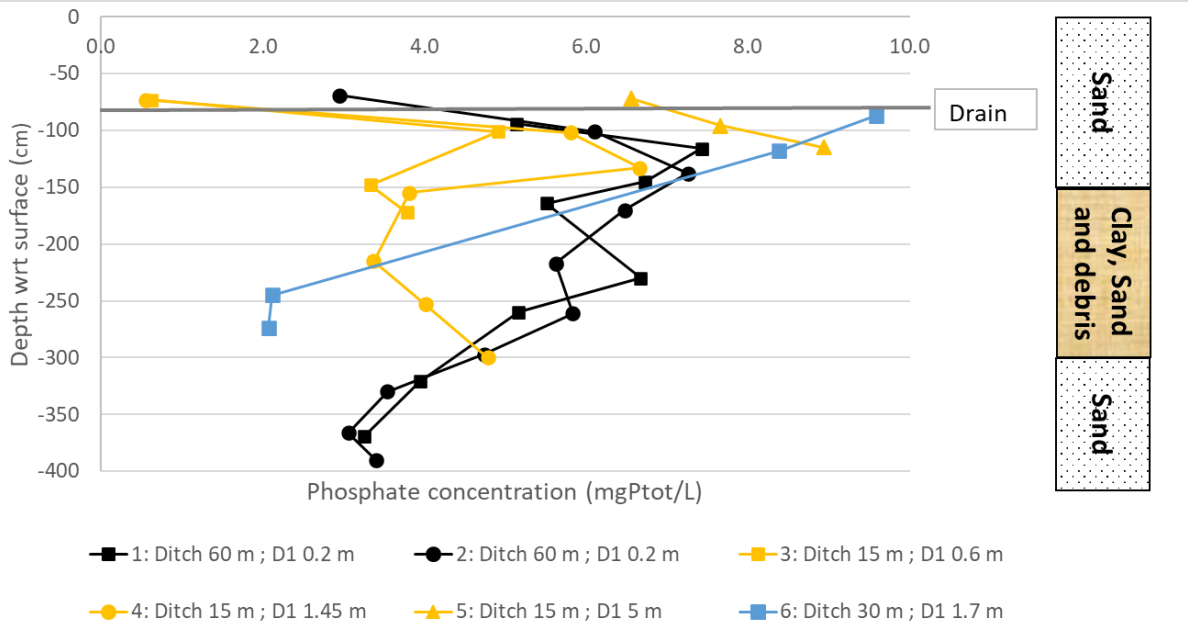

Figure 3.16: Total phosphorus profiles in Hogervorst from groundwater samples extracted with the gvp. The legend indicates the order of sampling (W1 to W6) and the location of sampling (distance to the ditch and D1). The results show (except for the sixth sample) an increase in concentration with depth, after which the concentration decreases again. The highest values (except for the sixth profile) are between 100 and 150 cm below the surface. Which is slightly below the drain level at 80 cm. In the horizontal plane, the overall picture shows a decrease in phosphorus from the end of the field towards the ditch.

Table 3.5 shows the sample number, the distance from the western ditch and the distance from D1 in the description. The depth of the samples is given in relation to the surface. At a depth of -10 cm, the phosphorus concentration in the uppermost layer decreases by a factor of 0.8 towards the ditch, except for the 4th measurement of soluble phosphorus (Pw). At the groundwater level (-60 cm), the total concentration of P increases towards the ditch by a factor of 1.8.

The highest groundwater concentrations of phosphate are found in the clay/debris layer between 100 and 150 cm, which is directly below the tile drains at a depth of -80 cm.

The groundwater samples 15 metres from the trench have lower concentrations than the values from 60 and 30 metres from the ditch. However, at -250 cm, a lower phosphorus concentration is found at 30 metres from the ditch than at 15 metres from the ditch. In addition, the 5th measurement also had higher phosphorus values. However, this measurement was taken 5 metres away from D1, while the other extractions were taken close to D1. When comparing the three P measurements at 15 metres from the ditch (yellow lines), the P concentrations increased with distance from D1.

3.3.2. P response

From 18th of March till the third of June the phosphate concentration at the outflow of the drain was captured by using an auto-sampler which extracted samples from B1 which collected water from D1. From 8 to 12 May 2021 there were three tile drain responses captured with a lowered drain extension tube. Figure 3.1 visualizes

Table 3.5: Phosphorus concentrations at the six depth profiles from soil samples in the unsaturated zone. The table presents the results of two different extraction methods P-tot and P-H2O. Where P-tot used HCL and P-h2O used water as the extraction solution. In the first column the depth profile number (W1 to W6) and location is given. The depth profile number is in the order of the date the depth profile was made. The location is marked as Ditch..; D1.. where ditch.. shows the distance from the ditch and D1.. the distance from D1. The second, third and fourth column show the concentration at the depth at which the samples were extracted with respect to the surface. At Hogervorst the topsoil is extracted at -10 cm and the subsoil at -60.

Description	**-10 cm** mg P_tot/kg	**- 60 cm** mg P_tot/kg	**-10 cm** mg P_H2O/kg
W1: Ditch 60 m ; D1 0.02 m	465	118	12
W2: Ditch 60m ; D1 0.2 m	358	143	14
W6: Ditch 30 m ; D1 1.7 m	348	129	10
W3: Ditch 15 m ; D1 0.6 m	369	217	9
W4: Ditch 15 m ;D1 1.45 m	382	268	13
W5: Ditch 15 m ; D1 5 m	361	216	9

the precipitation, drain response, water levels, phosphorus concentrations and phosphorus load during the three tile drain responses. The full time frame (18 march to 3 June) during the auto-sampler measurements are presented in Appendix C. The time frames where the extension tube was lowered can be found in Appendix D.

Six vertical dashed lines indicate the three responses observed over four days, which in total discharged a volume of 2.8 m^3. Since the auto-sampler collects the water samples from B1 it is important that the water is refreshed regularly. The pump to empty the barrel was started about 100 times between the three responses. However, there was no discharge at the drain between the responses and the same water was measured in the barrel. Therefore, no change in concentration was observed between and after the three responses.

The measured Total Phosphorus (TP) concentrations from the monitoring wells (P1 to P6) are shown in the third graph together with the measurements from the automatic sampler. Note that there are two scales for the measurements taken with the automatic sampler. The thicker blue line is scaled on the right axis. Before the first reaction starts on 07.05.2021, the concentration in the barrel is comparable to P6 (green line), the monitoring well 1 metre from the ditch. During the first, second and third tile drain response the concentration keeps increasing. After the third response an concentration of 5.5 mgPtot/L is reached. This concentration is comparable to the monitoring well P5 (purple line) and the measured concentrations with the GVP as shown in Figure 3.16. During the third response the P concentration is still climbing and does not show a decrease in incline. These concentrations are high compared to the dutch standard of 0.15mg/l [37]. To reduce the concentrations in tile drainage at Hogervorst to the commonly used Dutch standard of 0.15 mg/l, a high efficiency of 97 % is required when 5 mgPtot/l is used.
The bottom graph shows the phosphate load which was calculated by:

$$L_{Pm} = \sum_{n=1}^{n} (Q_{(\Delta t)} * C_{(\Delta t)}) * \Delta t \tag{3.1}$$

The P-load was than extrapolated for the entire year:

$$\left(\frac{V_{tm}}{V_{Pm}} * L_{Pm}\right) * \frac{Prec._t}{Prec._{tm}} \tag{3.2}$$

Q = tile drain discharge.
C = total phosphate concentration.
L_{Pm} = phosphate load during the measured concentration and discharge of the tile drain
V_{tm} = total measured volume through the tile drain between December 2020 and August 2021
V_{Pm} = measured volume through the tile drain while phosphate was measured (2021-05-07 to 2021-05-15)
$Prec._t$ = average yearly precipitation in the Netherlands (850mm)
$Prec._{tm}$ = total precipitation between dec. 2020 to aug. 2021 (500 mm)

Δ t is the time step between a discharge measurement. Since the P concentrations had a lower frequency than the Q measurements the P measurements joint to the Q measurements with their nearest value.

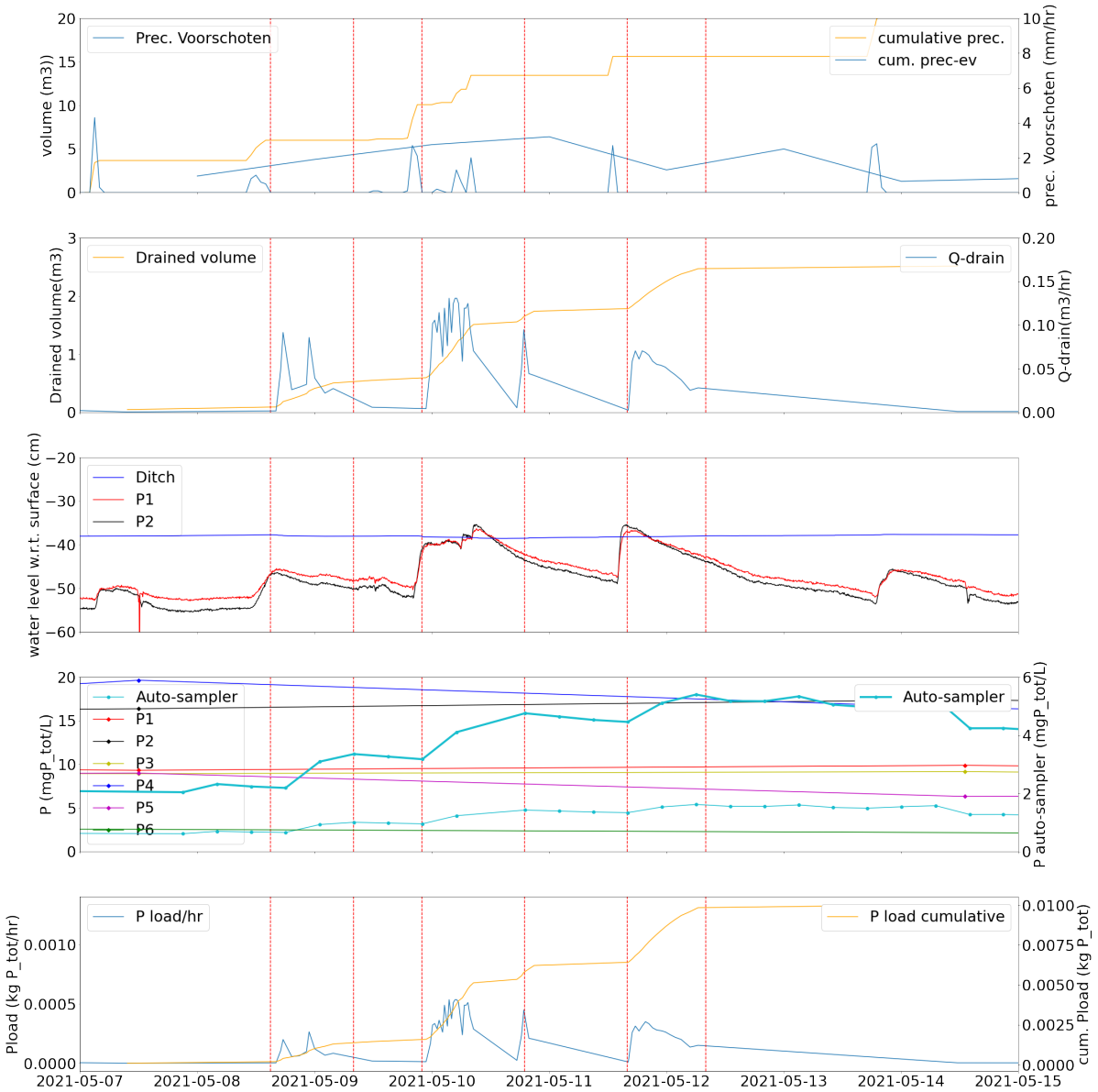

Figure 3.17: This figure shows the three drain responses during which the phosphorus concentration was measured at the drain outflow. The duration of each drain response is indicated by vertical red dashed lines. Five sub-plots are used to interpret the results, showing the event, drain response, the water level, phosphorus concentration and phosphorus load. Since the observed phosphorus concentration at the drain outflow is important, an additional y-axis on the right side of the fourth diagram shows the increase in phosphorus concentration in more detail.

4

Discussion

First, the phosphate concentrations found at Hogervorst are put into perspective based on the literature (see section 4.1). Secondly, the dynamic behaviour of the system and the connection to C-Q is discussed in section 4.2. Third, the mass balance under dry summer and wet winter conditions is discussed in section 4.3. Fourthly, the transport and oxidation times are discussed in section 4.4. Finally, the limitations of the research are presented.

4.1. High Phosphate Concentrations and Leaching Loads at Hogervorst and the 'Bollenstreek'

To put the found results of the phosphate concentration in the soil and at the outflow of the tile drain at Hogervorst in perspective, the values were compared to other locations. First, the phosphate in the soil, the soil's sorption capacity (Fe + Al concentration), and the soil's phosphate saturation degree (PSD)[1], which is a quantification of the P leaching potential, will be compared to two plots (HUB and JUB) in close proximity to Hogervorst and in one other plot located in the east of the Netherlands (Huppel). All values can be found in Table 4.1. The exact locations of HUB and JUB can be found in Appendix I. The data from HUB and JUB were extracted in this study in the same way as at Hogervorst. Huppel's data comes from the study Barcala *et al.* [22].

Table 4.1: Soil and sediment results: number of samples (n), average TP, oxalate extractions, and Phosposphorus saturation degree (PSD) in the "Bollenstreek" (two other locations and Hogervorst) and at Huppel.

	n	TP [mg/kg]	Fe_{ox}+Al_{ox} [mg/kg]	Molar PSD
Hogervorst				
Depth 0 – 10 cm	4	381 (348-465)	395 (282-410)	0.49 (0.45 – 0.54)
Depth 40 – 70 cm	6	192 (118-268)	165 (99-209)	0.33 (0.12 – 0.48)
Depth 150 cm (clay)	2	1355	4239 (3079 – 5400)	0.41 (0.38 – 0.44)
JUB				
Depth 0 – 10 cm	1	406	730	0.17
Depth 40 – 70 cm	1	152	320	0.17
Depth 150 – 200 cm (clay)	2	737 (791-683)	4287 (3969-4805)	0.13 (0.13-0.13)
HUB				
Depth 0 – 10 cm	1	609	675	0.57
Depth 40– 70 cm	1	257	373	0.29
Huppel				
Depth 0 – 10 cm	24	601	400 (251-732)	0.26 (0.19-0.33)
Depth 40– 50 cm	24	165	426 (252 – 943)	0.06 (0.01-0.11)
Depth 70 – 80 cm	4	113	228 (147-320)	0.03 (0.01 – 0.05)

It is evident that the TP content of the sandy soil in the top 10 cm at Hogervorst is lower than of the soil in HUB and Huppel, but comparable to the TP content in JUB. Moreover, the TP at Hogervorst and JUB was at

[1] PSD is the molar ratio of P : Fe + Al in soil which quantifies the P leaching potential [38]

the lower end of the found content in non-calcareous sandy soils [2] in the Netherlands, which normally ranges between 280 and 500 mg/kg [39]. The average TP load in the top 30 cm is 1121 kg/ha/y[3] at Hogervorst, which is lower than 2500 kg/ha/y in the Huppel catchment and the 2050 kg/ha/y in the average agricultural soils in the Netherlands [22, 40]. On the other hand, the TP content from the two samples taken 150 cm below the surface at the top of the clay/debris layer had much higher content exceeding the previous references. In general, it can be seen that the all plots in the Bollenstreek (JUB, HUB and Hogervorst) are characterised by a decrease in TP content to -150 cm. However, at Hogervorst very high TP concentrations were found at -150 cm below the surface from extracted clay. At JUB, clay was also found, but it is not known whether these are just clay patches. The decrease in TP content with depth was also found in the plot in the east of the Netherlands. More importantly, Mol *et al.* [23] found a median value of 654 mg P/kg in the topsoil and 44 mg P/kg in the subsoil (below 60 cm) in the sandy soils throughout the Netherlands. The decrease observed at Hogervorst was thus at the lower end of the average phosphate decrease in the Netherlands since the concentrations in the top (10 cm) are relatively low and at a depth between 40 to 70 cm relatively high. The topsoil thus contains relatively low phosphate concentrations, the subsoil high values and the extracted clay in the clay/debris layer very high phosphate concentrations.

Although the sandy topsoil contains relatively low P concentrations compared to other agricultural land with sandy soils in the Netherlands, the Pw is still classified as high. Since the Dutch Fertilization Grassland and Plants Commitee's for sandy soils classifies Pw values above 9.8 mg/kg for sandy soils as high [41]. Groenendijk and Kroes [42] Calculated it would take about 30 years for top soils with Pw of 10 mg/kg to reach low values (below 4.4 mg/kg). The Pw measured at Hogervost ranged between 9 and 14 (see Table 3.5).

The critical PSD value for non-calcareous sandy soils is 0.25 [43], which is exceeded at all measured sites in the Bollenstreek and at Huppel. At Hogervorst, the values for the PSD of the clay were the same as in the overlying sand layer, as both P and Fe+Al were much higher in the clay layer. This also appeared to be the case at the clay found at JUB around one to three meter below the surface. The HUB measurements did not include clay measurements. At Huppel, the PSD value at the bottom was much lower than at the top, which was not the case at Hogervorst, where phosphate concentrations decreased less over depth. Therefore, the subsoil at Hogervrost is more saturated with P, which increases the potential for P leaching. As the tile drains causing quick transport are at - 80 cm, this is even more problematic.

Groundwater (GW) concentrations far exceed the value that King *et al.* [17] often considers problematic for concentrations in surface waters: 0.02 mg/l. It also exceeds the Dutch standard of 0.15 mg/l, which is often used [37]. A low P/Fe ratio is important for co-precipitation or adsorption of phosphate on iron hydroxides. Critical values for P release from sediments during summer anoxia are 0.12 for lakes and 0.4 for lowland rivers [44], [32]. In groundwater samples from Huppel and fields in the Bollenstreek, the P/Fe ratio is high. Especially at JUB and Hogervorst very high P/Fe ratios were found (see Figure 4.1b). This means that the iron concentrations are too low to bind all the phosphate (see Appendix H).

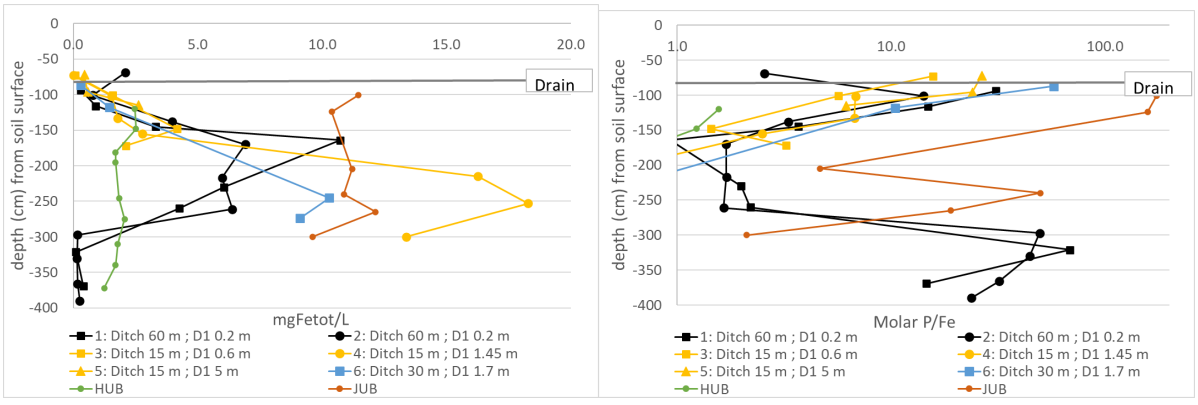

(a) Fetot

(b) molair P/Fe ratio at Hogervorst, HUB and JUB

Figure 4.1: TP and Fe_{tot} at Hogervorst, HUB and JUB

[2] At Hogervorst, calcium concentrations between 0.13 and 0.15 % were found in the top 10 cm. Mol *et al.* [23] has shown that in the Netherlands the calcium concentration in the top 20 cm of sandy soils is 0.07 % in the 25th percentile (P25) and 0.3 % in the 75 th percentile (P75). The sandy soil in Hogevorst is therefore not calcium-free, but lies between P25 and P75.

[3] Assuming: soil 1330 kg/m^3 and using the average TP concentration of the measurements at 0-10 and 40-70 cm (281 mg/kg)

At Hogervorst, the TP concentrations in the GW are an order of magnitude higher than in the field in Huppel, where concentrations around 0.1 mg/l were found. As the clay layer contains much higher phosphate concentrations, this could have an influence. However, high P concentrations in GW were also found in Hub and Jub, although it was not clear whether both sites contained large amounts of clay below the subsoil (-60 cm). The tile drain concentrations measured at Voorhout, which was also a field in the Bollensteek [1], also contained high P concentrations at the outlet, as will be discussed (see Table 4.2). Therefore, the high P concentrations in the subsoil don't need to be the cause of the clay.

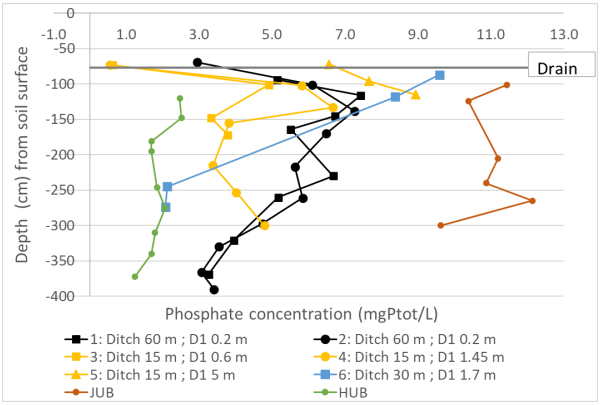

Figure 4.2: PT

The interaction of the clay layer with the subsoil and topsoil also depends on the amount of seepage. The water level area at Hogervorst is maintained between NAP - 0.12 cm and -0.27 cm. East of Hogervorst, the water level is maintained at NAP -0.61 to -0.64. Since Hogervorst is just below sea level and the area east of Hogervorst has a water level half a metre lower, this is the first indication of low seepage. Secondly, groundwater profiles at Hogervorst contained low Cl concentrations (see Figure 4.3). Five of the six measurements were below 70 mg/L (safe for all plants) [45]. Measurement W6 showed concentrations up to 120 to -3.5 m, where a concentration of 40 mg/l was found. It is not known why the concentrations of W6 were higher in the top but these measurements show that CL concentrations are relatively low. So there does not seem to be much infiltration with high cl concentrations. However, infiltration with lower cl concentrations could still occur. But, infiltration often has higher concentrations (600 to 1100 mg/l) [46]. Furthermore, the case study of Rijnland in Coa [47], showed that higher Cl concentrations of 2500 to 5000 mg/l were found in deeper soil layers at 45 metres below the surface at Hogervorst. Thirdly, the LHM model indicates a leakage of -0.25 mm/day at Hogervorst. However, the LHM model included a large grid size of 250 m and an average infiltration value from 2011 to 2017, so seasonal variations were not considered. The MF6 wet winter model showed an increase in groundwater level and drain discharge of 3 cm and 0.12 m^3/d, respectively, in the sensitivity analysis when the maximum head below the clay/debris layer was increased to NAP 0 m (see Figure 3.11). In the dry summer model, the maximum groundwater level was increased by 10 cm (see Figure 3.7). However, the increase in groundwater level and discharge also depends on the conductivity of the clay/debris layer, for which a constant conductivity was used. While the actual clay/debris layer has greater heterogeneity, there could be patches of clay that result in some areas having much higher conductivity in practice. This would result in a greater increase in groundwater level and discharge, if there was indeed a greater head beneath the clay/debris layer. The tile drains themselves did not cause upward flow in either dry summer or wet winter (see Figure 3.9, Figure 3.10). Based on the arguments given, it is suspected that the transport path to the ditches comes from above. However, the P concentrations in the topsoil were similar to those in Huppel and were on the lower side of the non-calcareous sandy soils in the Netherlands. It is therefore unclear why the phosphate concentrations in the subsoil were relatively high. It could be that the soil at Hogervorst is less able to retain phosphate compared to other fields.

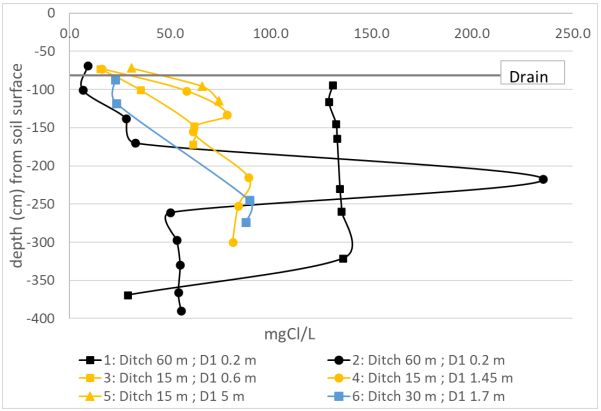

Figure 4.3: Chloride. The results clearly show a lower chloride concentration from the second profile made after the rain event. The other profiles show similar values as the second profile.

Table 4.2 shows a overview of hydrological and chemical data at the tile drain outflow found at Hogervorst and other studies. The table shows that Hogervorst contained high concentrations compared to Hupsel [19]. This was a tile drained field in the east of the Netherlands, where transport through the tile drain as well as through the soil was measured. King *et al.* [17] showed the wide ranges at which phosphate is found. Hogervost is at the upper end of these findings. The high concentrations at Hogervorst correspond with the

Table 4.2: Data overview of tile drain outflow at Hogervost and other studies. $_1$ = In the Hupsel catchment area, 3 tile drains captured 0.283 m^3. An estimate for 10 tile drains for one Ha like Hogervorst was made by multiplying by 10/3. $_2$ = Average of 76 measurements, values range from 0.8 to 0.107 with a 95 % confidence interval. $_3$ = The samples were not filtered

Study	Location	Ratio drain : soil %	Drained P concentration and load	
			Mg/l	Kg/ha/y
Hogervorst	Bollenstreek	70	2 - 6	5.5
King *et al.* [17]	Amerika , EU		< 0.01 to > 8	0.4 - 1.6
Huppel [22]	Gelderland	-	-	0.04
Hupsel [19]	Gelderland	80 (0-95)	0.091	0.94 $_1$
King *et al.* [21]	Big Walnut Ohio	41	-	-
Buijert *et al.* [1]	Bollenstreek	-	4 - 10 $_2$	-

high P concentrations in groundwater and subsoil. On another field in the Bollenstreek area, high phosphate concentrations were also found at the tile drain outflow, between 4 and 10 mg/l [1]. Note, however, that these samples were not filtered. The P load at Hogervorst is an order of magnitude higher compared to other studies found by King *et al.* [17]. The estimated load from Hupple, based on the lower groundwater concentrations, is also much lower. This indicates that phosphate leaching at Bollenstreek is relatively large. The proportion of rainwater transported into the drain is comparable to that of Hupsel. Another study in Ohio found that a lower percentage was transported through the tile drains [21]. There are many different factors that influence runoff through the drainage. However, at the case study in Ohio, the drainage systems were traditional tile drained systems that were above the water level, which could mean that the storage capacity for this field was larger.

4.2. Dynamic Behaviour of the System and the Link to the C-Q Relation

Besides seasonal fluctuations between summer and winter conditions a fastly changing groundwater level was observed Figure 3.1. The box-plots showing the groundwater level observations 60 m from the ditch in summer and winter have a large number of outlines (see Figure 3.13). Also the drain discharge in summer and winter conditions show these outlines. These high groundwater levels and discharges shown as outlines in the box plots are no measurement faults but were caused by one large or multiple rain showers quickly after another. When precipitation stopped, the groundwater level decreases to a level below the west ditch. The speed at which the groundwater level decreases after the rain shower depends on the groundwater level after the rain shower. The higher the groundwater level the faster it decreases. Especially when the groundwater level exceeds the west ditch which activated the tile drain a fast decrease of the groundwater level was observed Appendix B. This could be due to the activated tile drain and the greater difference in water level between the field and the ditch which causes greater runoff from the field into the ditch. The consequence of this is that a greater amount of precipitation is required in a shorter period of time to achieve a similar increase in groundwater level. This indicates that the regulated tile drains played an important role in the groundwater level management and water-transport during wet conditions where the groundwater level exceeds the ditch as should be the case [2]. That there was indeed tile drain discharge when the groundwater level exceeded the west ditch was also confirmed by comparing the difference between ditch and groundwater level to the drain response (subsection 3.1.3). This calculation showed that 100 percent of the time when the groundwater level 60 meter from the west ditch was exceeded there was tile drain discharge Table 3.1. However, this data also showed that there often was a response when the groundwater level 60 meter from the ditch was not exceeded (b = 20 % Table 3.1). Indicating that the groundwater level close to the ditch exceeds the ditch water level more often.

Rozemeijer and Broers [12] found that in Noord-Braband (province in the Netherlands) the poor chemical status of upper and shallow groundwater leads to exceedance of quality standards in receiving surface waters, especially during quick flow periods. However, the contribution of the different flow paths was unknown and depends on the local hydrological situation. This study looked into a local hydrological situation at Hogervorst. Which gave more insights into the activation of various flow paths. Overland flow on flat sandy soils with a high permeability are unlikely. Therefore, the activation of a flow path in the Bollenstreek depend on the ditch levels, the type of tile drainage and the groundwater levels. However, the water table itself depends on storage capacity, ditch levels, tile drain type, effective precipitation and seepage. This dependence on so many different factors probably explains the large fluctuations in the ratio between drain discharge and rainfall. At Hogervorst, this ratio varied between 0 and 83 %. King *et al.* [21] showed fluctuations between 0 and 100%. Since the tile drain discharge is directly dependent on the groundwater level, it was very effective to measure the change in groundwater level and tile drain discharge to find a relationship between groundwater

level and tile drain discharge. The rd tile drain should respond when the groundwater level exceeds the water level of the ditch [2]. Groundwater measurements are therefore effective in assessing the hydrological system of a rd tile drained field.

The observations showed a higher percentage transported by tile drains in winter than in summer, which is probably due to the additional evaporation. Which is also confirmed by the model and the groundwater level observations which showed a greater storage capacity in summer. However, the large fluctuations during the season show that this is only part of the explanation and that the system is more complex. It was found that not only the fluctuations of the groundwater level over time are important, but also the spatial distribution of the groundwater level. The hydrological model has shown that when the effective rainfall amount is increased, a larger area exceeds the drain head and discharges into the western ditch via the tile drain (see Figure 3.13). Furthermore, the tracer experiment showed that under the conditions of the experiment, only the first 15 metres of the field were connected to the tile drain outlet. The hydrological model (see Figure 3.13) and the measured groundwater level distribution (see Figure 3.7) also showed a decreasing groundwater table towards the east during dry conditions. So the distance between the groundwater level and the water level of the West Ditch is therefore greater in the east before a precipitation event occurs. Therefore, it is also likely that the area near the West Ditch reacts earlier and more frequently. Furthermore, the hydrological model showed that at the layer below the clay/debris the field drains to the east in wet winter and dry summer. It also showed that increasing the water level in the eastern ditch had less effect on the discharge below the clay/debris than on the upper layer. Therefore, the discharge below the clay/debris layer proved to be more consistent. Based on the high-frequency measuring data, tracer experiment and two steady-state models an expectation of the change in groundwater level and flow paths from a dry to wet situation was visualised in a conceptual model (see Figure 4.4). Which shows the complexity of a local hydrological situation in a tile drained agricultural field. t0 shows the dry situation and t3 the situation after one large or multiple rain showers within 1 to 15 days. In the actual field the groundwater level dropped between the rain showers and t3 is only reached in very wet conditions. The conceptual model visualized this by the yellow (t1), orange(t2) and red (t3) colors inside the tile drain. In the dry situations where the groundwater table not exceeded the ditch, ditch water infiltrated the drain which is indicated with the green arrow t0.

Instead of using steady-state models an effort could be made to construct a transient model. However, by using a steady-state model it was also possible to model a situation which corresponded with the measured groundwater level and discharge in a wet period. Using a transient model would increase the complexity and by adding a storage factor the models risk is likely to increase [48]. Furthermore, the porosity can change over time [49]. However, in the sandy soil in the Bollenstreek this change is probably less compared to bedrock aquifers. Estimations of the porosity can be based on literature values [50]. However, estimations based on literature were found to be 50 to 90 % greater than the field calibrated value and is highly dependent on the chosen model and is best obtained by laboratory or field tracer tests [51]. To gain an idea of the hydrological situation it was therefore decided that two steady state models combined with a sensitivity analysis and calibrated to actual wet and dry conditions was sufficient.

The observed phosphate concentrations at the tile drain outlet increased during the measured response. This indicates higher phosphate concentrations at the drain outflow after a long wet situation with large discharged volumes. Based on the studied hydrological system and the phosphate distribution in the field, it was found that a more active field near the drain and ditch could be an important factor, as indicated in Figure 4.5. First, the measured concentrations of dissolved P in the field showed higher P concentrations further away from the tile drain and the western ditch. Second, the model showed that the area contributing to the tile drain outflow increased with rainfall duration (see Figure 4.4). Third, actual measurements of groundwater level and discharge indicated that storage capacity increased with distance from the ditch (see Figure 3.7 and subsection 3.1.3). Fourth, the tracer experiment showed that during the experiment there was only a connection between the first 5 to 15 metres of the field (see subsection 3.1.5). So, all in all, the argument is that a small area near the ditch is more active, but leaches relatively low concentrations of P into the ditch. However, if there is a long wet period with several rain showers, a larger area of the field is activated and leaches higher P concentrations into the ditch via the drain. For a similar tile drain discharge the same phosphate concentrations are expected. The results from the groundwater extractions at 60 meter from the ditch were taken before and after a large rain event (see Appendix G). This data showed that the phosphate concentration in the groundwater was the same after the precipitation event. Which indicates that phosphate stored in the soil functions as a phosphate buffer and releases phosphate to the diluted groundwater until the same concentration as before the rain event is found. Also the PSD showed high values in the top and subsoil (see Table 4.1). However, how many rain events are required before the P reserves are used is not known [52].

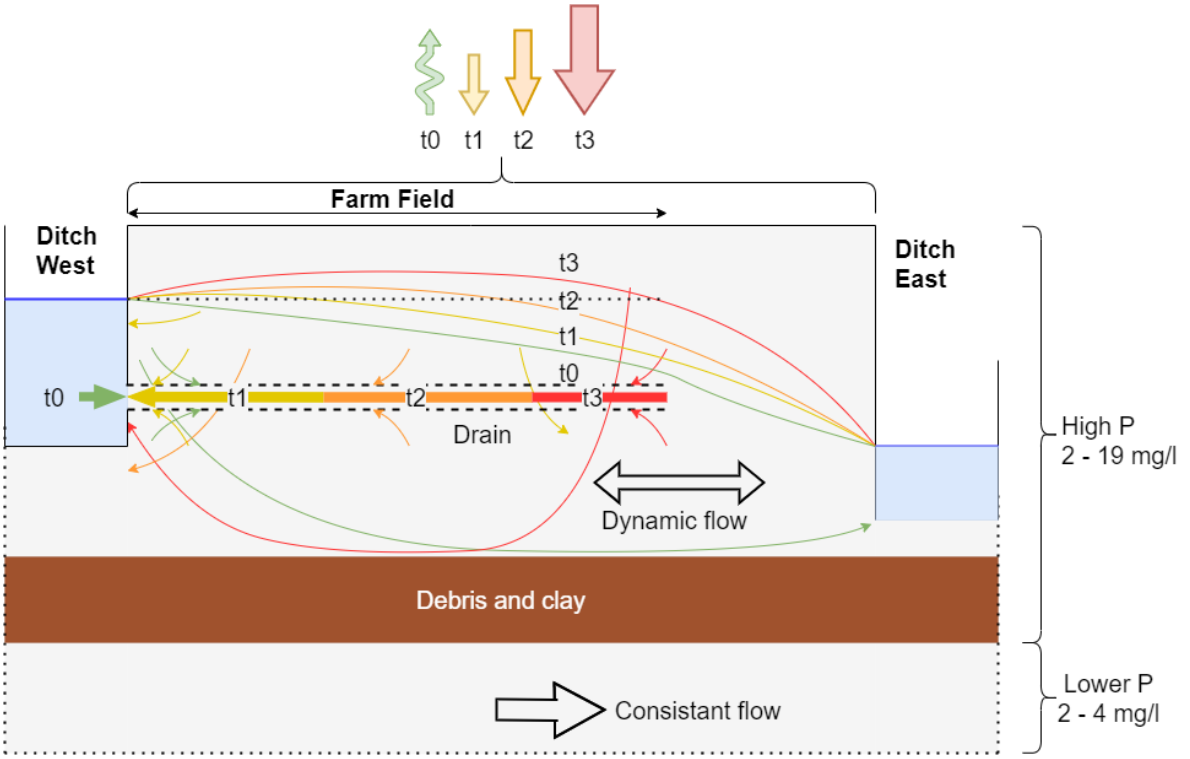

Figure 4.4: Consistent and dynamic flow of the field during one or more large rain showers in quick succession. t0 shows the situation before the start of a rain period. t3 shows the situation after a large amount of rain has entered the field. t3 is only reached when the amount of rain is large enough. When the rainfall decreases, the water table drops until the situation at t0 is reached again, which takes a few days. Note that in situations t1 and t2, the entire tile drain does not discharge water into the western ditch. Only when t3 is reached does the entire tile drain discharges into the western ditch.

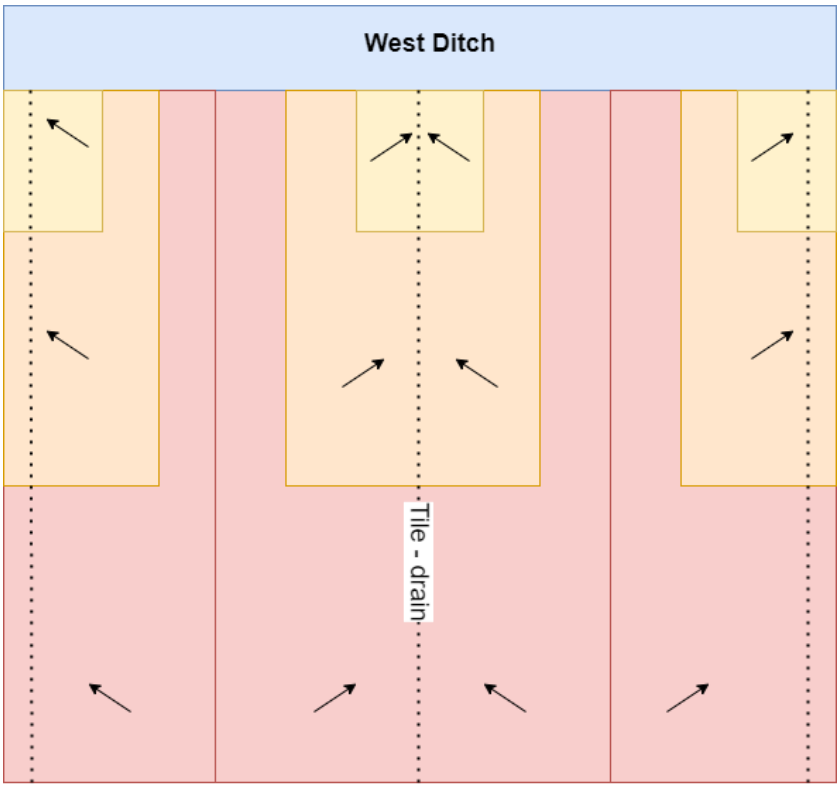

Figure 4.5: Top view of the conceptual model. Illustration of how the zone of influence is expected to increase with tile drained volume for one large or multiple tile drain responses in rapid succession. The zone of influence increases as the groundwater level exceeding the western ditch water level shifts east. The colours represent the t1 (yellow), t2 (orange) and t3 (red) situation as shown inFigure 4.4.

4.3. Wet Winter and Dry Summer Conditions

The results for the flow paths above the clay/debris from the two final models are shown in Table 4.3. Under winter conditions, water originates from rainfall and flows into the ditches to the west and east. In the west, the rainwater flows through the tile drains (25 m^3/d) and the soil (11 m^3/d). Most of the rainwater flows into the east Ditch (66 m^3/d). In dry summer, the water flows from the west ditch, where 88 % is evaporated and 22 % flows through the Hogervorst field and drains into the East field. This water balance showed that the largest amounts of water above the clay/debris layer are transported to the east. In dry summer conditions, this transport could be minimized by raising the weir on the neighboring property to the east of Hogervorst. According to the model, an elevation of 20 cm was sufficient to stop the transport to the east. Since most of the rainwater seeps to the west through the tile drains, the ICS filters are an effective measure. However, 29 % is still transported into the ditch via groundwater. Therefore, the construction of a buffer zone in combination with the ICS filter is the way to reduce most of the phosphate leaching into the western ditch. The wet winter model was a good representation of the average percentage of effective precipitation transported through the tile drain. 32 % of the precipitation was discharged via the tile drain during the period 2020-12-08 to 2021-03-16, while the model indicated a percentage of 25 %.

Table 4.3: Wet Winter and Dry summer mass balance. *: Discharge from the entire field(100 * 125 m).

Conditions	Effective precipitation	East boundary (No Drain, Soil)		West Ditch (tile drain)		West Ditch (soil)	
(-)	Discharge* (m3/day), %	origin	Discharge (m3/day), %	origin	Discharge (m3/day), %	origin	Discharge (m3/day), %
Wet Winter	+ 97, 100	Rain	-64, 66	Rain	-24, 25	Rain	-10, 10
Dry summer	- 42,	West Ditch	-11, 22	West Ditch	+31	West Ditch	+21

For the calibration of the winter model, $k_h k_v$ and the drain conductance were used. Where the ratio between $k_h k_v$ was fixed by an anisotropy ratio of 10. El-Rawy *et al.* [53] used the same ratio for the model calibration. The analysed groundwater level measurements showed a 10-day period during the wet winter conditions with a continuous discharge. This was considered to be a sufficient period to validate the wet winter model. With the two calibration parameters, a combination was found that matched the tile drain discharge and groundwater level observations.

The dry summer model used the same $k_h k_v$ values as the wet winter model. This left the drain conductance as the only calibration parameter for the measured groundwater level at three locations. The usable time frame for the summer groundwater measurements was a period of 10 days (6 to 17 June 2021), when the western ditch was set to its summer level and no precipitation fell. The fit for these conditions agreed with the measured groundwater level at 15 and 30 metres from the West ditch. However, the groundwater level 60 metres from the western ditch differed from the measured groundwater level by 8 cm. It was not known whether the neighbouring property had raised its weirs during the used 10 day calibration period (6 to 17 June 2021). In dry conditions the farmer sometimes raised the weirs to increase the water level in its field, which was not documented. The model showed that when raising the eastern groundwater level by 20 cm the flow to the east in the top 1.5 meter of the soil was reduced to almost zero. Furthermore, the modelled groundwater level with a 20 cm higher eastern head agreed with all three measurement locations (see Figure 3.7). Since, it was unknown what the actual head in the east ditch was during 6 to 17 June 2021 it increased the uncertainty of the model during summer. However, in winter the east ditch was always in open connection with the main ditch. Therefor this uncertainty is not present during winter conditions. In addition, the east CHD boundary was set at the boundary for the neighbors field. Thereby an assumptions was made that the groundwater level was the same over the full width. The disadvantage of this simplification is that there was no difference in groundwater level between the middle of the field and the side ditches, which also affects the mass balance. However, this simplification made it easier to study the effects of changing the head in the east. This is because it depends on a single variable, whereas constructing a model with side ditches requires the depth of the ditch, the conductivity of the ditch and the levels of the weirs.

The boundary condition in the west was set to the average measured water level in the ditch. Which seemed to be a proper assumption since the water level in the ditch only had small fluctuations compared to the groundwater levels in the field. The north and south boundary were set as no flow boundaries. Since the tile drains function as separate ditches the effect of these boundaries is assumed to be limited. A larger assumption was made by constructing CHB for the east and west over the full depth of the model. To limit the effect of these boundary conditions at the deeper groundwater layers a larger groundwater model could be

constructed. By increasing the size of the model the boundary conditions have a lower influence on the field. Ond [54] showed that when using three times the leakage factor the boundary conditions almost have no influence anymore. At Hogervorst using a resistance (C) of 75 for the clay/debris layer and a 20 meter deep sand layer showed a area of one by one kilometer is required. However, at Hogervorst the problem stays that the conductance of the clay/debris layer below the field is unknown. Therefor it is not possible to know to which extent seepage is blocked. Furthermore, section 4.2 explained why large quantities of seepage are unlikely. Moreover, there was a lot of information about the distribution of the groundwater level, the water level in the ditch,tile drain discharge. Therefor it was decided to limit the size of the model and calibrate the model to the well known groundwater levels and tile drain discharge. The flow paths below the clay and debris layer are therefor less reliable. However, these were considered of lower importance since the phosphate concentrations were almost 10 times lower compared to the top (see Figure 3.16).

The model used pointwater heads and did not take into account the effect of density flow. Figure 4.3 shows the Cl concentrations in the field. These concentrations are between 50 and 150 mg/l. Calculating the density from a CL concentration of 150 mg/l gives 1000.2 kg/m3 [55, 56]. Calculating the head difference between freshwater and groundwater with 150 mgCL/l gives a head difference of 0.02 cm [57]. Since the chloride concentrations are low, the effect of the density flow was very small.

4.4. Transport vs Oxidation Times

Test 3 with the second tracer experiment showed that the transport times from the shell layer 5 metres from the ditch are about half an hour when the (ground)water level difference between the ditch and the field is about 13 cm. However, there are many different transport times and the time from a raindrop through the unsaturated and saturated zone into the ditch is longer.

Based on the wet winter model, a calculation of the transport time from the maximum groundwater level (60 metres from the western ditch) to the east and west was made. This resulted in a transport time of 30 days to the eastern ditch and a shorter transport time of 23 days to the western ditch through the tile drains. However, the calculation was based on the time to discharge the old groundwater which depended on the water levels. In the west, the distance between the west ditch water level and the location of the tile drain was used. As the MF6 model showed that mainly groundwater was extracted from above, this seemed to be a reasonable assumption (see Figure 3.9). In the east, the distance between the surface and the clay/debris layer was used. Therefore, a stronger horizontal flow to the eastern ditch would result in shorter transport times.

A field study at Hogervorst showed an oxidation time between 14 and 21 days, reducing P by about 30 per cent (see Appendix H). However, the oxidation rate and maximum precipitation depend on the iron and phosphate concentrations, which varied greatly in the field. Furthermore, PH and temperature are also not constant values in the field (see Appendix G). Nevertheless, the calculated transport time to the east and west at 60 meters from the west ditch exceed the oxidation time, which has a positive effect on P precipitation. However, at shorter distances the transit time does not exceed the oxidation time, which increases the risk of P leaching. In rd systems, shorter distances between the location of the tile drain and the water level in the ditch seem to reduce the transport time. When precipitation enters the field and the water level in the connected ditch is not exceeded, there is no flow to the ditch and the water is stored. Only when the groundwater level rises above the threshold can the water flow through the tile drain into the ditch. Therefor reducing the distance between the water level in the ditch and the location of the tile drain seem to reduce the transport time. Reducing the distance between the water level in the ditch and the location of the tile drain therefore seems to reduce the transport time.

4.5. Limitations

An indication for seepage was found by using the: LHM 4.1 model, Hogervorst model calibrations, observed (ground)water quality measurements and the debris/clay layer. However the LHM 4.1 model showed average values from 2011 to 2017 with a coarse 250 m grid while the field is only 100 by 100 meter. Furthermore, these measurements could not be used to determine the variability between wet winter and dry summer conditions. Actual head measurements below the debris/clay layer were not measured. Observations from the DINOloket were found at 18 meter deep a few kilometers from Hogervorst which was considered too deep and far away. Since, DINOloket showed a clay layer at 18 meter deep and the location was situated in a different 'peilvak'. Furthermore, the conductivity of the clay/debris layer and its heterogeneity was unknown.

The steady state model simplified the actual situation considerably. Here average input (effective rainfall,west ditch water level) and calibration (Qdrain, groundwater level) values were used. While in reality these values largely fluctuate over time, especially during wet winter conditions with heavy rainfall. To get a first indication on the flow paths in the system when the water level increased above the ditch level the steady state model is an effective tool. However, to get a deeper understanding of the flow paths including the actual dynamic behaviour, a transient model might better represent reality. During dry summer conditions the situation is more constant. Therefore the difference between a steady state and transient model is probably less significant.

The boundary condition in the east uses a head across the entire width of the field. In reality, this head is not consistent. This could affect the mass balance and the modelled water level distribution. However, in wet winter conditions the side ditches were in open connection with the main ditch to the east, whose level was known. And the field consists of a sandy soil with a high conductivity, which limits groundwater fluctuations between the ditch and the field. For the dry summer model, it was not known whether the weirs in the side ditches were set to raise the ditch level.

The conductance between the sand and debris/clay layer differs by a factor of 100. Little information was known about the conductance of the clay/debris layer in particular. The heterogeneity of this soil could be very high due to the combination of clay and debris. This made it difficult to estimate the effects of the clay/debris layer on infiltration from the deeper layer.

In the dry summer conditions there was no discharge calibration since drain water infiltrates the system which could not be measured.

The weather station data from KNMI in Voorschoten was used to study the discharge/effective rainfall correlation and recharge values in dry summer and wet winter conditions. However, the station is located 13 km from Hogervorst and could therefore deviate from the actual weather conditions.

The actual evaporation in the dry summer conditions was estimated by reference evapotranspiration from KNMI. The model did not include an extensive calculation for the unsaturated zone.

5

Conclusions

The purpose of this study is to gain insights into water transport dynamics to support the understanding of hydrochemical processes involved in phosphate leaching from agricultural fields and to implement effective mitigation measures. This case study is a step forward in understanding the concentration-discharge relations that will allow to determine effective mitigation measures to improve the water quality in the region. For this purpose, high-frequency measurements were extracted and an MF6 model was created for the tile drained field of Hogervorst. Where the distribution of the groundwater level, drain discharge, soil characteristics (physical and chemical) and ground water / ditch water characteristics were monitored in space and time.

An efficiency of 97 % is required to reduce the P concentration by tile drainage to the Dutch standard
The groundwater concentrations, tile drain outflow concentrations and P load (5.5 kg/ha/year) from the tile drains, were an order of magnitude higher compared to field studies outside the Bollenstreek. At other locations in the Bollenstreek, similar concentrations were found in the field and at the outflow of the tile drain. Since this study has shown that 70 % of the total flow to the west at Hogervorst is transported by tile drains, it becomes clear how important it is to find effective measures to contain phosphate leaching in the Bollenstreek. However, local hydrological conditions should be taken into account. In this study, the other water level area to the east was found to play an important role.

Most of the phosphate leaching into the drain is expected to originate from the top soil
Two possible sources of phosphate were found in the field. A high phosphate concentration at the surface and the clay/debris layer at a depth of 1.5 m below the surface. The soil at three measured sites in the Bollenstreek had a relatively low amount of P at the surface and a high P concentration at 0.7 m depth compared to non-calcareous sandy soils in the Netherlands. Since the depth of the tile drain at Hogervorst is 0.8 m below the surface, there is an increased risk of leaching of high P concentrations. To determine the effect of the clay/debris layer on P leaching, the boundaries of the water level areas, the effect of the tile drains, groundwater level compared to mean sea level, the LHM4.1 model, CL concentrations and soil properties were considered. Each of these factors indicates that large amounts of seepage are unlikely. Therefore, the main source of phosphate is expected to come from above. However, if seepage or upward flow (due to drain response) is not negligible, the clay/debris layer could be an important source of phosphate.

Longer transport times to the east, but large flows and high phosphate concentrations
The study showed that the water flows towards the east in both dry and wet conditions. In dry summer, a 0.5 metre water level difference between the east and west ditches transports 22 % of the infiltrated water from the west to the east ditch and the other 88 % evaporates. During wet winter conditions, the groundwater level increases by precipitation and 66 % of the outflow leaches into the eastern field. Since ditch and rainwater contain more oxygen than groundwater, iron oxidation can occur if the transport times exceed the oxidation time, which was the case at 60 meter flow the west ditch. However, as the phosphate concentrations in the field are high, between 2 and 10 mgPtot/l, only part of the phosphate can be oxidised. The laboratory analysis showed a maximum phosphate reduction of 28 %. To mitigate leaching the model showed that increasing the east groundwater level by 10 to 20 centimetre in dry summer conditions is enough to stop leaching to the neighbour. However, as infiltration exceeds evaporation during drought, the Eastern flow increases the risk of phosphate leaching.

Peak flows to the west during rain showers with short transport times through the tile drains.
Leaching into the West ditch only occurs when the groundwater level exceeds the West ditch. In the winter observations (2020-12-08 to 2021-03-16), 32 % of the rainfall was leached through the tile drains and 68 % took other flow paths, which is close to the wet winter model where 25 % was transported through the tile drains. In addition, only 10 % of the precipitation leaches through the soil into the western ditch (the other 65 % to the east). At 60 meter from the west ditch the transport time to the west was shorter compared to the east. Still the iron oxidation time was exceeded. However, when the distance to the ditch and tile drain was reduced, these transport times became shorter than the iron oxidation time.

Larger tile drain outflow volumes increase the leaching of phosphate.
Larger discharged volumes caused by heavy rainfall increased the phosphate concentration at the tile drain outflow. There are two possible hydrological reasons for this. First, the distance perpendicular to the tile drain contributing to leaching increased. Second, the groundwater level exceeding the western ditch water level shifts to the east when the field becomes wetter. Therefore, the area which discharges to the west ditch increases. Only during very wet conditions the entire drain length is discharging into the west ditch. As the phosphate concentration increased with increasing distance from the drain and ditch, these hydrological effects play an important role.

6

Recommendations

Further study
By examining the chemical characterises of both the field and the outlet of the tile drain in combination with the hydrological situation, a clue was found as to why the phosphate concentration at the tile drain outlet changed. This suggests that studying field and outlet concentrations could help improve knowledge of the relationships between phosphate concentrations and tile drain discharge. This approach could also be suitable for studying other concentration-discharge relationships and is therefore recommended.
Study the effect of the hydrological system on the P response on other agricultural land. This study focused on Hogervorst, where a large difference in groundwater level was found between the east and the west. Additional research is needed to know how the field would respond if this is not the case. By adjusting the current MF6 model of Hogervorst, a first indication is obtained. Measuring the P concentration at different locations of another field in combination with an analysed hydrological situation with a constant water table around the field would provide additional information. Understanding the water flow is key to understanding phosphate leaching. This is important because it would help to understand the C-Q relationship, which in turn will help to construct effective mitigation measures. For example, adjust the amount of fertiliser applied to the field. If P concentrations are already high at the end of the field, additional manure application would not be necessary. In addition, tile drains with ICS at the end of the field would only be effective in very wet conditions or sometimes may never leach to the outflow. We recommend that further studies consider the depth and distance to the ditch at which groundwater samples are taken. Different from what we first thought, there was a large heterogeneity in the groundwater concentrations in the field. The water flow determines the phosphate discharge concentrations; therefore, any further study or evaluation of mitigation measures should consider the groundwater levels and drain discharge and not only the phosphate concentrations. To take the groundwater level into account, it is advisable to measure it directly, as the flow paths in sandy soils are directly connected to the groundwater level.

Investigate the effects of seepage on P leaching. In order to assess whether high P concentrations leaching from an agricultural field are directly due to the fertilisation of that field or may also originate from deeper soil layers, it is important to know the seepage rate. At Hogervorst, this proved to be difficult to model, as there were no measurements of the head below the clay/debris layer and little data on the conductivity of the clay/debris layer. Since the uncertainty of the clay/debris layer at Hogervorst was very high, there is still the problem of not knowing to what extent the clay/debris layer blocks seepage when creating a larger model. However, there was a lot of information about the distribution of the groundwater level, the water level in the ditch,tile drain discharge. Moreover, the LHM 4.1 model indicated no seepage. It was therefor decided to minimize the size of the model and focus on the flow paths on top of the clay/debris layer. Due to the uncertainty of the clay/debris layer, it is recommended to investigate a different field to study the effect of seepage. To include seepage it is advised to use a model size tree times the leakage factor [54]. Since the head at deeper ground layers is influenced by a larger area than the boundaries of the field itself. By using three times the leakage factor the influence of the boundary conditions is low. Which is important since the head especially at deeper groundwater layers is often unknown. Furthermore is is recommended to measure the head at various depths in the field to calibrate and or validate the model. A more refined grid size may be required at the field site. Although this larger model is also subject to many uncertainties, the effects of model boundary conditions will be smaller and seepage can be better simulated.

Study which phosphate loads are discharged into surface waters through tile drains and how often they occur for various wet conditions in the 'Bollenstreek'. For the design of the ICS filter at the tile drain outflow it is important to understand which phosphate concentrations and flow rates are to be expected. The measurements at Hogervorst have shown that phosphate concentrations increase when larger volumes are discharged and therefor a overflow would not be advisable. However, the measured data set of phosphate leaching at Hogervorst showed a discharge response at a single tile drain. It is therefore recommended to measure phosphate leaching from tile drains on different fields and to use already available data (e.g. Buijert *et al.* [1]). With the field at Hogervorst, adding the chemical transports to the current model is also a quick way to get additional information.

It is important to know what is happening in the east, and that is something that is missing in this study. We don't know if there is a water quality problem in the east or not. This result can help to take the best measures.

Framework to mitigate phosphate leaching
When installing mitigation measures taking into account the managed groundwater tables can be a simple indication where phosphate leaching risks are high. The head differences at the boundaries of a water level area cause groundwater to flow to the water level area with lower heads and therefor have an increased risk in phosphate leaching. The mitigation measures should take into account the peak flows as this is the time where more phosphate is transported. Mitigation measures with an overflow that are unable to treat peak flows are not recommended in the bollenstreek. Since Hogervorst and Voorhout showed high P concentrations at the drain outflow and at Hogervorst concentrations increased during the response. The mitigation measures should include infiltration from the ditch into the field, as this could favour iron precipitation, which contributes to phosphate storage.

Mitigation at Hogervorst
Since only during very wet conditions the entire drain length at Hogervorst is causing a response it would be more effective to construct a ICS filter at the end of the drains instead of implementing ICS around the drains. Furthermore, the ICS filters could filter 70% of the west flow, the other 30% is transported through the soil into the west ditch. To filter the other 30% a buffer zone could be installed. To mitigate the expected phosphate leaching to the east, increasing the head of the east weirs in dry summer conditions by 10 to 20 cm would minimize its transport to zero. Ditch water from the west ditch will than still infiltrate the field, reducing phosphate concentrations in the groundwater through dilution and oxidation. However, all infiltrating water can be evaporated, limiting the transport to the east.

Bibliography

[1] A. Buijert, R. Talens, W. Chardon, B. J. Grounenberg, S. Jansen, and J. Gerritse, *PILOT EFFECTGERICHTE VERWIJDERING FOSFAAT BOLLENSTREEK*, Tech. Rep. (Hoogheemraadschap van Rijnland, 2015).

[2] Stowa, *Meer water Met regelbare drainage?* (2012).

[3] *h2020-P-TRAP | General project description,* .

[4] J. Rozemeijer and Y. Van Der Velde, *Temporal variability in groundwater and surface water quality in humid agricultural catchments; Driving processes and consequences for regional water quality monitoring,* Fundamental and Applied Limnology **184**, 195 (2014).

[5] R. J. Diaz, *Overview of Hypoxia around the World,* Journal of Environmental Quality **30**, 275 (2001).

[6] J. C. Makarewicz, P. E. D'Aiuto, and I. Bosch, *Elevated nutrient levels from agriculturally dominated watersheds stimulate metaphyton growth,* Journal of Great Lakes Research **33**, 437 (2007).

[7] M. J. Weijters, J. H. Janse, R. Alkemade, and J. T. Verhoeven, *Quantifying the effect of catchment land use and water nutrient concentrations on freshwater river and stream biodiversity,* Aquatic Conservation: Marine and Freshwater Ecosystems **19**, 104 (2009).

[8] H. J. M. Van Grinsven, H. F. M. Ten Berge, T. Dalgaard, B. Fraters, P. Durand, A. Hart, G. Hofman, B. H. Jacobsen, S. T. J. Lalor, J. P. Lesschen, B. Osterburg, K. G. Richards, A.-K. Techen, F. Vertès, J. Webb, and W. J. Willems, *Management, regulation and environmental impacts of nitrogen fertilization in northwestern Europe under the Nitrates Directive; a benchmark study,* Biogeosciences **9**, 5143 (2012).

[9] L. Bouwman, K. K. Goldewijk, K. W. Van Der Hoek, A. H. Beusen, D. P. Van Vuuren, J. Willems, M. C. Rufino, and E. Stehfest, *Exploring global changes in nitrogen and phosphorus cycles in agriculture induced by livestock production over the 1900-2050 period,* Proceedings of the National Academy of Sciences of the United States of America **110**, 20882 (2013).

[10] J. C. Rozemeijer, A. Visser, W. Borren, M. Winegram, Y. Van Der Velde, J. Klein, and H. P. Broers, *High-frequency monitoring of water fluxes and nutrient loads to assess the effects of controlled drainage on water storage and nutrient transport,* Hydrology and Earth System Sciences **20**, 347 (2016).

[11] S. Baken, M. Verbeeck, D. Verheyen, J. Diels, and E. Smolders, *Phosphorus losses from agricultural land to natural waters are reduced by immobilization in iron-rich sediments of drainage ditches,* (2015), 10.1016/j.watres.2015.01.008.

[12] J. C. Rozemeijer and H. P. Broers, *The groundwater contribution to surface water contamination in a region with intensive agricultural land use (Noord-Brabant, The Netherlands),* Environmental Pollution **148**, 695 (2007).

[13] S. Vandermoere, N. A. Ralaizafisoloarivony, E. Van Ranst, and S. De Neve, *Reducing phosphorus (P) losses from drained agricultural fields with iron coated sand (- glauconite) filters,* Water Research **141**, 329 (2018).

[14] J. C. Rozemeijer, Y. Van Der Velde, F. C. Van Geer, G. H. De Rooij, P. J. Torfs, and H. P. Broers, *Improving load estimates for NO3 and P in surface waters by characterizing the concentration response to rainfall events,* Environmental Science and Technology **44**, 6305 (2010).

[15] C. Stamm, H. Flühler, R. Gächter, J. Leuenberger, and H. Wunderli, *Preferential Transport of Phosphorus in Drained Grassland Soils,* Journal of Environmental Quality **27**, 515 (1998).

[16] A. L. Heathwaite and R. M. Dils, *Characterising phosphorus loss in surface and subsurface hydrological pathways,* The Science of the Total Environment **251**, 523538 (2000).

[17] K. W. King, M. R. Williams, M. L. Macrae, N. R. Fausey, J. Frankenberger, D. R. Smith, P. J. A. Kleinman, and L. C. Brown, *Phosphorus Transport in Agricultural Subsurface Drainage: A Review,* Journal of Environmental Quality **44**, 467 (2015).

[18] P. A. I. Ehlert, P. H. M. Dekker, J. R. Van Der Schoot, R. Visschers, J. C. Van Middelkoop, M. P. Van Der Maas, A. A. Pronk, A. M. Van, and D. Alterra, *Uitloop 0 lijn 10 mm 15 mm 20 mm 5 mm,* .

[19] J. C. Rozemeijer, Y. Van Der Velde, F. C. Van Geer, M. F. Bierkens, and H. P. Broers, *Direct measurements of the tile drain and groundwater flow route contributions to surface water contamination: From field-scale concentration patterns in groundwater to catchment-scale surface water quality,* Environmental Pollution **158**, 3571 (2010).

[20] J. E. Groenenberg, W. J. Chardon, and G. F. Koopmans, *Reducing Phosphorus Loading of Surface Water Using Iron-Coated Sand,* Journal of Environmental Quality **42**, 250 (2013).

[21] K. W. King , N. R. Fausey, and M. R. Williams, *Effect of subsurface drainage on streamflow in an agricultural headwater watershed,* (2014), 10.1016/j.jhydrol.2014.07.035.

[22] V. Barcala, J. Rozemeijer, L. Osté, B. Van Der Grift, L. Gerner, and T. Behrends, *Processes controlling the flux of legacy phosphorus to surface waters at the farm scale,* Environmental Research Letters **16**, 15003 (2021).

[23] G. Mol, P. v. Gaans, J. Spijker, G. v. d. Veer, G. Klaver, and G. Roskam, *Geochemische atlas van Nederland,* (2010).

[24] J. (Janine) de Wit, C. (Coen) Ritsema, J. (Jos) van Dam, G. (Gé) van den Eertwegh, and R. (Ruud) Bartholomeus, *Development of subsurface drainage systems: Discharge – retention – recharge,* Agricultural Water Management **269**, 107677 (2022).

[25] J. Oriffloen', *Envlron. Sci. Technol*, Tech. Rep. (1994).

[26] *Rozemeijer_etal_kwel-P,* TNO-rapport (2005).

[27] Y. Liang, *VU Research Portal Groundwater-surface water interaction in urban lowland catchments*, Tech. Rep. (2021).

[28] B. Van Der Grift, J. C. Rozemeijer, J. Griffioen, and Y. Van Der Velde, *Iron oxidation kinetics and phosphate immobilization along the flow-path from groundwater into surface water,* Hydrology and Earth System Sciences **18**, 4687 (2014).

[29] R. Bol, G. Gruau, P. E. Mellander, R. Dupas, M. Bechmann, E. Skarbøvik, M. Bieroza, F. Djodjic, M. Glendell, P. Jordan, B. Van der Grift, M. Rode, E. Smolders, M. Verbeeck, S. Gu, E. Klumpp, I. Pohle, M. Fresne, and C. Gascuel-Odoux, *Challenges of reducing phosphorus based water eutrophication in the agricultural landscapes of Northwest Europe,* Frontiers in Marine Science **5** (2018), 10.3389/FMARS.2018.00276.

[30] A. C. Senn, R. Kaegi, S. J. Hug, J. G. Hering, S. Mangold, and A. Voegelin, *Composition and structure of Fe(III)-precipitates formed by Fe(II) oxidation in water at near-neutral pH: Interdependent effects of phosphate, silicate and Ca,* Geochimica et Cosmochimica Acta **162**, 220 (2015).

[31] D. A. Robinson, I. Lebron, and J. I. Querejeta, *Determining Soil–Tree–Grass Relationships in a California Oak Savanna Using Eco-GeophysicsAll rights reserved. No part of this periodical may be reproduced or transmitted in any form or by any means, electronic or mechanical, including photocopying, recording, or any information storage and retrieval system, without permission in writing from the publisher.* Vadose Zone Journal **9**, 528 (2010).

[32] E. Smolders, E. Baetens, M. Verbeeck, S. Nawara, J. Diels, M. Verdievel, B. Peeters, W. De Cooman, and S. Baken, *Internal Loading and Redox Cycling of Sediment Iron Explain Reactive Phosphorus Concentrations in Lowland Rivers,* Environmental Science and Technology **51**, 2584 (2017).

[33] J. D. Hughes, *Documentation Prepared in cooperation with the U.S. Geological Survey Water Availability and Use Science Program Documentation for the MODFLOW 6 Groundwater Flow Model*, Tech. Rep.

[34] B. B. B. Bot, *Grondwaterzakboekje,* (2011).

[35] R. A. Feddes, *Crop factors in relation to Makkink reference-crop evapotranspiration,* (1987), 10.3/JQUERY-UI.JS.

[36] *Validatie en toetsing LHM 4.1 : samenvattend hoofdrapport - Rijkswaterstaat Rapportendatabank,* .

[37] E. v. boekel, J. Roelsma, H. Massop, H. mulder, P. Jansen, L. renaud, R. Hendriks, and P. Schipper, *Boekel_2015,* Alterra (2015).

[38] O. F. Schoumans, C. Van der Salm, and P. Groenendijk, *PLEASE: A simple model to determine P losses by leaching,* Soil Use and Management **29**, 138 (2013).

[39] G. F. Koopmans, W. J. Chardon, P. H. Dekker, P. F. Römkens, and O. F. Schoumans, *Comparing different extraction methods for estimating phosphorus solubility in various soil types,* Soil Science **171**, 103 (2006).

[40] *Phosphate saturation degree and accumulation of phosphate in various soil types in The Netherlands | Elsevier Enhanced Reader,* .

[41] H. Schoonvelde, *Grasland - 2008 - Commissie Bemesting Grasland en Voedergewassen,* Samenstelling Commissie Bemesting Grasland en Voedergewassen (2017).

[42] P. Groenendijk and J. G. Kroes, *Modelling the nitrogen and phosphorus leaching to groundwater and surface water with ANIMO 3.5,* (2000).

[43] O. F. Schoumans, W. J. Chardon, M. E. Bechmann, C. Gascuel-Odoux, G. Hofman, B. Kronvang, G. H. Rubæk, B. Ulén, and J. M. Dorioz, *Mitigation options to reduce phosphorus losses from the agricultural sector and improve surface water quality: A review,* Science of the Total Environment **468-469**, 1255 (2014).

[44] H. S. Jensen, P. Kristensen, E. Jeppesen, and A. Skytthe, *Iron:phosphorus ratio in surface sediment as an indicator of phosphate release from aerobic sediments in shallow lakes,* Sediment/Water Interactions , 731 (1992).

[45] *Bauder, T.A., R.M. Waskom and J.G. Davis, 2003. Irrigatio... - Google Scholar,* .

[46] P. G. B. De Louw, G. H. P. Oude Essink, P. J. Stuyfzand, and S. E. A. T. M. Van Der Zee, *Upward groundwater flow in boils as the dominant mechanism of salinization in deep polders, The Netherlands,* 10.1016/j.jhydrol.2010.10.009.

[47] *Coastal Aquifer Management-Monitoring, Modeling, and Case Studies - Google Boeken,* .

[48] J. C. Wu, L. Lu, and T. Tang, *Bayesian Analysis for Uncertainty and Risk in a Groundwater Numerical Model's Predictions,* http://dx.doi.org/10.1080/10807039.2011.618419 **17**, 1310 (2011).

[49] S. R. H. Worthington, A. E. Foley, and R. W. N. Soley, *Transient characteristics of effective porosity and specific yield in bedrock aquifers,* (2019), 10.1016/j.jhydrol.2019.124129.

[50] *Applied Groundwater Modeling: Simulation of Flow and Advective Transport - Mary P. Anderson, William W. Woessner, Randall J. Hunt - Google Boeken,* .

[51] D. B. Stephens, K.-C. A. Hsu Mark Prieksat, M. D. Ankeny Neil Blandford, T. L. Roth, J. A. Kelsey Julia R Whitworth, K.-C. Hsu, M. A. Prieksat Mark D Ankeny, N. Blandford, T. L. Roth James A Kelsey Daniel B Stephens, and J. R. Whitworth, *A comparison of estimated and calculated effective porosity,* Hydrogeology Journal **6**, 156 (1998).

[52] P. Ehlert, C. Morel, M. Fotyma, and J. P. Destain, *Potential role of phosphate buffering capacity of soils in fertilizer management strategies fitted to environmental goals,* Journal of Plant Nutrition and Soil Science **166**, 409 (2003).

[53] M. El-Rawy, F. De Smedt, O. Batelaan, U. Schneidewind, M. Huysmans, and W. Zijl, *Hydrodynamics of porous formations: Simple indices for calibration and identification of spatio-temporal scales,* Marine and Petroleum Geology **78**, 690 (2016).

[54] *onder een deklaag (De Glee),* .

[55] C. D. Langevin, S. Panday, and A. M. Provost, *Hydraulic-Head Formulation for Density-Dependent Flow and Transport,* Groundwater **58** (2020), 10.1111/gwat.12967.

[56] *The Effect of Brackish Water Extraction on the Brackish Upconing Below the Horstermeer Polder | TU Delft Repositories,* .

[57] J. Jiao and V. Post, *Coastal Hydrogeology* (2019).

Appendices

A

Test setup details

Unwanted factors which could have influenced the drain extension tubes surface level:

- Material stiffness: the drain tubes extension caused a small gap of 1 to 2 cm above the ditch level.
- Floating material in the ditch which accumulates on the drain. Aquatic plants sometimes gathered at the drain. These were removed during fieldwork sessions.
- Weight of water inside the drain extension tube. The weight of the tube increases when water enters the tube this caused the drain to lower a view cm.
- Siphon effect: This could theoretically occur when there is a very high discharge and the drain extension tube fully fills itself with water.

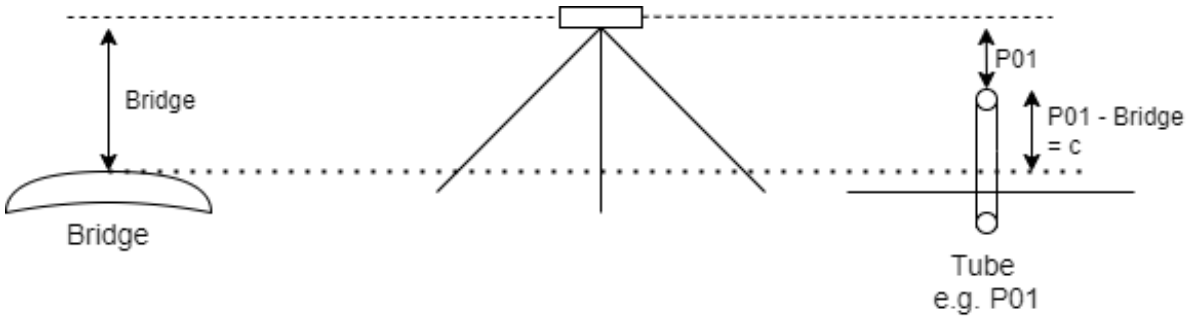

Figure A.1: Schematic Overview Measuring c Levels

Table A.1: Installed monitoring devices. The name column shows the monitoring wells P1 to P12, Baro meter, barrel 1 and 2, the Soil Moisture Probe (SMP) and the auto-sampler (auto-s). The start and stop column show the installation and removal. The Frequency column presents the interval of a measuring device. However not all monitoring wells were equiped with a measuring device. The type and SN show which device was installed. Depending on the device it can measure: pressure (P), temperature (T), electrical conductivity (EC), water content (WC), relative humidity (RH) and dew point (DewPt).

Name	Start	Stop	Frequency	SN.	Type	Measures	Note
P1	12/9/2020	9/13/2021	5 min	W6041	Cera-Diver (DI701)	P, T	
P2	12/9/2020	9/13/2021	5 min	L8009	Mini-Diver (DI501)	P, T	
P3a	12/9/2020	4/28/2021	5 min	S9905	Mini-Diver (DI501)	P, T	After 4/28 diver moved to P06
P3b	6/3/2021	9/13/2021	5 min	K2877	Mini-Diver (DI501)	P, T	
P4	-		-			-	
P05	3/11/2021	3/18/2021	5 min	K28777	Mini-Diver (DI501)	P,T	
P06a	4/16/2021	4/28/2021	5 min	K2877	Mini-Diver (DI501)	P,T	After 4/28 diver moved to B2
P06b	4/28/2021		5 min	S9905			
P07	6/3/2021	7/9/2021	5 min	K2877	Mini-Diver (DI501)	P,T	
P08	6/3/2021	7/9/2021	5 min	M8878	CTD-Diver (DI271)	P,T, EC	
P09	6/3/2021	7/9/2021	-				
P10	6/3/2021	7/9/2021	-				
P11	6/3/2021	7/9/2021	-				
P12	6/3/2021	7/9/2021	-				
Baro.	10/29/2020	9/13/2021	5 min	BH326	TD-Diver (DI800)	P, T	No measurements between 6/3 and 6/14 since the barometer was needed for an other project
B1	12/9/2020	9/13/2021	11/3/2021 Before: 5min after: 1 min	M8878	CTD-Diver (DI271)	P,T, EC	No measurements beween 6/3 and 7/9 barrel was disconnected because of dry conditions.
B2a	3/18/2021	4/9/2021	1 min	K7113	Mini-Diver (DI501)	P,T	No response measured
B2b_p	4/28/2021	6/3/2021	1 min	K2877	Mini-Diver (DI501)	P,T	
B2b_ctd	4/16/2021	6/3/2021	1 min	V5491	CTD-Diver (DI271)	T,EC	Pressure meter is broken
SMP	12/9/2020	9/13/2021	5 min	-	HOBO	WC, T, RH, DewPt	Two water content measuring depths
Auto-s.	3/18/2021	6/3/2021	Variable			-	

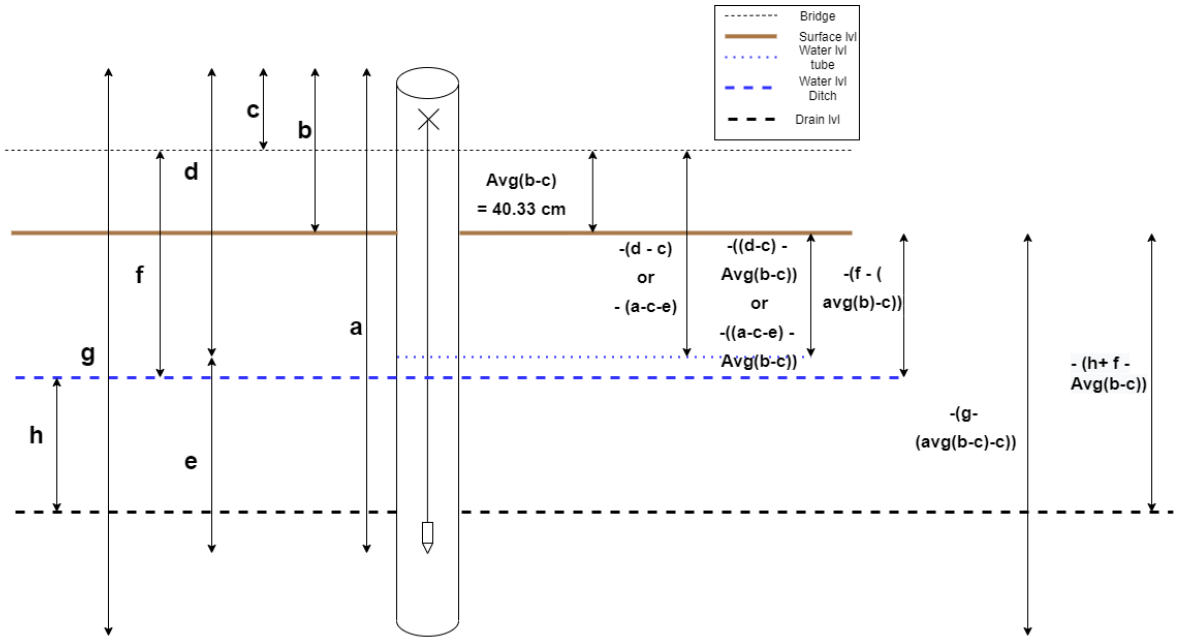

Figure A.2: Schematic Overview of Measured (left side of the figure) and calculated Levels(right side of the figure) With Respect To the Bridge

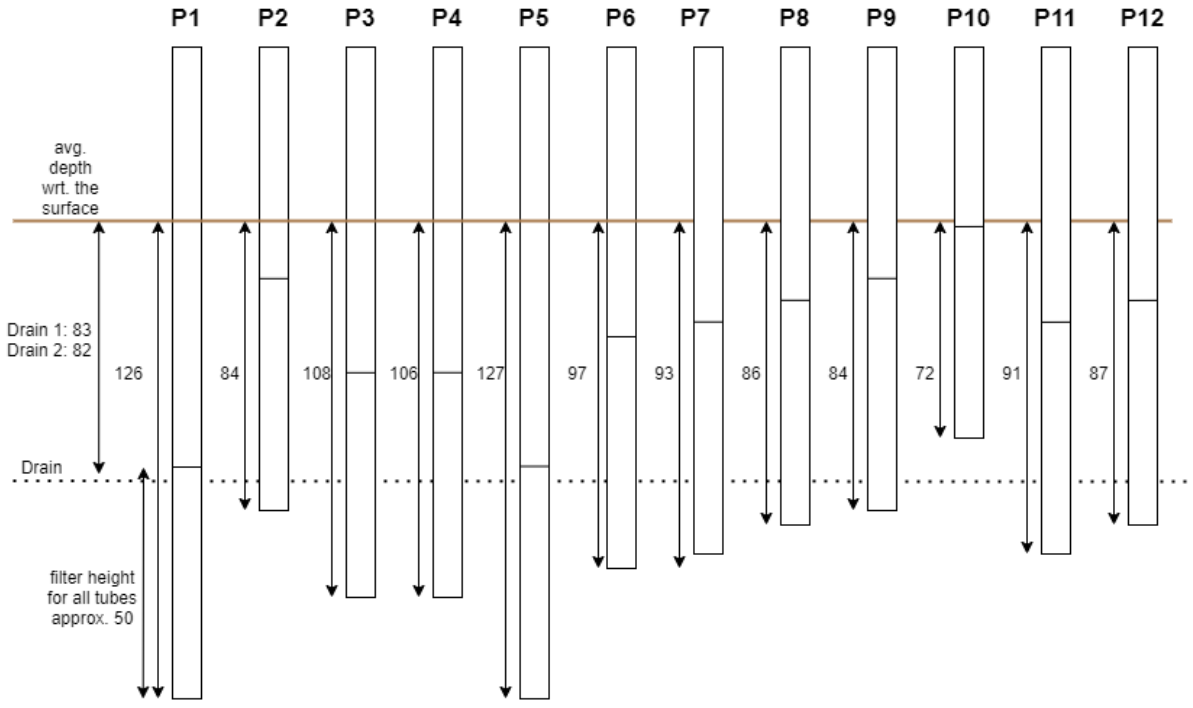

Figure A.3: monitoring wells depth and drain depth

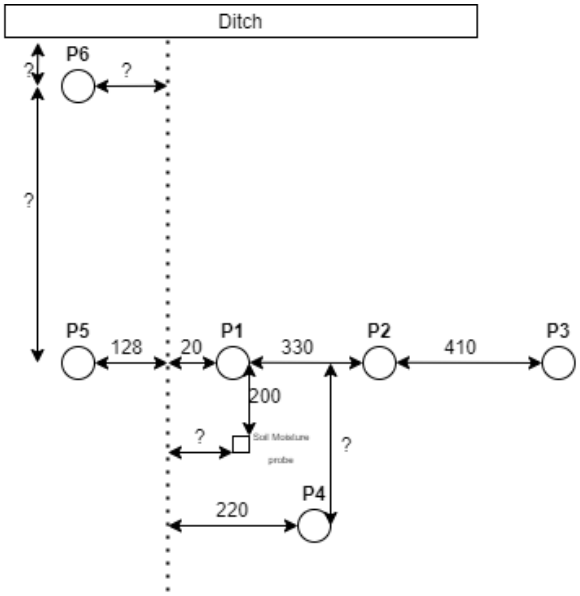

Figure A.4: setup detail of P1 to P5

Table A.2: Location of monitoring wells, soil moisture probe (SMP) and depth profiles (W1 to W6). The locations are measured with respect to the outflow of D1 at the edge of the ditch. Where L is the distance from the ditch and W is the distance from D1 as indicated in Figure 2.4

Description	L	W	note
P1	59	0.2	
P2	59	3.5	
P3	59	7.6	
P4		2.2	
P5	59	1.28	
SMP	59.2	0.2	close to P1
P6			
P7	14.3	1.7	
P8	29	1	
P9	59	9	
P10	14.3	8.4	
P11	29	7.5	
P12			
W1	59	0.2	close to P1
W2	59	0.2	close to P1
W3	14.3	0.6	close to P7
W4	14.3	1.45	close to P7
W5	14.3	5	close to P7
W6	30	1.7	close to P8

B

Hydraulic and EC response

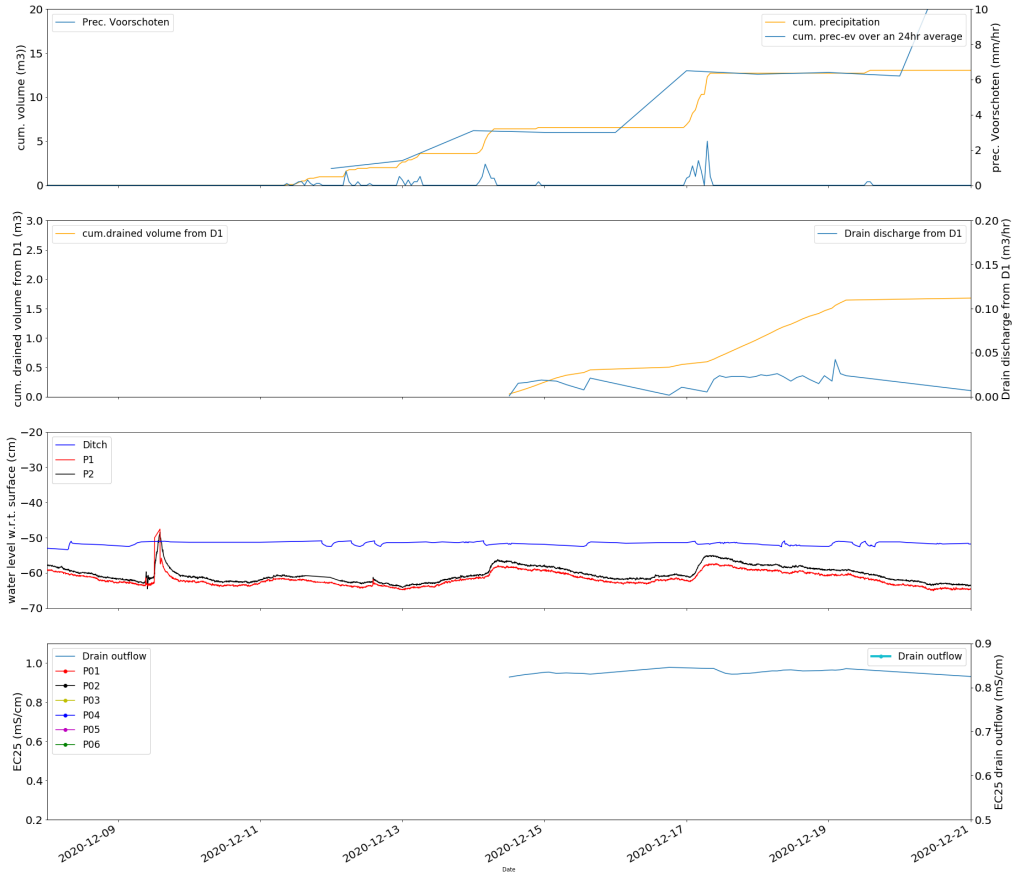

Figure B.1: part 1

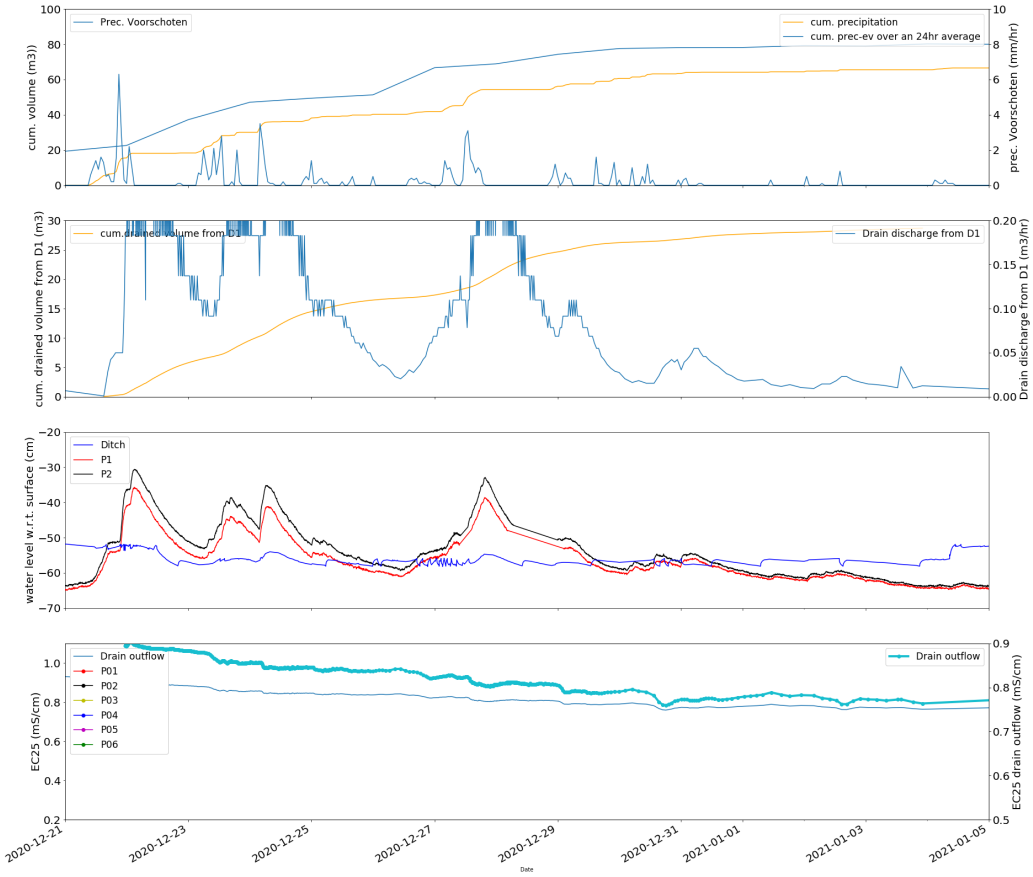

Figure B.2: part 2

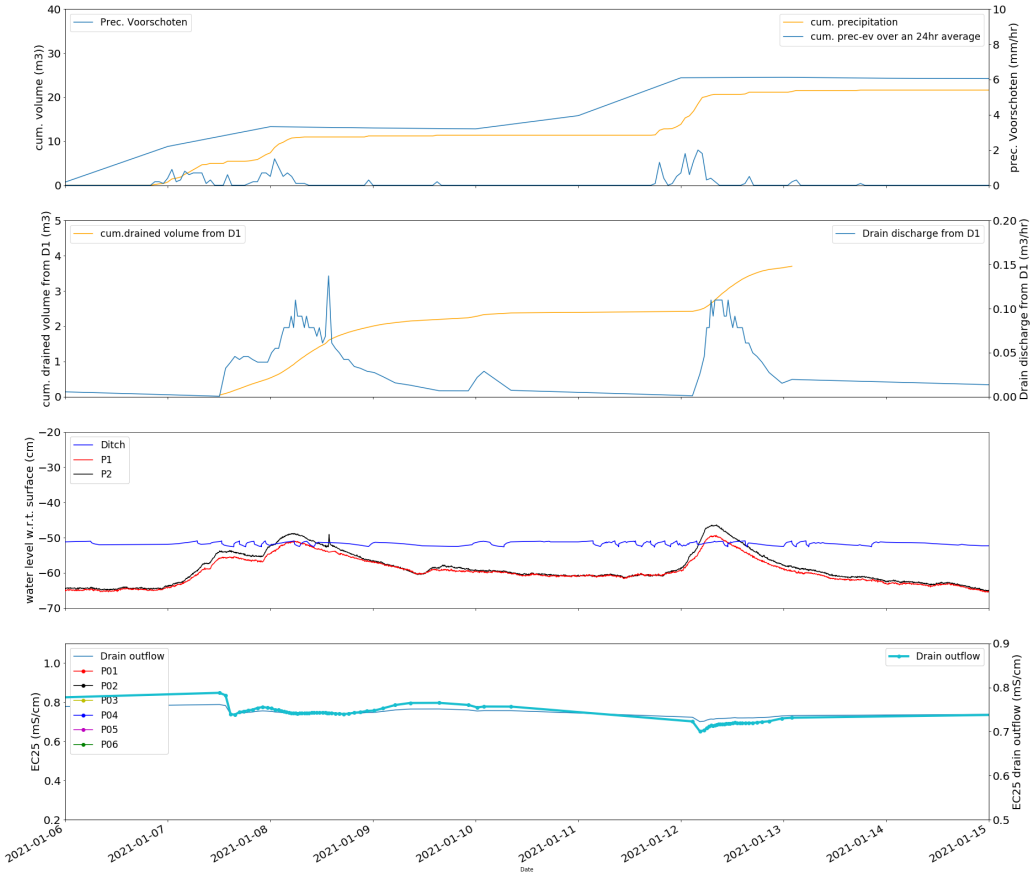

Figure B.3: part 3

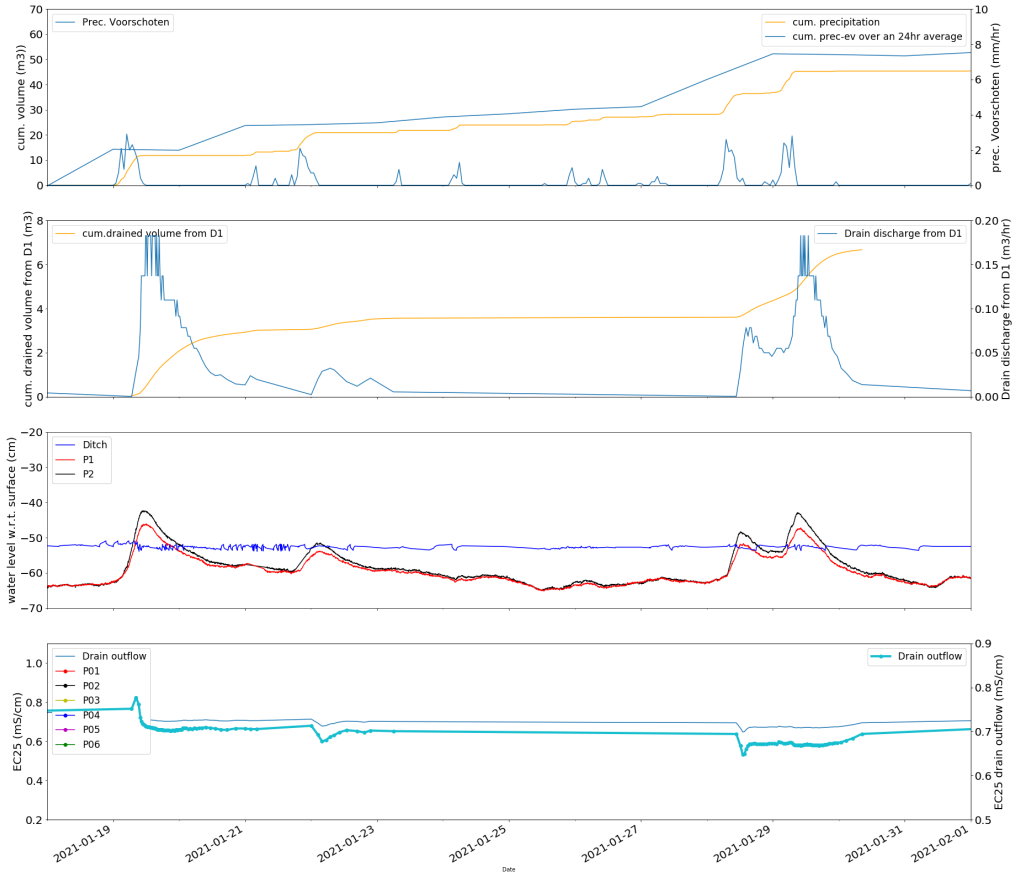

Figure B.4: part 4

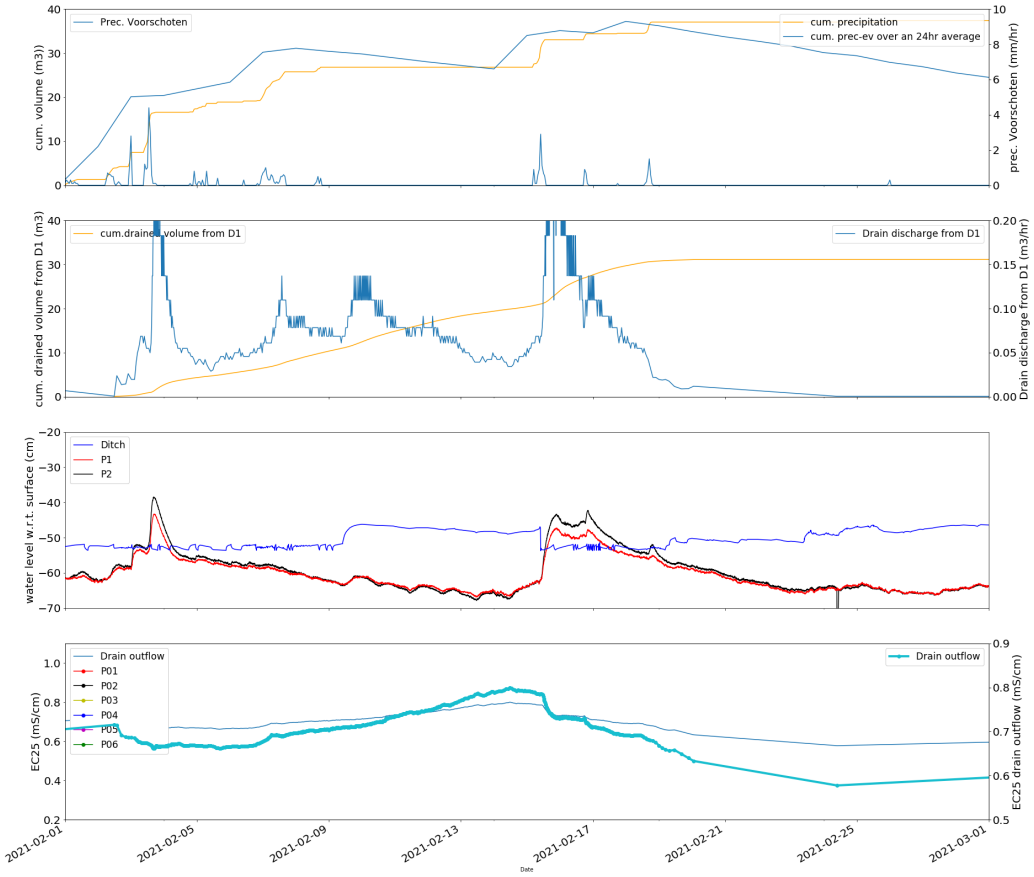

Figure B.5: part 5

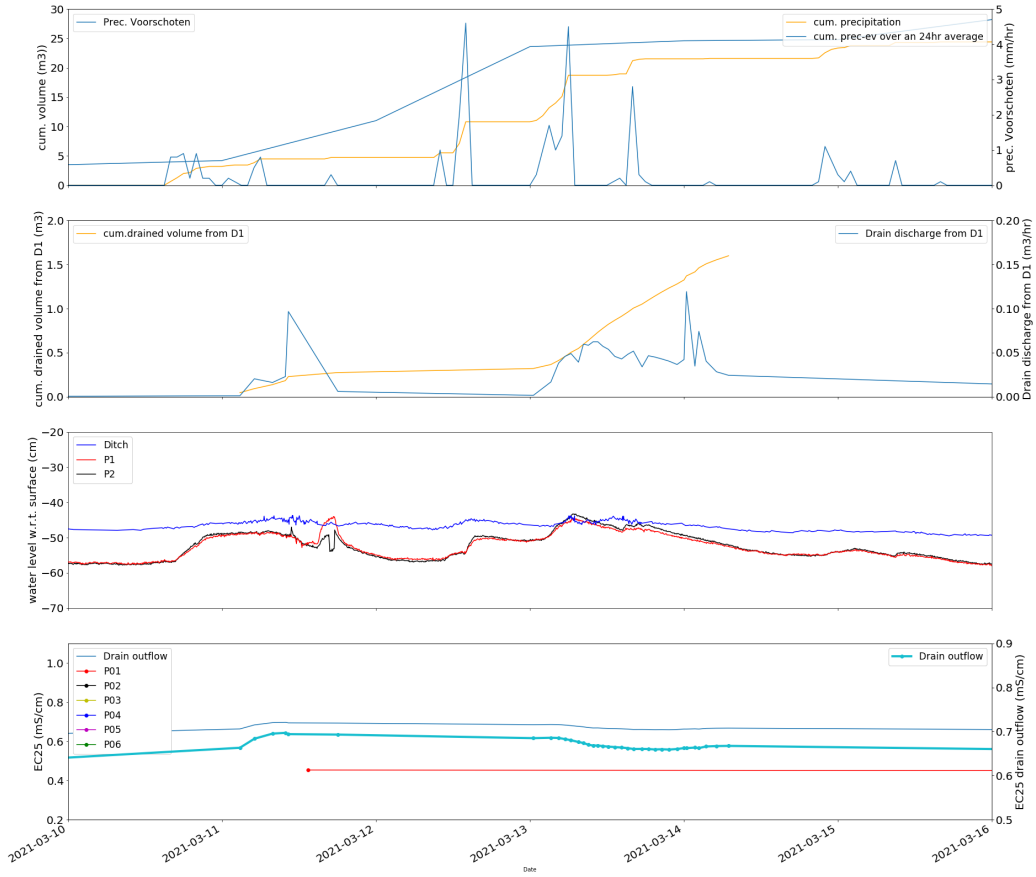

Figure B.6: part 6

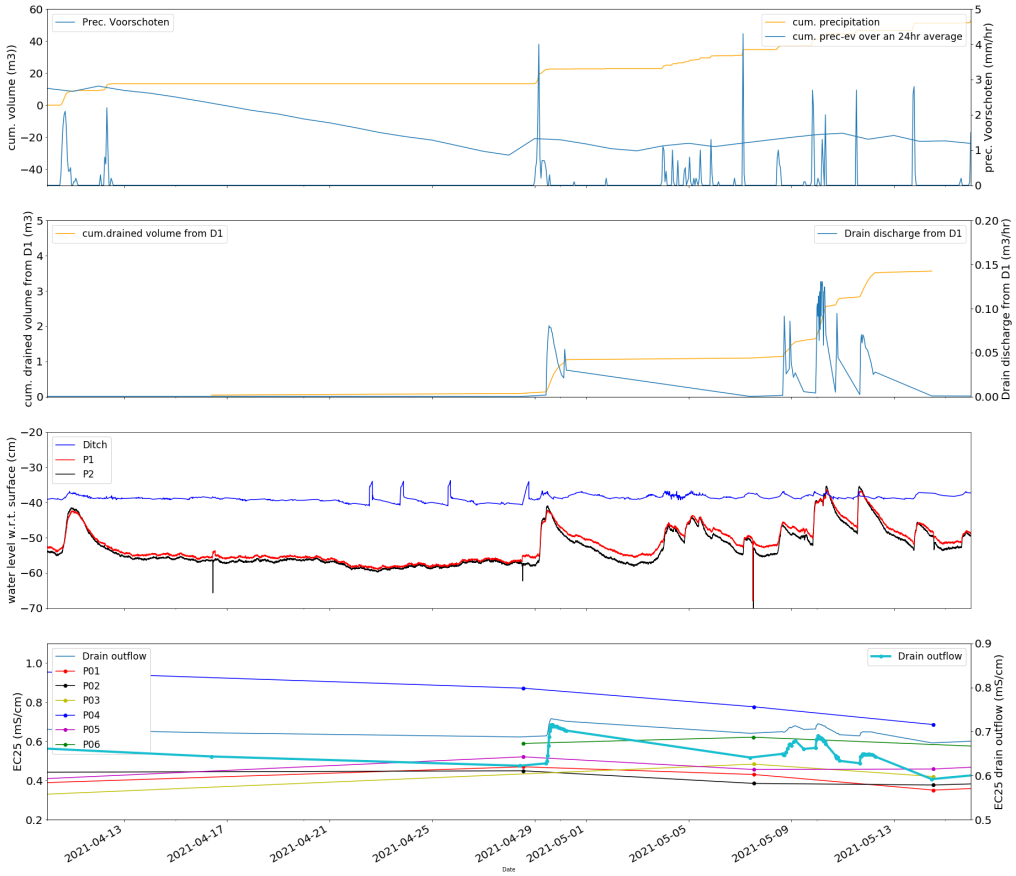

Figure B.7: part 7

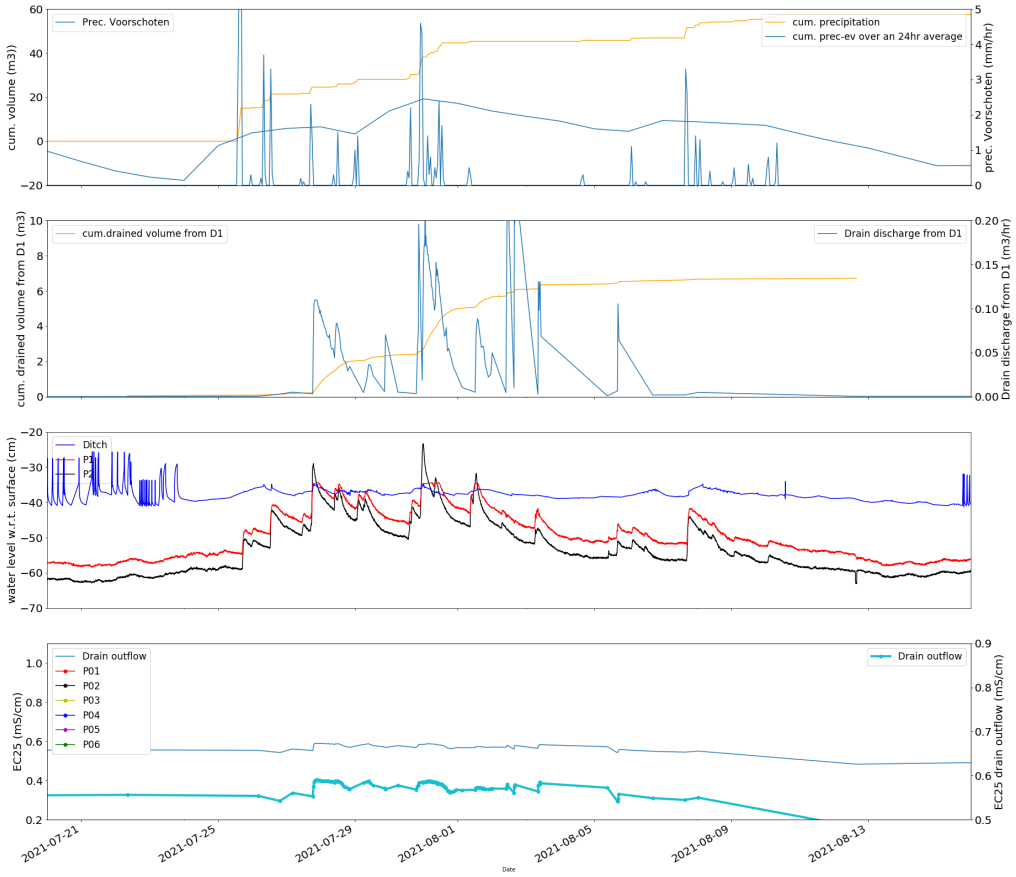

Figure B.8: part 8

C

P response complete data set

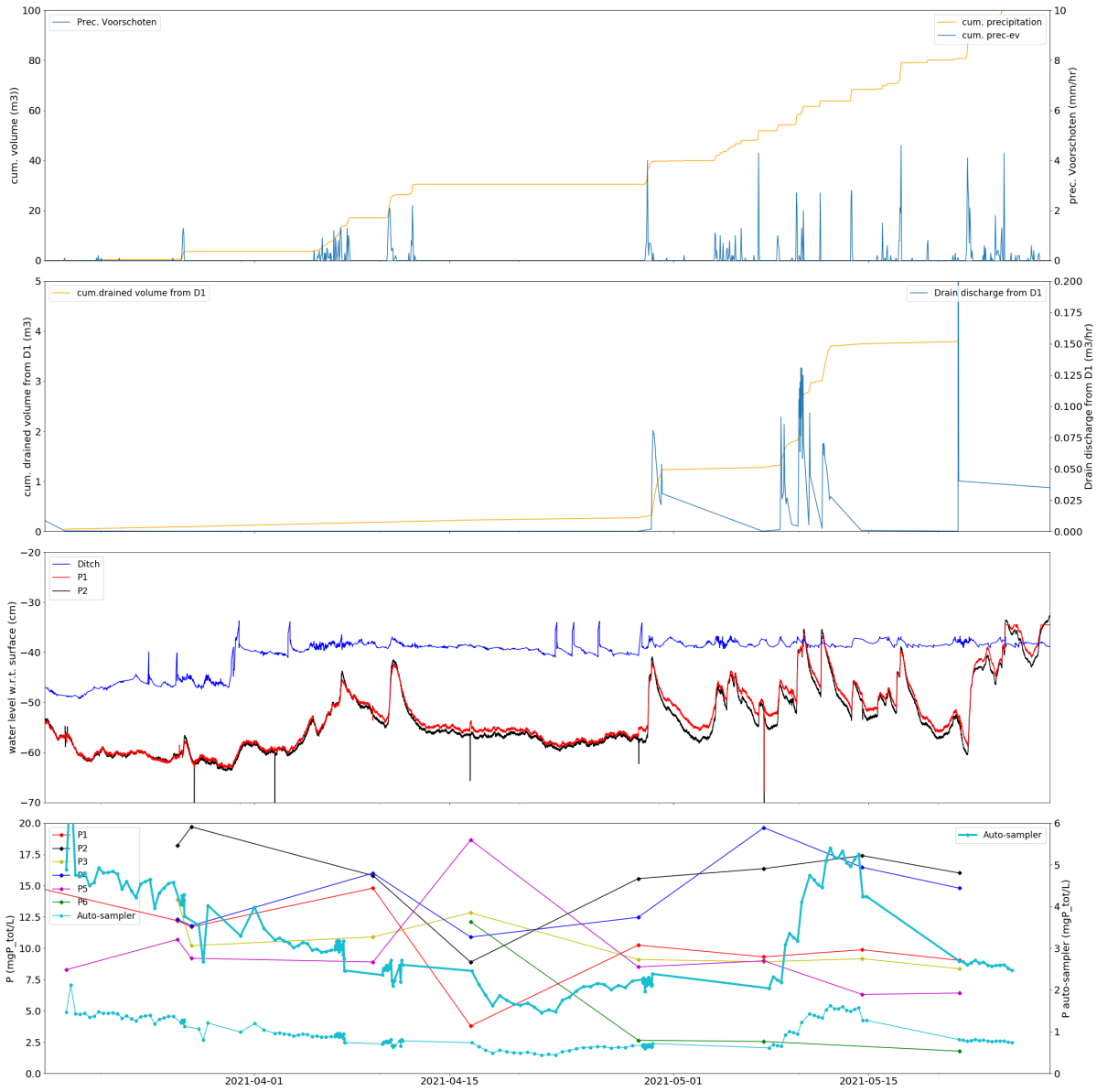

Figure C.1: P response complete data set

D

Adjustments to the Test Setup

For this study at two drains (D1 and D2) two barrels (B1 and B2) were installed. However, B2 faced many problems and was therefor often not operational. The barrel was mounted to four wooden poles which kept the barrel in place. To prevent the barrel from lifting because of the uplifting water force additional weight was added to the barrels.

The installation of the two barrels were at different dates. B1 was installed on 2020-12-09 and B2 was installed somewhat later on 2021-02-24. After the installation of barrel 1 there were no mayor problems and therefor no adjustments needed till the 5^{th} of May. Since, than the barrel was lifted by the water force and a new calibration was required. B2 faced problems with malfunctioning pressure sensor, uplifting of the barrel and a too high maximum water level in the barrel. The malfunctioning pressure sensor (diver) was replaced which its details can be found in Table A.1. The uplifting was solved by increasing the weight. To reduce the maximum water level a slightly different system was used to fixate the cable length of the float switch compared to B1. For B2 the float switch was fixed to a wooden pole as showed in Figure D.1. The functioning of B1 and B2 was however still the same.

Figure D.1: Temporal single drain-water tank barrel 2. In this barrel the cable tie is not fixated to the pump itself but to the installed wooden poll in the barrel. This was required to activate the pump before the maximum water level inside the barrel was above the water level in the ditch.

Table D.1: Adjustments to the drain extension tube of barrel 1 in 2021

date	description
18 - march	installation auto-sampler
16 - april 13:00	drain extension tube lowered
8 to 14 may	drain response with auto-sampler
14 - may	extension tube flows on top of the ditch
21 - may	extension tube flows on top of the ditch
3 - june	auto - sampler removed
3 - june	extension tube removed from the drain outflow
9 - july	extension tube connected to the drain outflow

Table D.2: calibrations barrel 1

b1	start	end	start pump number (m3)	stop pump number (m3)
installation ctd_diver	2020-12-09 14:43	-		
calibration	2020-12-09		5.8102	6.1523
drain lowered	2020-12-09 13:50	2020-12-12		
autosampler	2021-03-26	2021-06-03		
calibration after setup repaired	2021-5-5 13:43	2021-5-5 14:30	92.5694	93.8532
pump kept pumping (vlotter on a brick)	-	05-21-10:45		92.4506
disconnect from the drain	2021-06-03 14:00			

Table D.3: calibrations barrel 2

b2	start	end	start number	stop number
installation	2021-02-24			
calibration	2021-02-24-13:00	24-02	0.4024	0.4885
calibration	03-11-13:34	03-11-16:26	2.006	2.2642
calibration	18-03-13:31	18-03-15:00	4.7269	4.7667
calibration	06-03 13:15	06-03 14:00	19.8561	20.0724
disconnect from the drain	06-03 14:00			

Table D.4: Calibration moments barrel 1 and 2

barrel	date	start time	stop	m3 pumped
1	9 - december	-	-	
2	11 - march	15:46	15:54	
2	18 - march	13:30	13:50	
1	25 - may	13:46	13:55	1.3455
2	3 - june	13:15	14:00	
start draintest	9 -sep	10:00		
1 and 2 removed	13 - sep	11:00		

E

Soil profile at Hogervorst from DINOloket

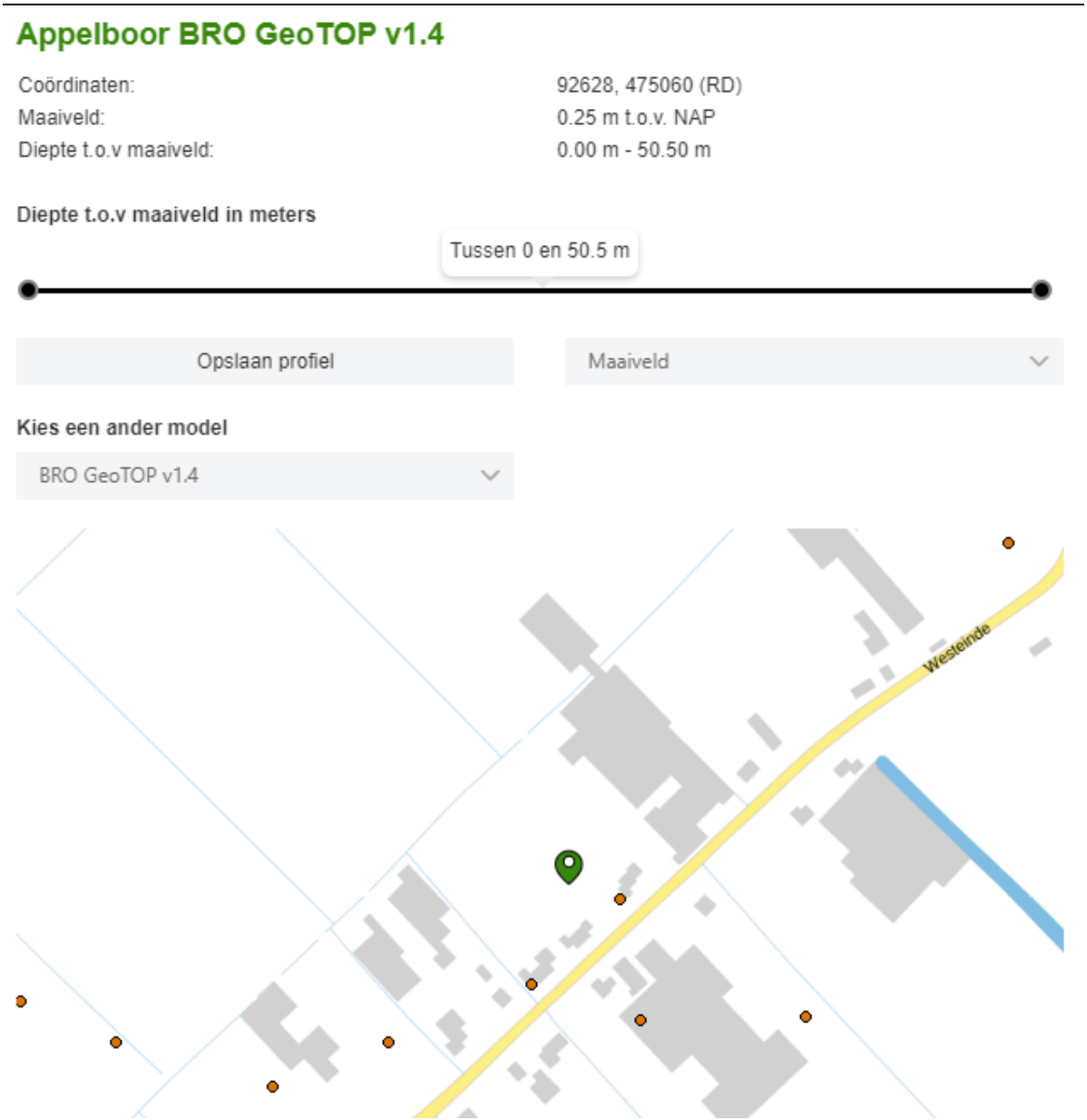

Figure E.1: Location of the soil profile from DINOloket taken at the farm plot of Hogervorst.

Figure E.2: Legend of the lithoklasse from the soil profile shown in Figure F.7

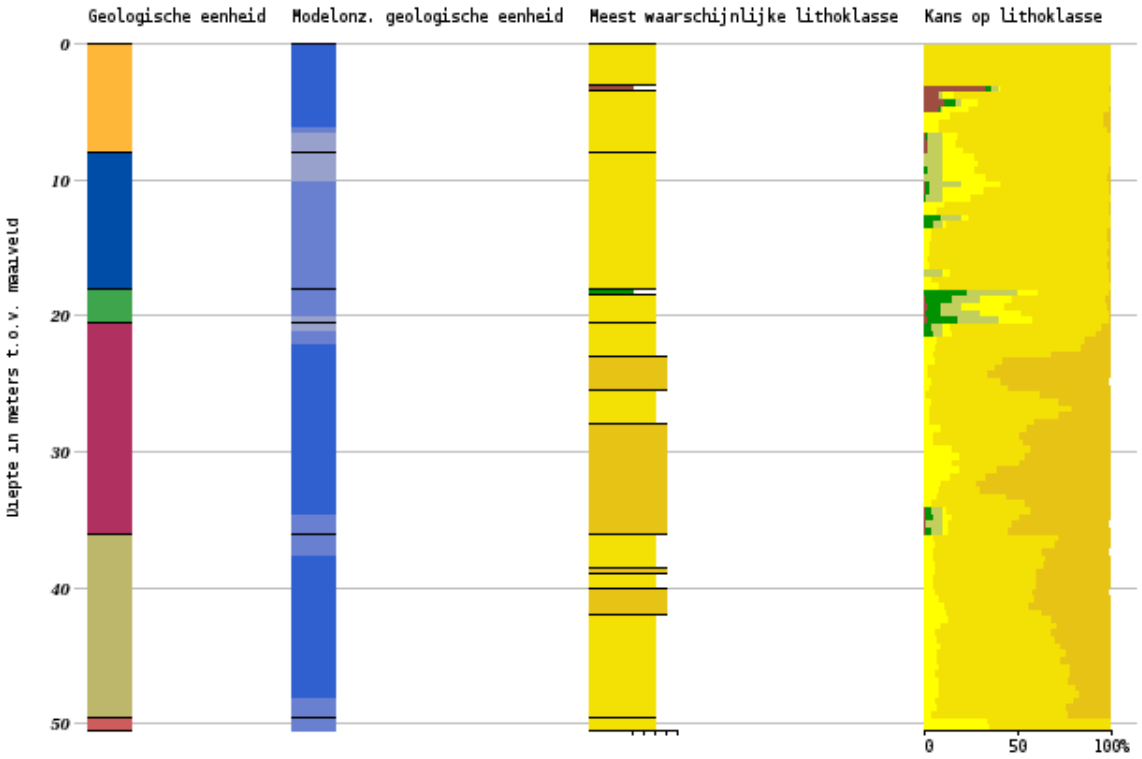

Figure E.3: Data from the depth profile at Hogervorst from DINOloket. At a depth of 18 meter it is likely that a thin clay layer is situated.

F

Sensitivity Analysis

This appendix shows the sensitivity analysis of Kv, Kh, drain conductance and effective precipitation. Each graph showing the sensitivity by changing one of the four parameters. The parameter values are shown in Table F.1. Note that the recharge boundary condition differs from Table 2.2. The CHD boundaries (virtual east, west ditch) and impermeable boundaries at the bottom, north and south are set as explained in subsection 2.3.1.

Wet Winter

Table F.1: Values used for the parameters in the sensitivity analysis.

Parameter	Kv	Kh	Drain conductance	Effective precipitation
Unit	m/d	m/d	m^2/d	m/d
Package	Node Property Flow (NPF)	NPF	General head boundary (GHB)	Recharge (RCH)
Value description	Value as indicated in figure 2.7	Value as indicated in Figure 2.7	Arbitrary number	Average precipitation in Jan. 2021
value	Kv_SEN	Kh_SEN	0.2	0.0025

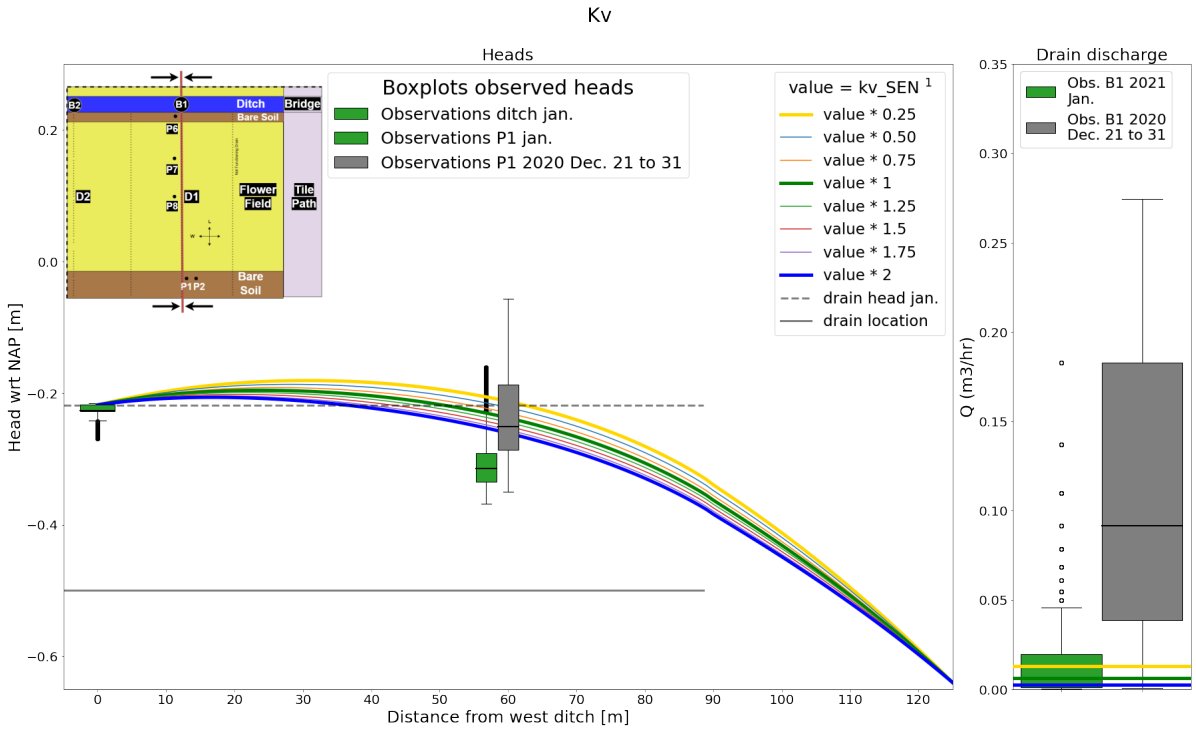

Figure F.1: Sensitivity of Kv
[1] the parameter kv_SEN as shown in Figure 2.6.

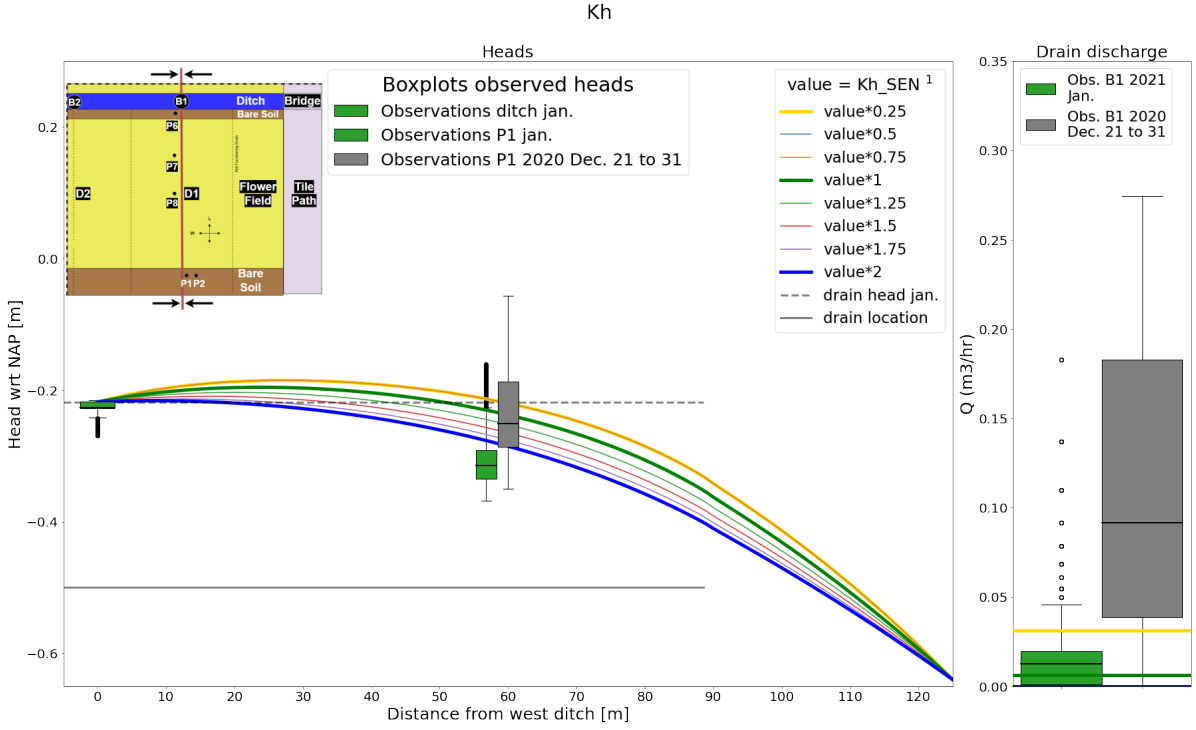

Figure F.2: Sensitivity of Kh
[1] the parameter kh_SEN as shown in Figure 2.6.

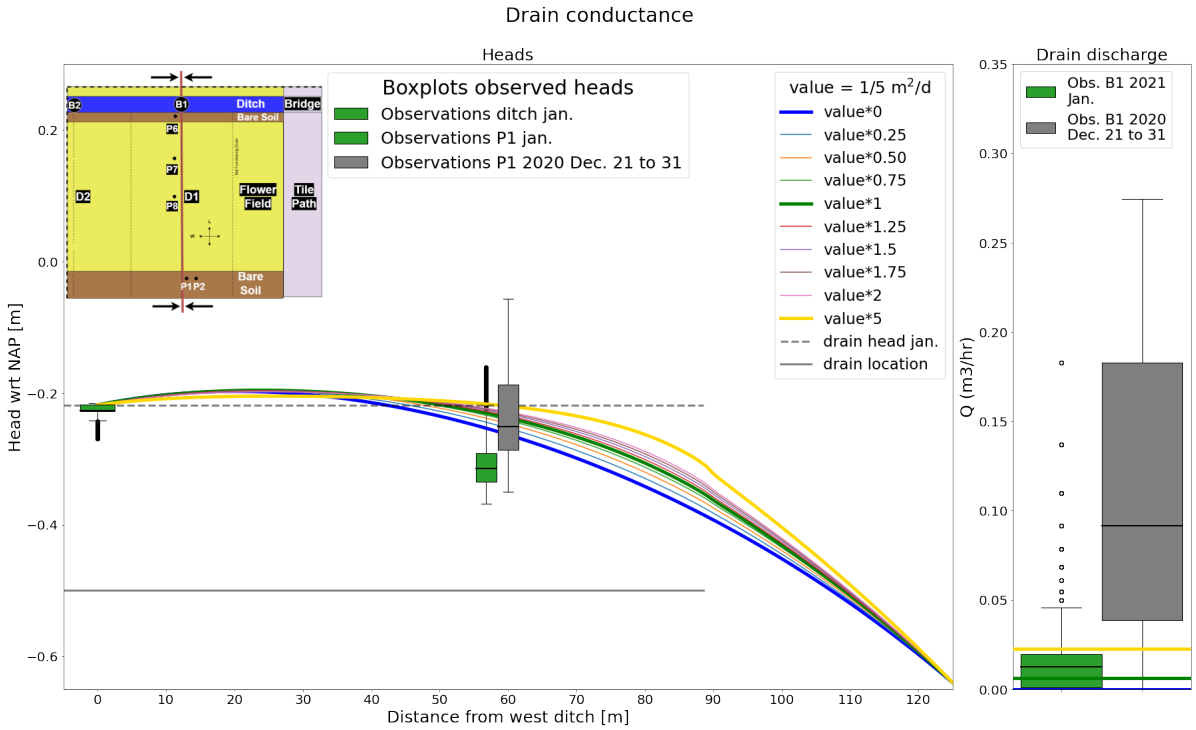

Figure F.3: Sensitivity of the drain conductance.

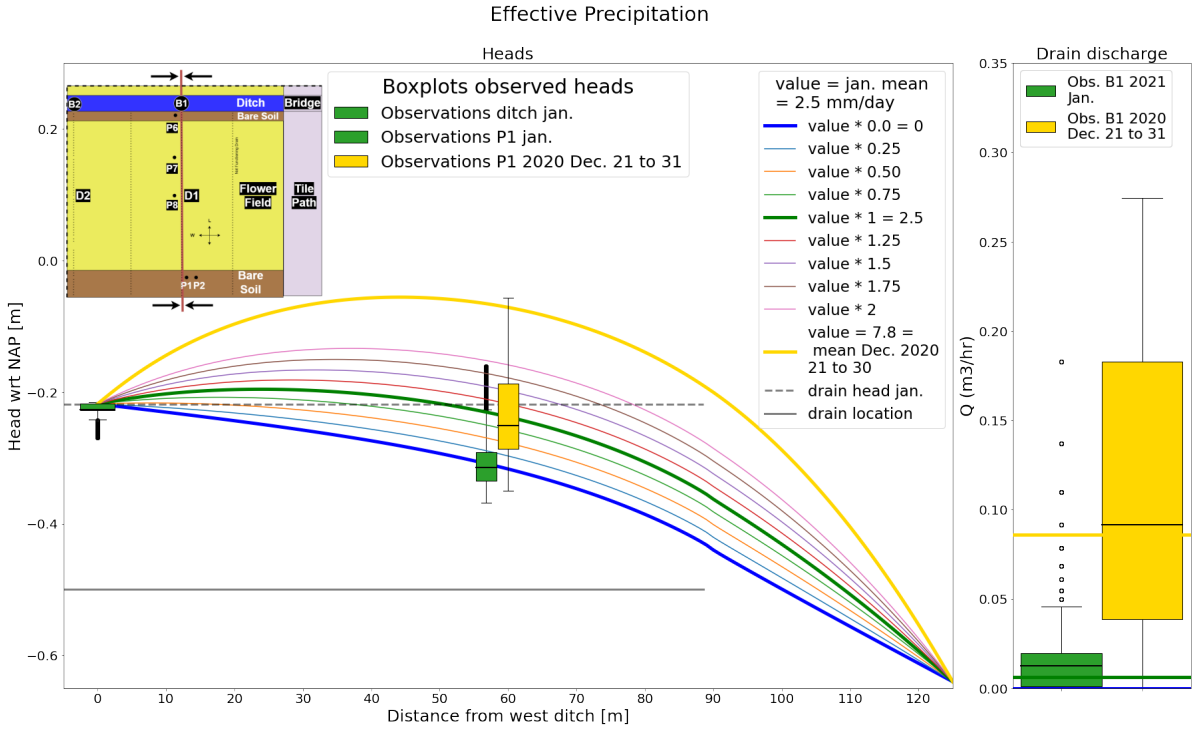

Figure F.4: Sensitivity of the effective precipitation.

Dry summer

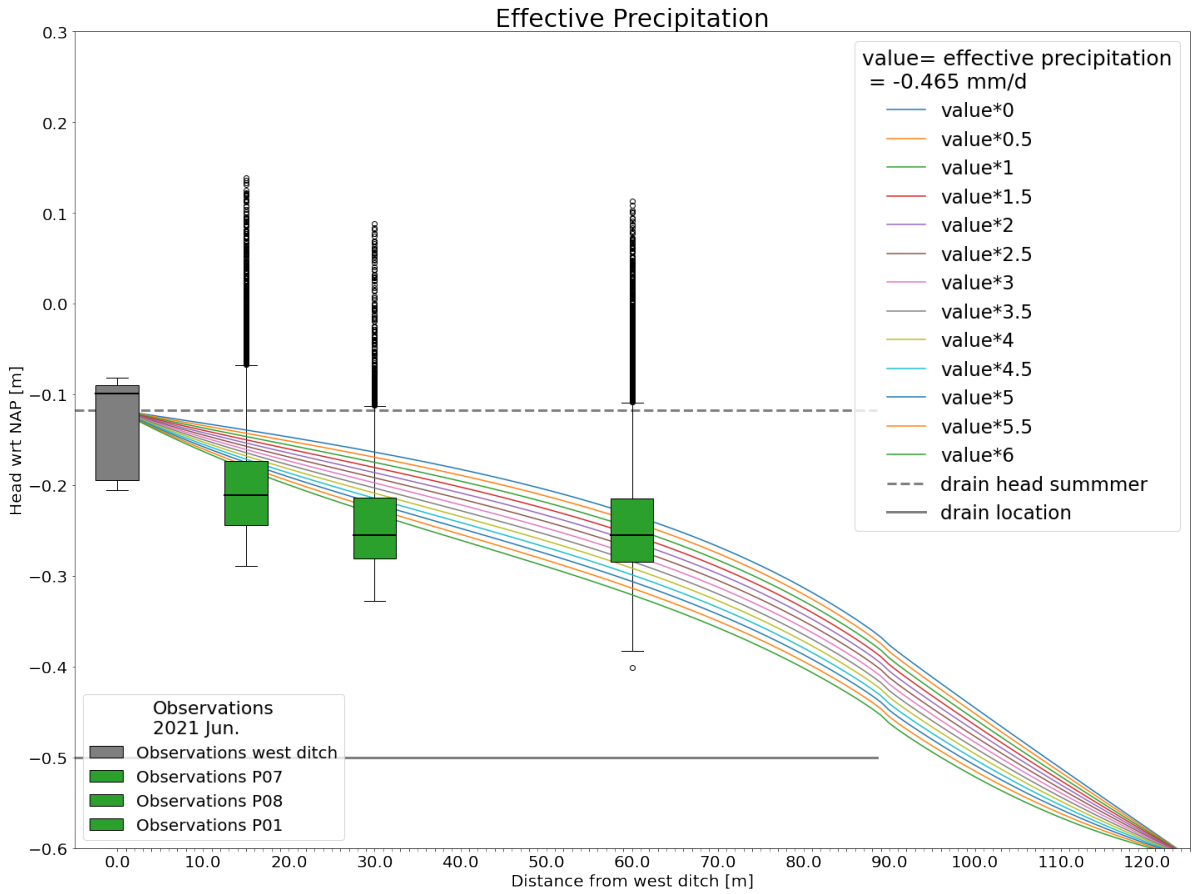

Figure F.5: Sensitivity of the effective precipitation.

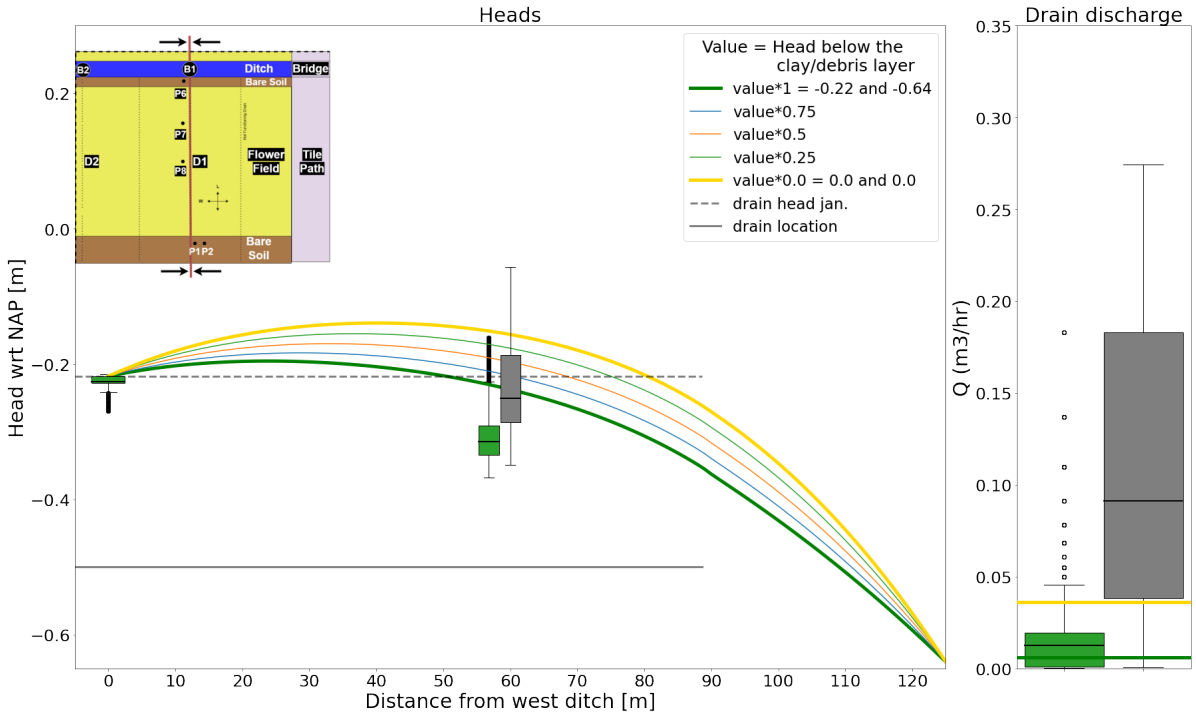

Figure F.6: Sensitivity analysis of the CHD parameter under the clay/debris layer for seepage in the wet-winter model. The START calibration parameters are used for the model input. The boxplots represent the head and discharge of the wettest month January (green boxplots) and the 10 wettest days, 21 to 31 December (grey boxplots). The CHD value below the debris layer is increased in four steps from -0.22 m NAP in the west and -0.64 m NAP in the east (green lines) to 0 (yellow lines).

Cross-section north south

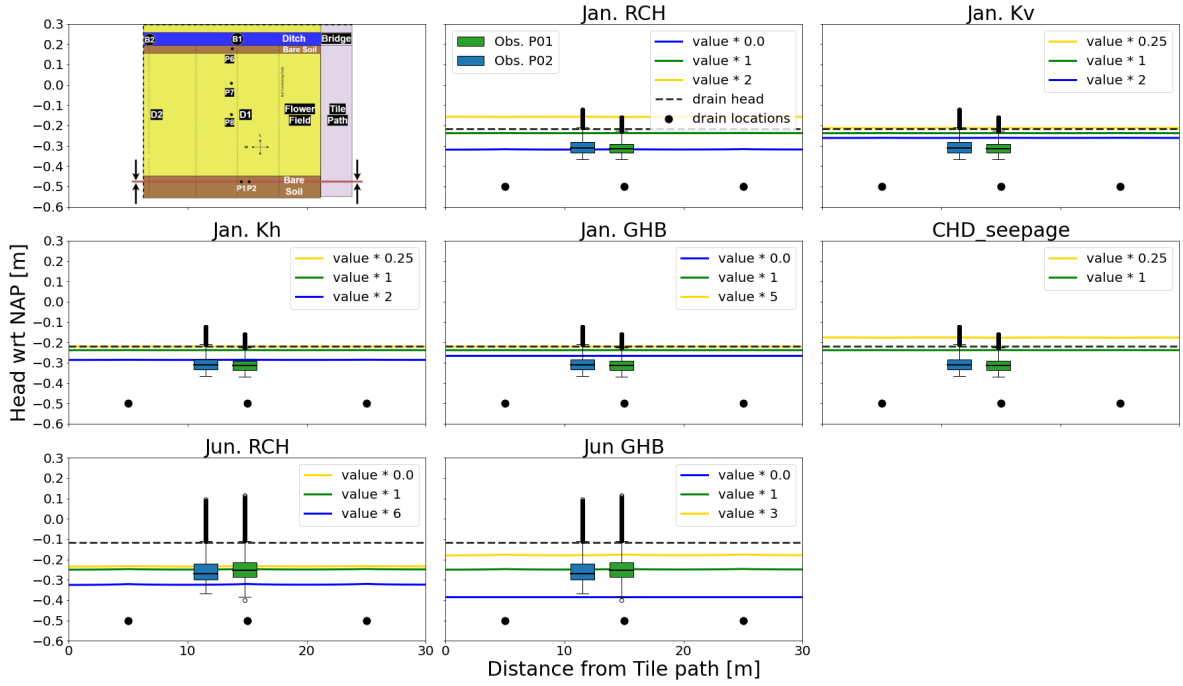

Figure F.7: Sensitivity overview of kv, kh, drain conductance, effective precipitation and seepage (increased heads below the clay/debris layer).

G

Groundwater Quality

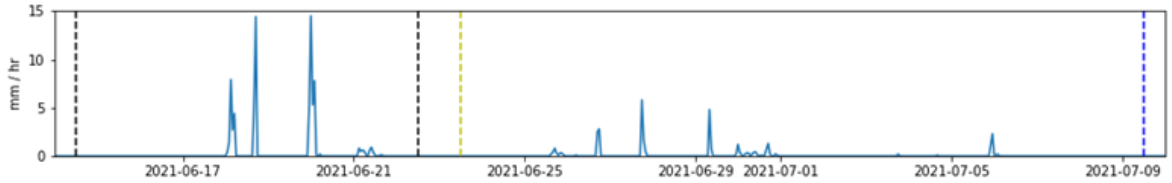

Figure G.1: precipitation during the gvp extractions. The dashed vertical lines show the dates at which soil profiles at Hogevervorst were made. The color indicates the location of the extraction with respect to the ditch. Black: 60 meter from the ditch (profile 1 and 2 respectively). Yellow: 15 meters from the ditch (profile 3,4,5). Blue 30 meter from the ditch (profile 6). These colors match with Figure 3.16.

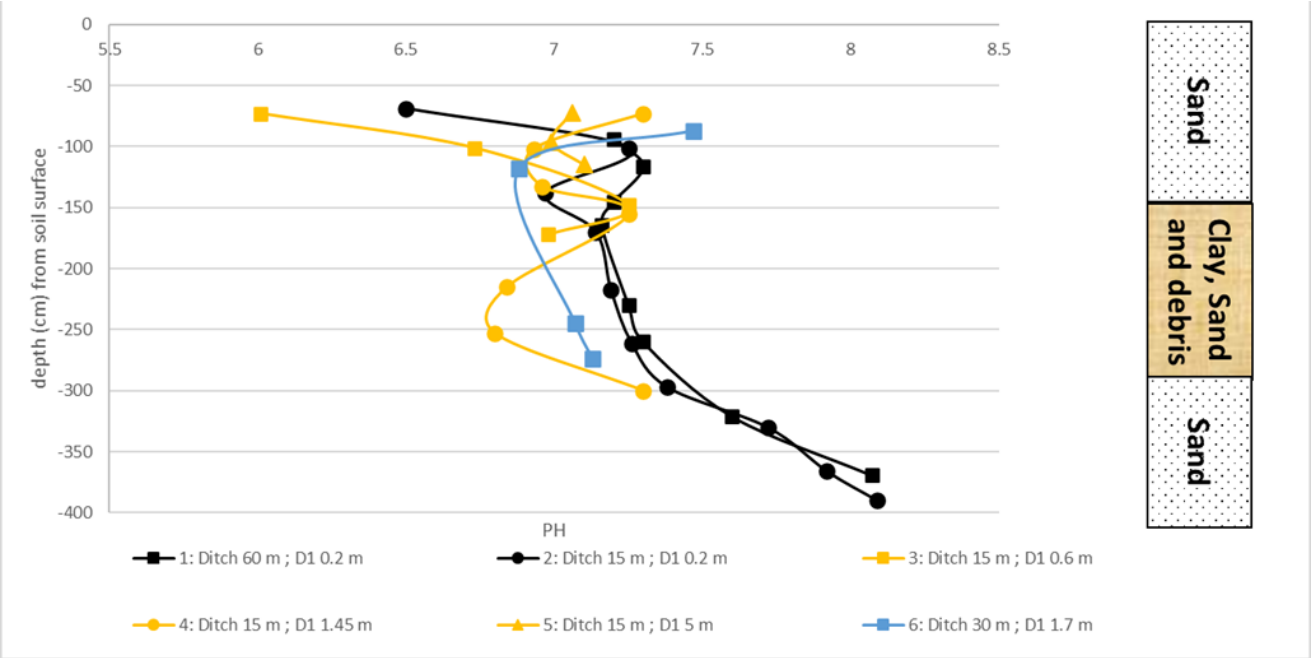

Figure G.2: PH

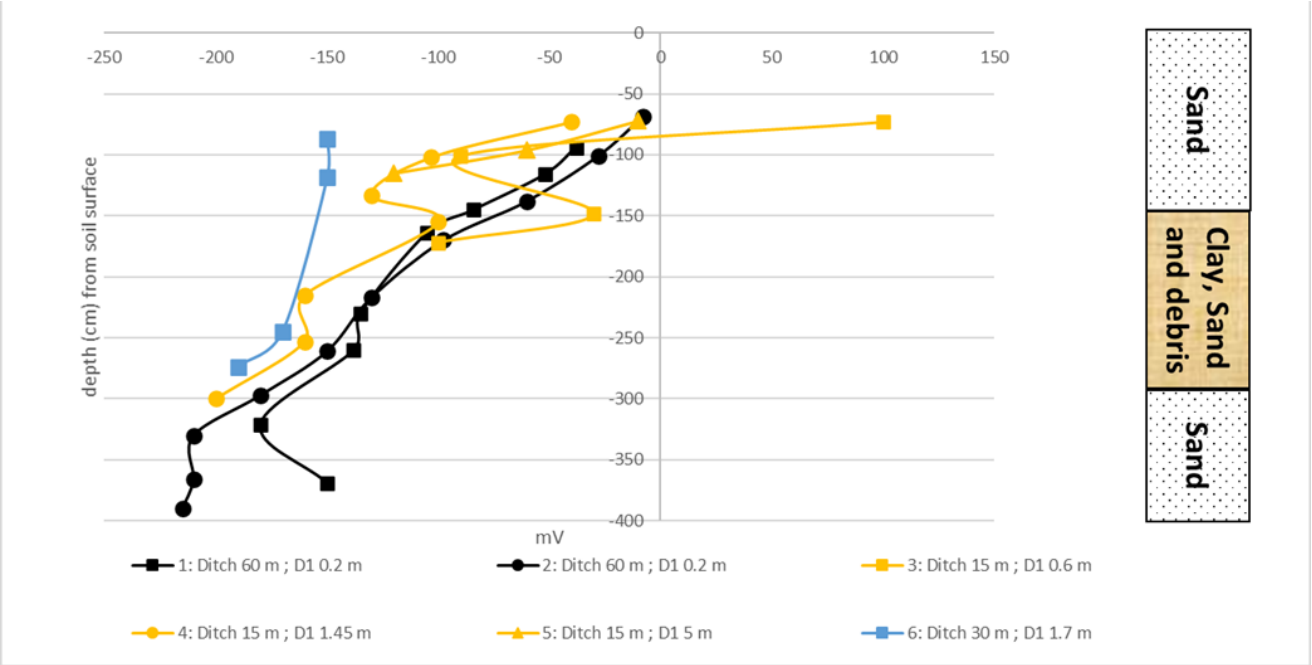

Figure G.3: redox potential

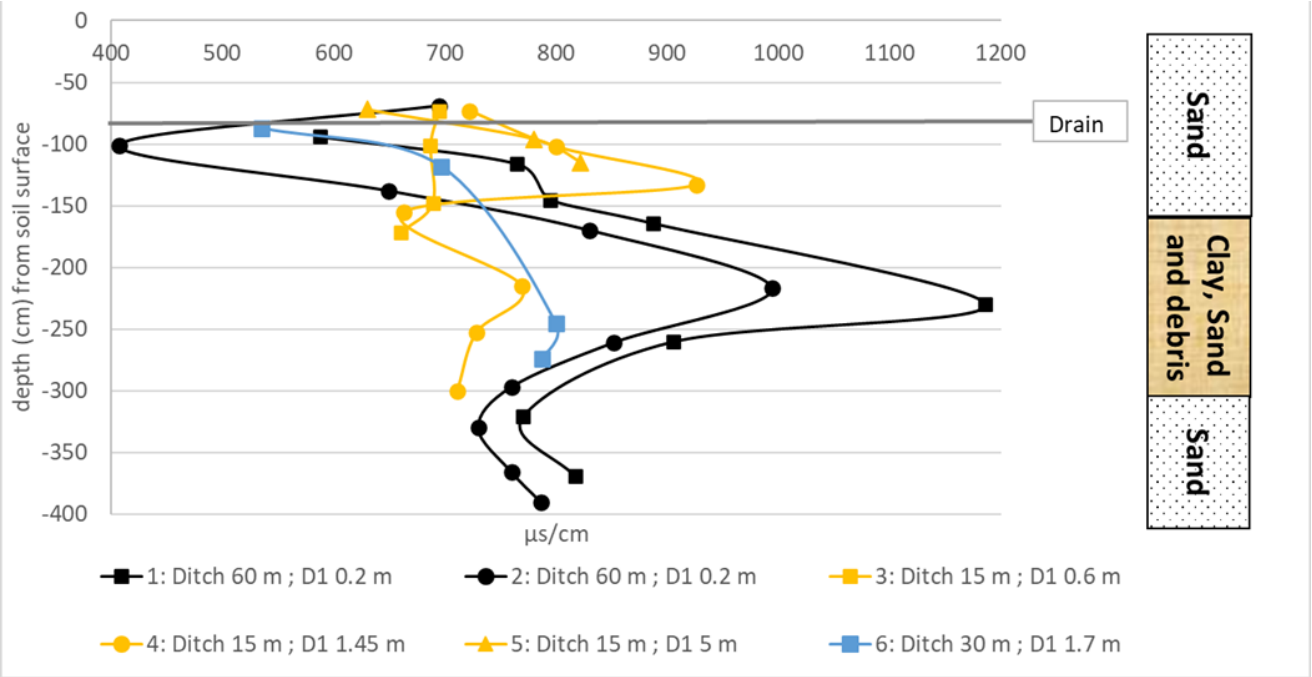

Figure G.4: EC. The results don't show a correlation between the distance of the drain and the ditch. However, in the vertical plane a difference in EC is found. first the EC increases where after is decreases again. Furthermore, a different EC between profile 1 and 2 is found which could be the result of the rain shower.

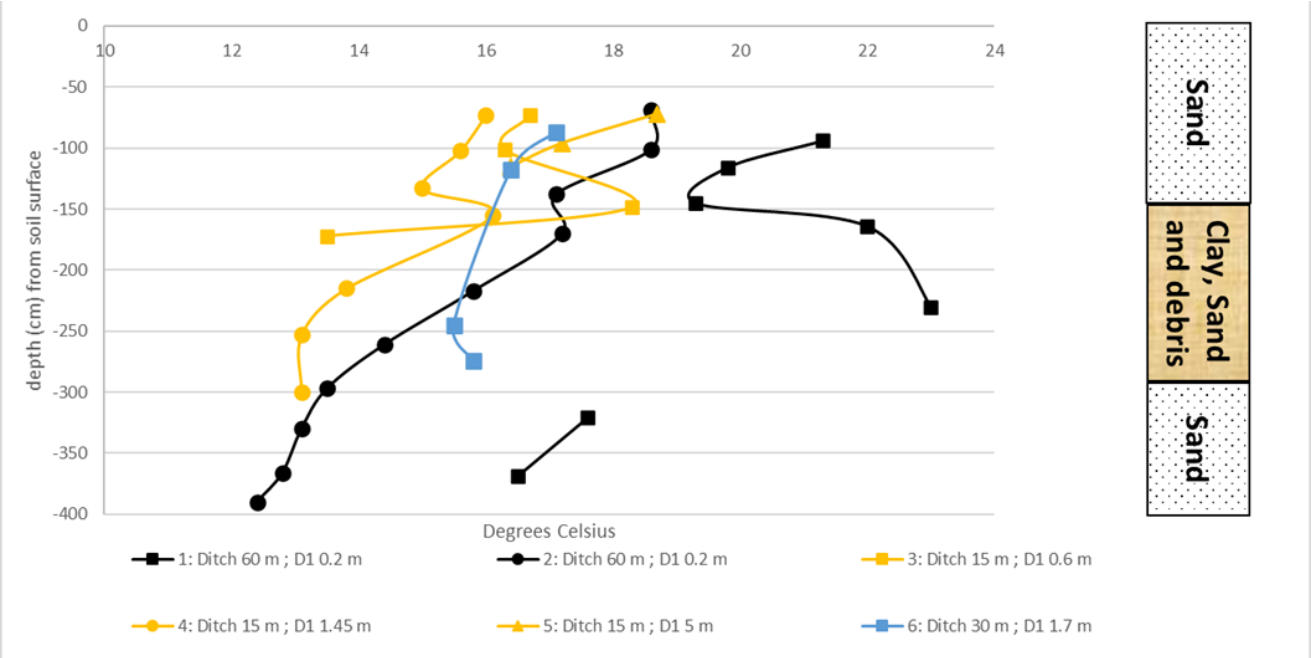

Figure G.5: temperature

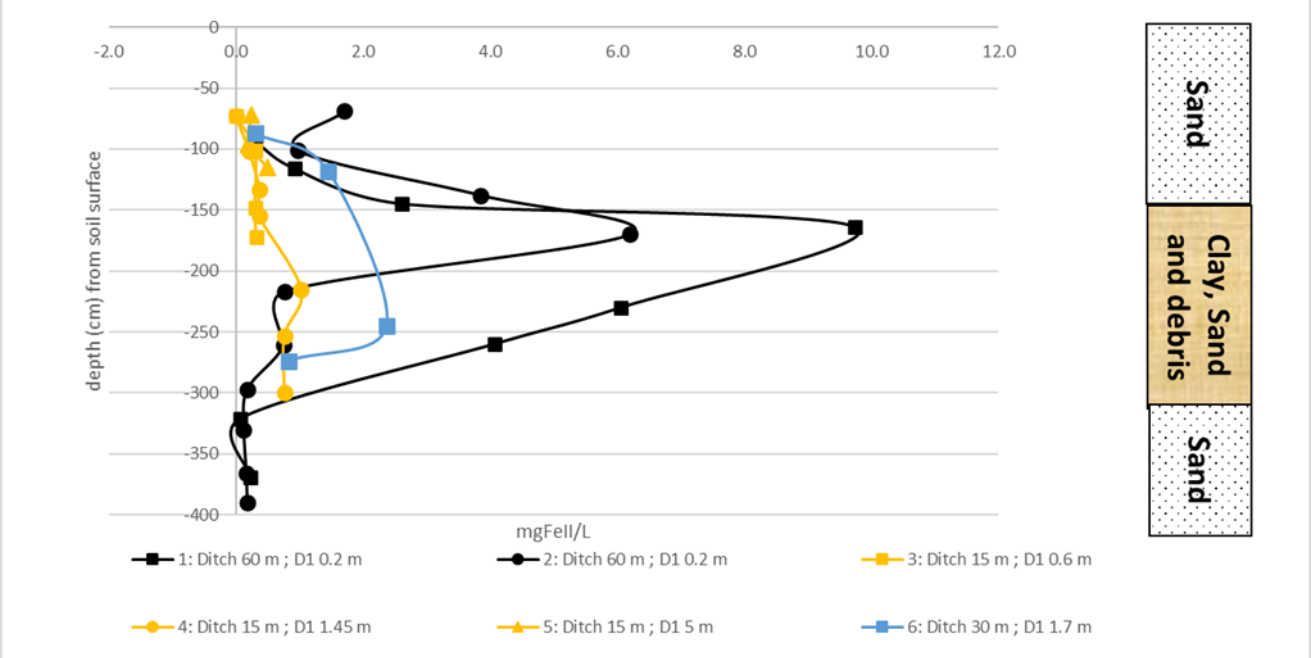

Figure G.6: precipitated iron

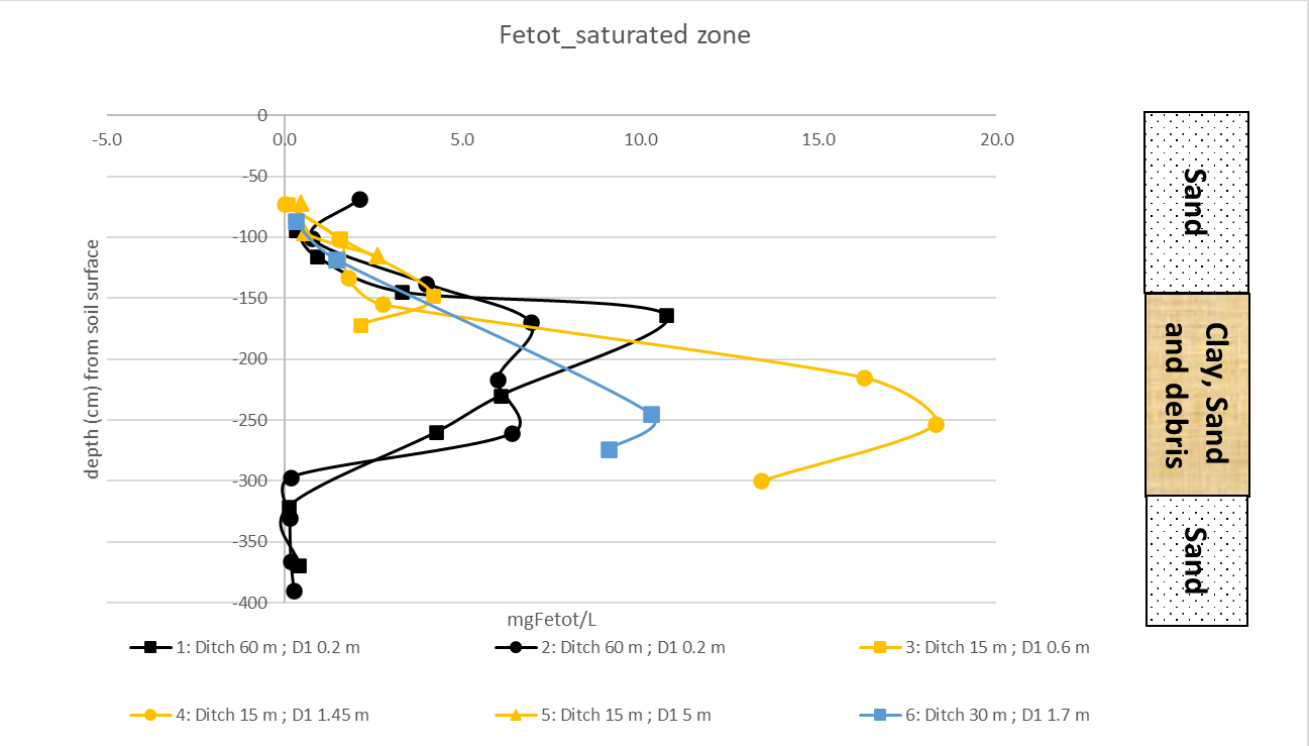

Figure G.7: Fetot profiles at Hogervorst from the water samples extracted with the gvp. Higher Fetot concentrations are found at the debris layer. Below the debris layer the iron concentration is almost zero.

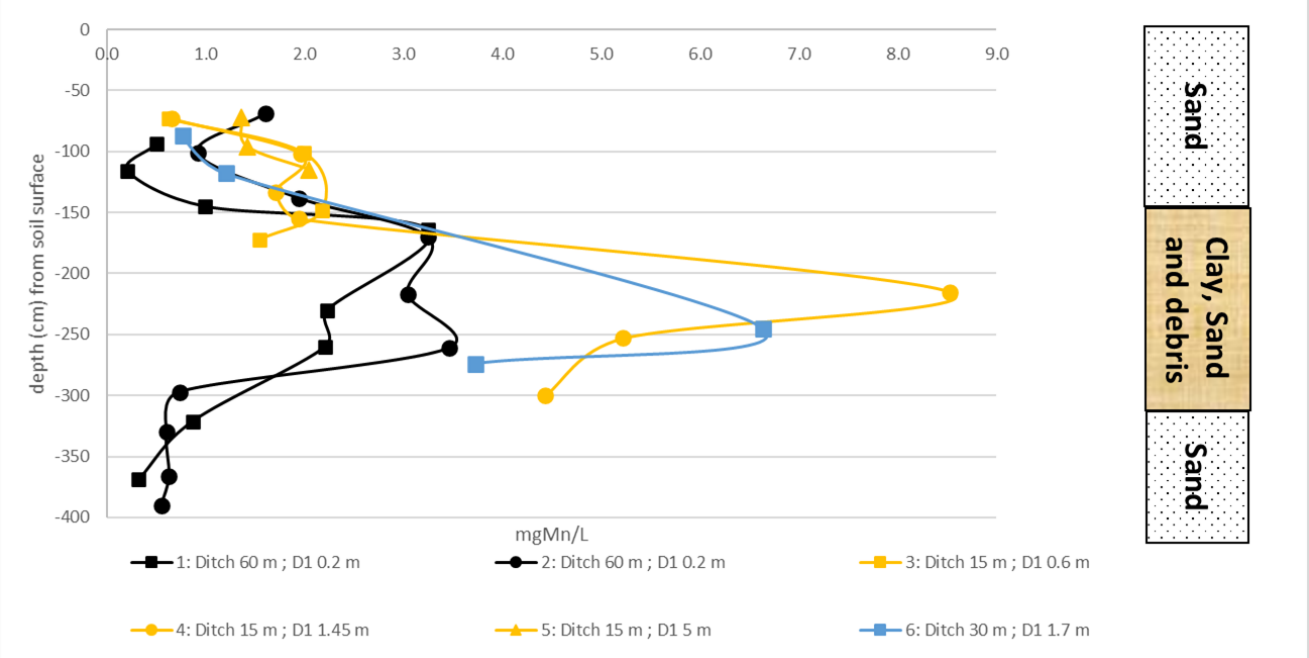

Figure G.8: Mn

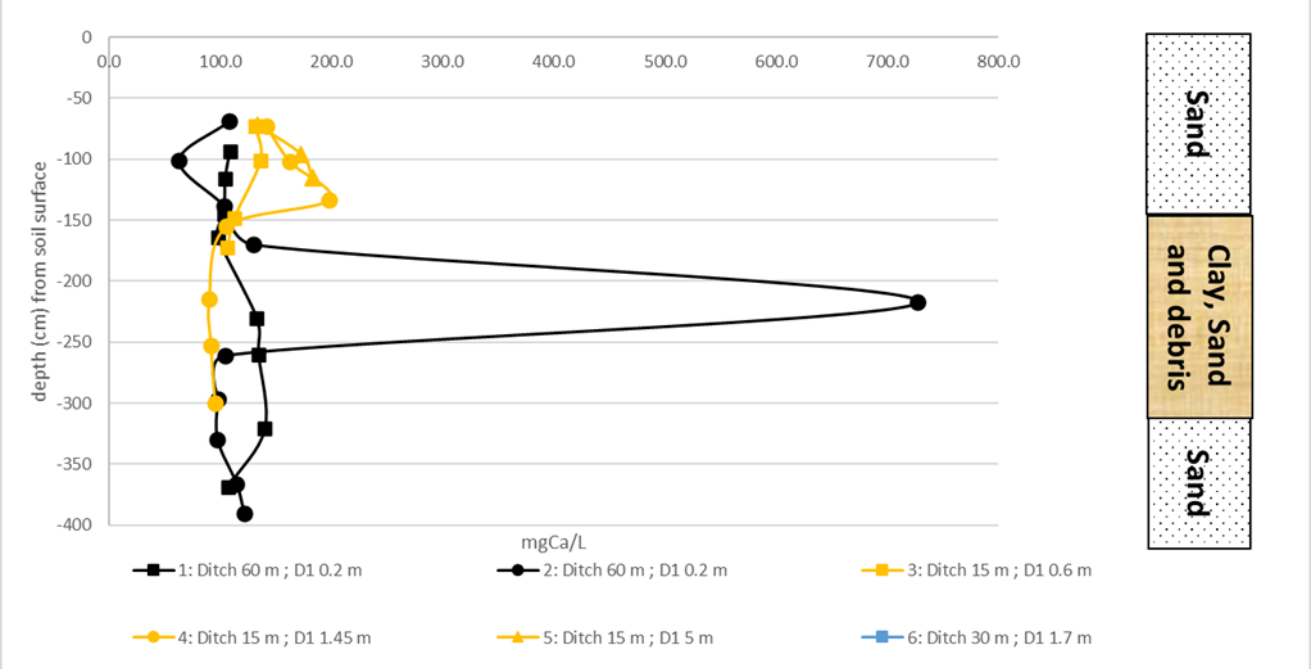

Figure G.9: Calcium

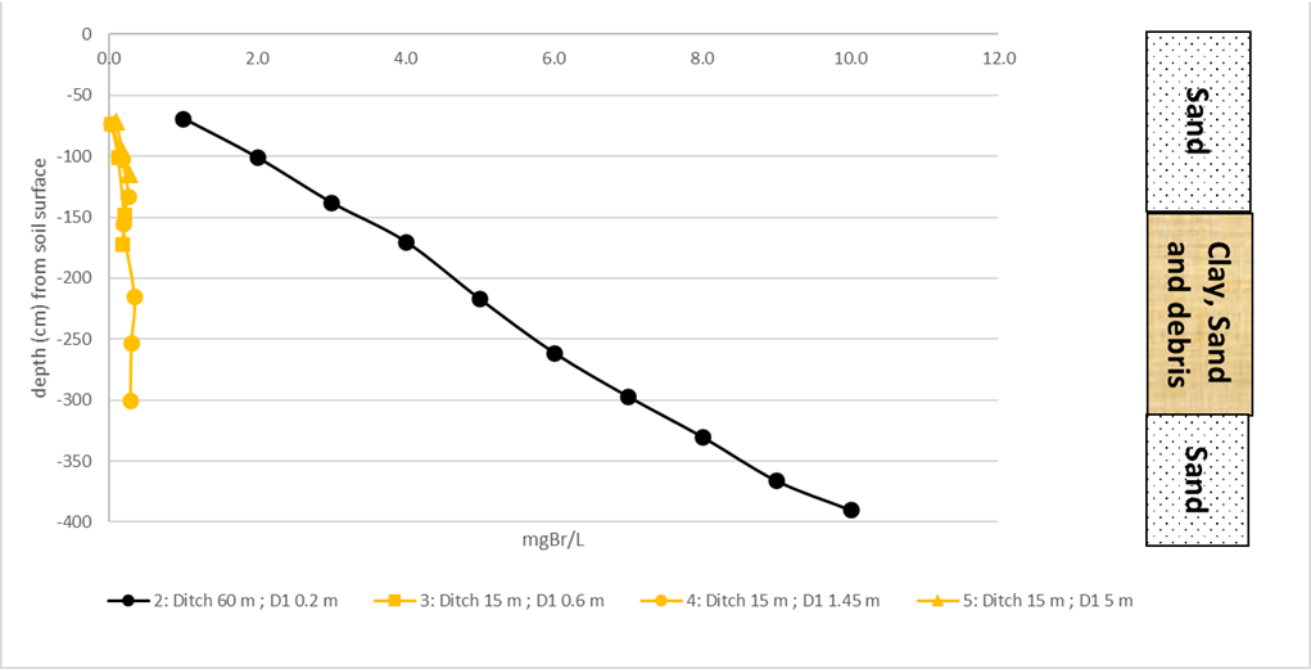

Figure G.10: Bromide

H

Oxidation of groundwater

Oxidation of groundwater from Hogervost field and precipitate formation
The data was produced by Ville Nenonen, Ville.Nenonen@eawag.ch on his secondment to Deltares.

Introduction

The groundwater in the field is reduced. When the groundwater is mixed with ditch water it is oxidized. Oxidation of the groundwater can take place in the field or in the ditch depending on the hydrological conditions. Upon oxidation iron is oxidized and precipitates. The P/Fe ratio of the iron hydroxyphosphates depends on the initial P/Fe concentrations in the water. The presence of phosphate delays the formation the iron oxides (Van der Grift et al., 2016). Other ions present in the groundwater as calcium (Ca), manganese (Mn), or silica (Si) can change the structure and composition of the precipitates. Ca and dissolved phosphate stabilize calcium iron (III) phosphates against transformation into ferrihydrite (Senn et al., 2017). Ca limits the P concentrations according to the calcium phosphate solubility constant. We want to know: (i) how oxidation affects P, Fe, and Mn concentrations in the groundwater, (ii) what precipitates are formed, (iii) the time it takes for precipitates to form.

Method summary

sampling We took 3 batches of groundwater on 14 June 2021:

- P1 at 1 m depth (60 m distance from the ditch)
- P1 at 3.2 m depth (w1.8) (60 m distance from the ditch)
- P7 at 1 m depth (15 m distance from the ditch)

Water chemistry during oxidation For each batch the initial unfiltered total concentrations in the water and the dissolved concentrations, filtered with 0.2 um, were measured with ICP-MS. The groundwater was oxidized in the lab at room temperature in the dark. Dissolved concentrations were measured after the oxidation with sampling interval of 1, 6, 14, 21, 24, 42, and 92 days. DOC and TOC was measured at the beginning for the 3 batches.

Precipitate chemistry After 92 days high resolution images of the precipitates were made with transmission electron microscopy (TEM) and energy dispersive x-ray spectroscopy (EDX). It was possible to make maps of the elements in the precipitates and quantify its composition. Fourier-transformed infrared spectroscopy (FTIR) was used to characterize the precipitates.

Result summary

Water chemistry The results agree with the measurements in P1, P7 and W1.8. ICP-MS is an independent measurement as we have measured concentrations before by colorimetry. The same pattern as before was observed. P concentrations in P1 are higher than in P7. The P concentration decreases as we approach the ditch. Samples from P1 and P7 were taken at 1m depth that is close to the level of highest concentrations. W1.8 was taken at the same distance from the ditch than P1 but at a deeper layer, below the clay. Below the clay the P concentrations are lower than above the clay layer. There is a large difference in Br concentrations

between the samples above and below the clay layer. Br is non-reactive and different Br concentrations can indicate dilution or a different water source. In the beginning at P1 at 1m depth the total P was 9.5 mg/L, total Fe was 1.5 mg/L, dissolved P was 9.0 mg/L, dissolved Ca was 90.2 mg/L, dissolved Fe 0.74 mg/L, dissolved Mn 0.41 mg/L, total Br 3.9 mg/L. The initial dissolved P/Fe molar ratio was 22 and DOC was 20.5 mg/L. On day 21 Fe and Mn concentrations had almost dropped to cero 0.05 mg/L and 0.04 mg/L respectively. The P and Ca concentrations were, on day 21, still high but lower than at the beginning, 7.5 mg/L and 84.5 mg/L respectively. Only 16.7Closer to the ditch at 1m depth, in P7, the initial concentrations were total P 4.2 mg/L, total Fe 2.2 mg/L, dissolved P 2.6 mg/L, dissolved Ca 113.8 mg/L, dissolved Fe 0.04 mg/L, dissolved Mn 0.42 mg/L, total Br 2.2 mg/L. The initial dissolved molar P/Fe ratio was 108 and DOC was 19.9 mg/L. In P7 there is almost no dissolved iron, most of the iron was forming precipitates before the oxidation experiment started. Before starting the oxidation experiment 38W18 is at the same distance from the ditch than P1 but 2m deeper, below the clay layer. In W18, the initial concentrations were total P 4.2 mg/L, total Fe 0.11 mg/L, dissolved P was 3.3 mg/L, dissolved Ca was 88.4 mg/L, dissolved Fe 0.05 mg/L, dissolved Mn 0.06 mg/L, total Br 7.6 mg/L. The initial P/Fe molar ratio was 122 and DOC was 23.9 mg/L. At the end of the experiment the P, Ca, Mn, and Fe concentrations were roughly the same.

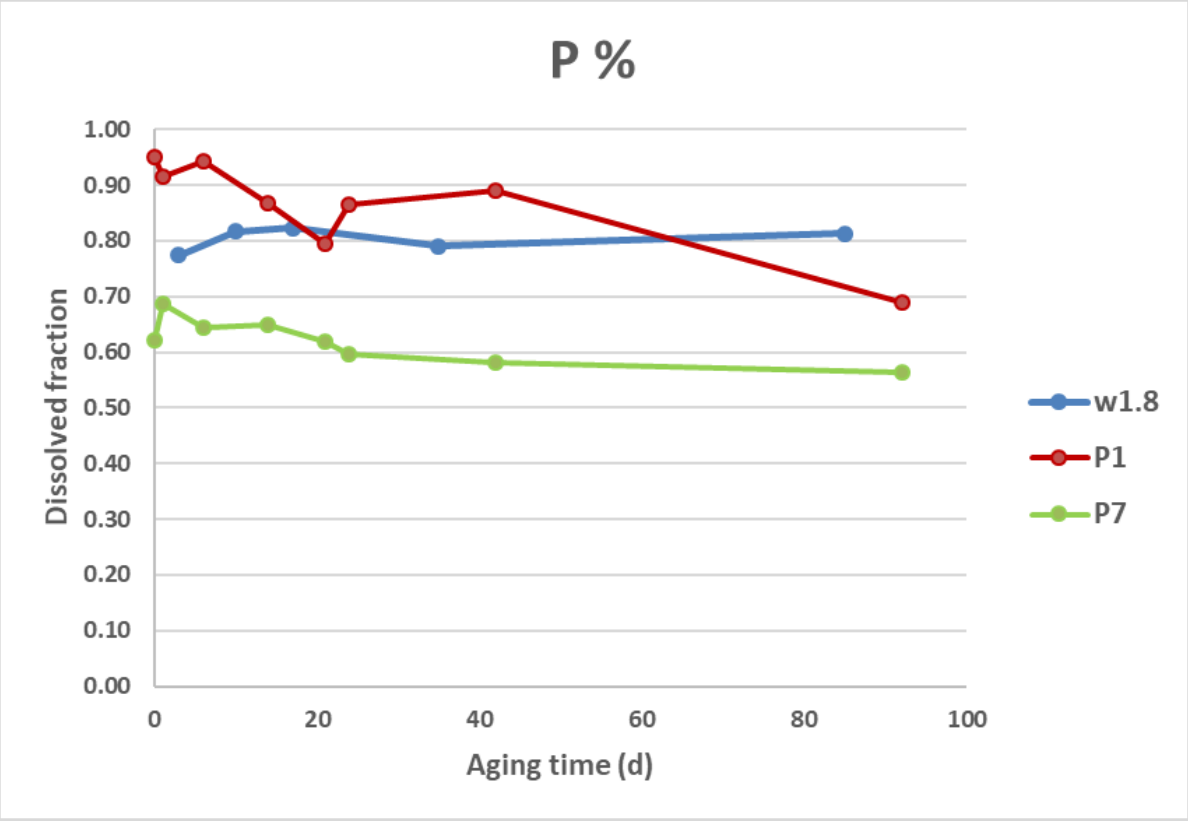

Figure H.1: Dissolved P fraction over the aging period.

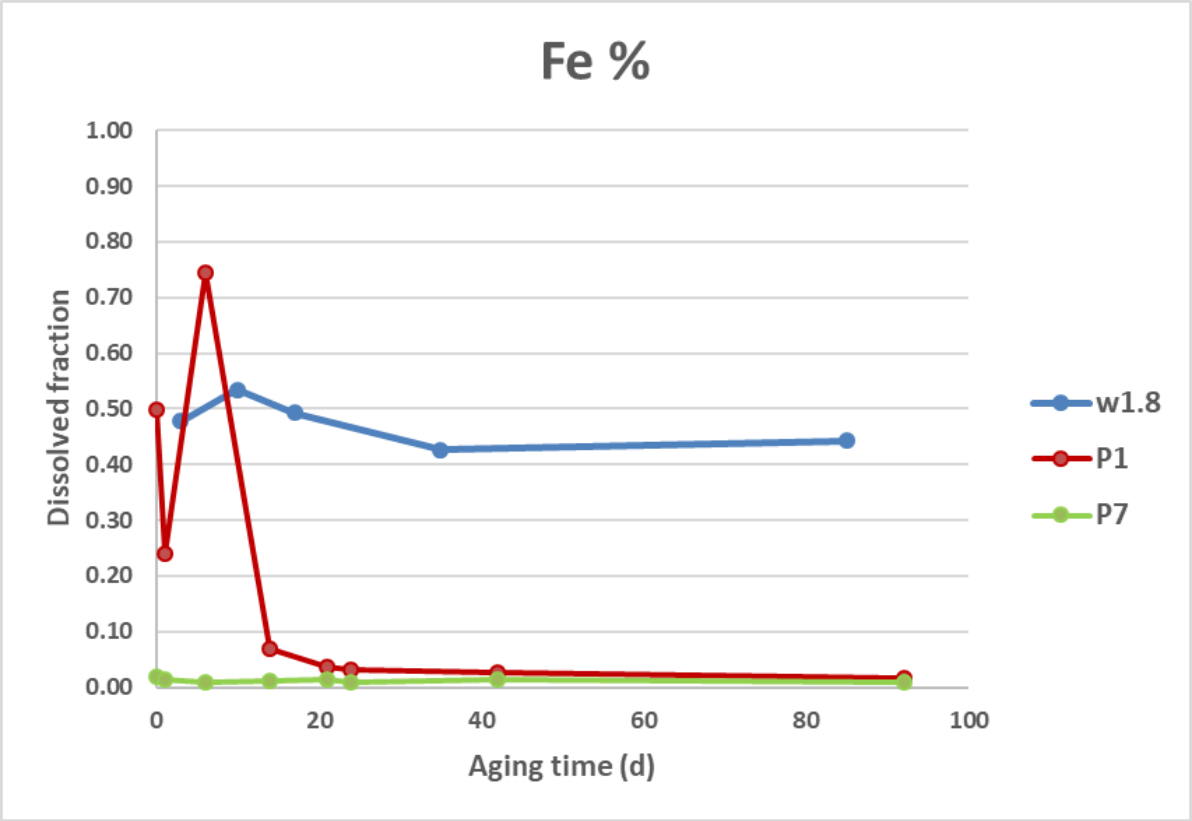

Figure H.2: Dissolved Fe fraction of Fe

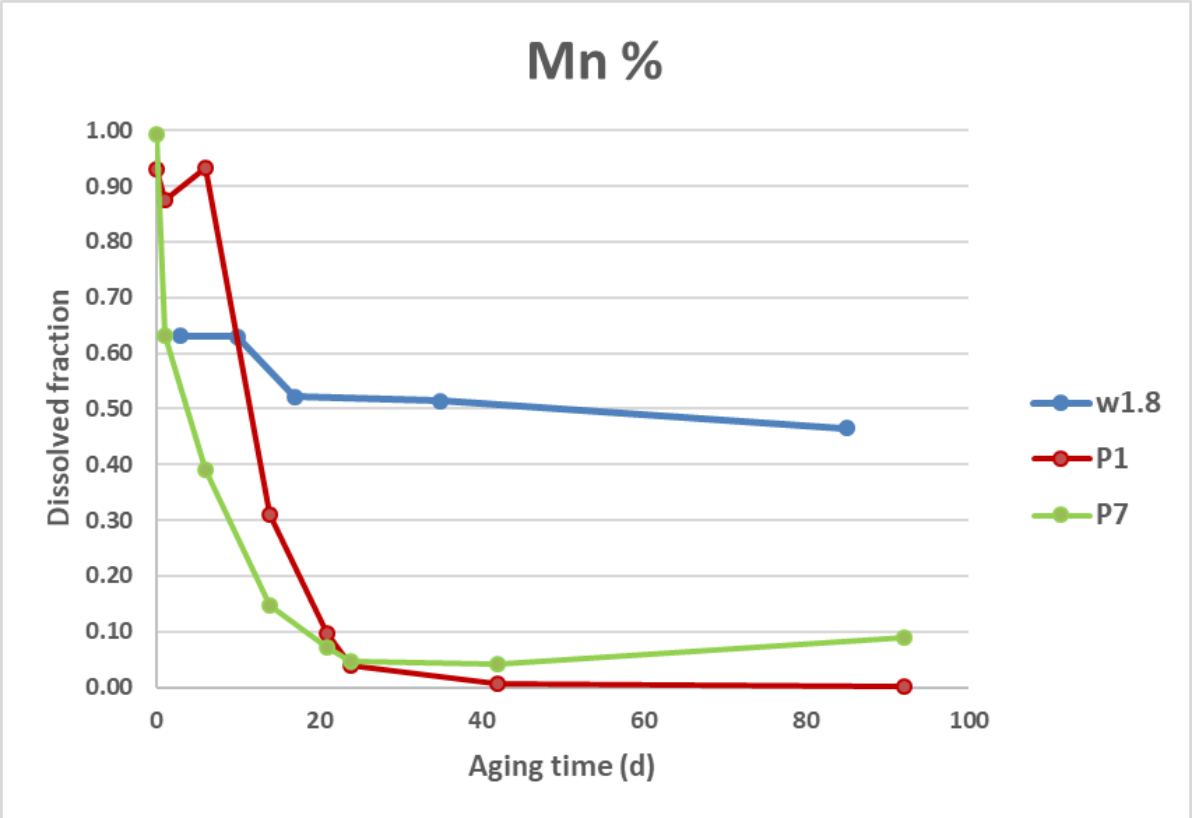

Figure H.3: Dissolved fraction of Mn

Precipitate chemistry The precipitates that formed in the water taken from P1 and P7 at 1 m depth look the same. FTIR results shows peaks for iron hydroxides, amorphous iron (III) phosp

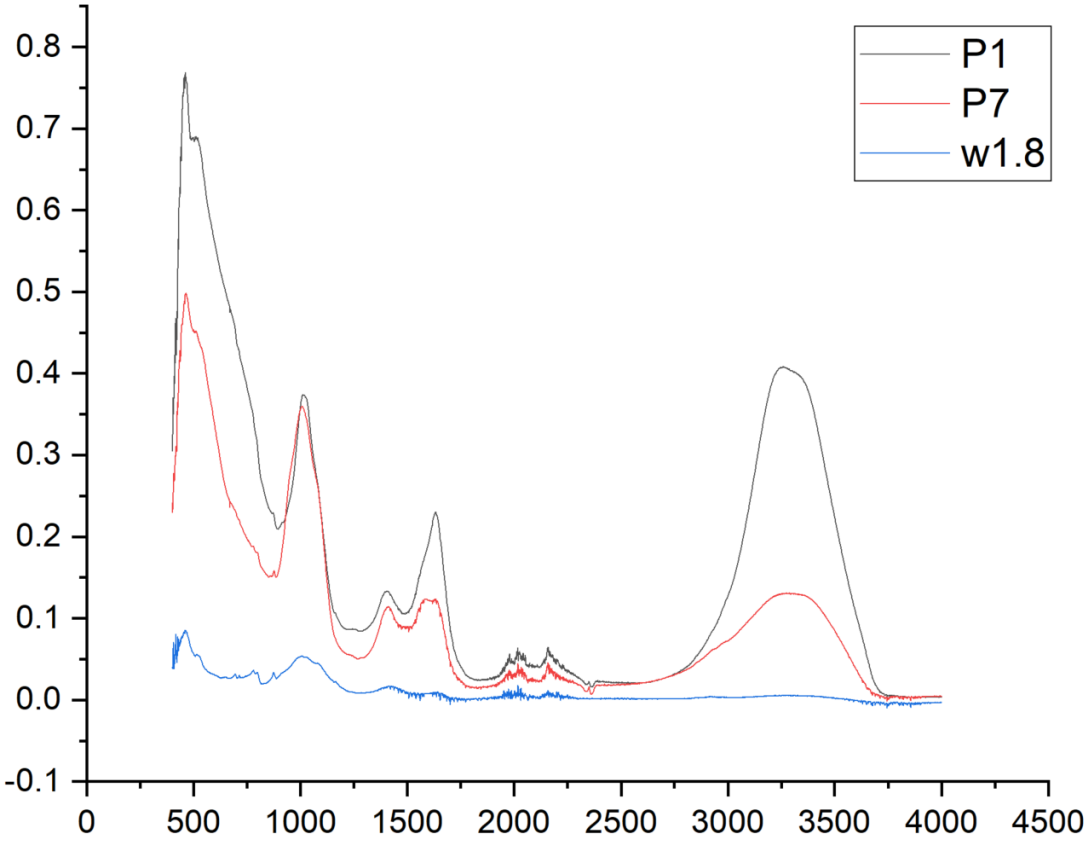

Figure H.4: FTIR results from precipitates from P1,P2 and W18

Figure H.5 and Figure H.6 show the TEM-EDX images of the precipitates from P1 and P7. The precipitates are calcium iron phosphates with a “webing” structure and P/Fe molar ratio of 0.86. The atomic fractions are 65 % O, 11.65% P, 7.67% Ca, 11.58% Fe. Mg and Na had a smaller presence with 0.41% and 0.68% atomic fraction respectively.

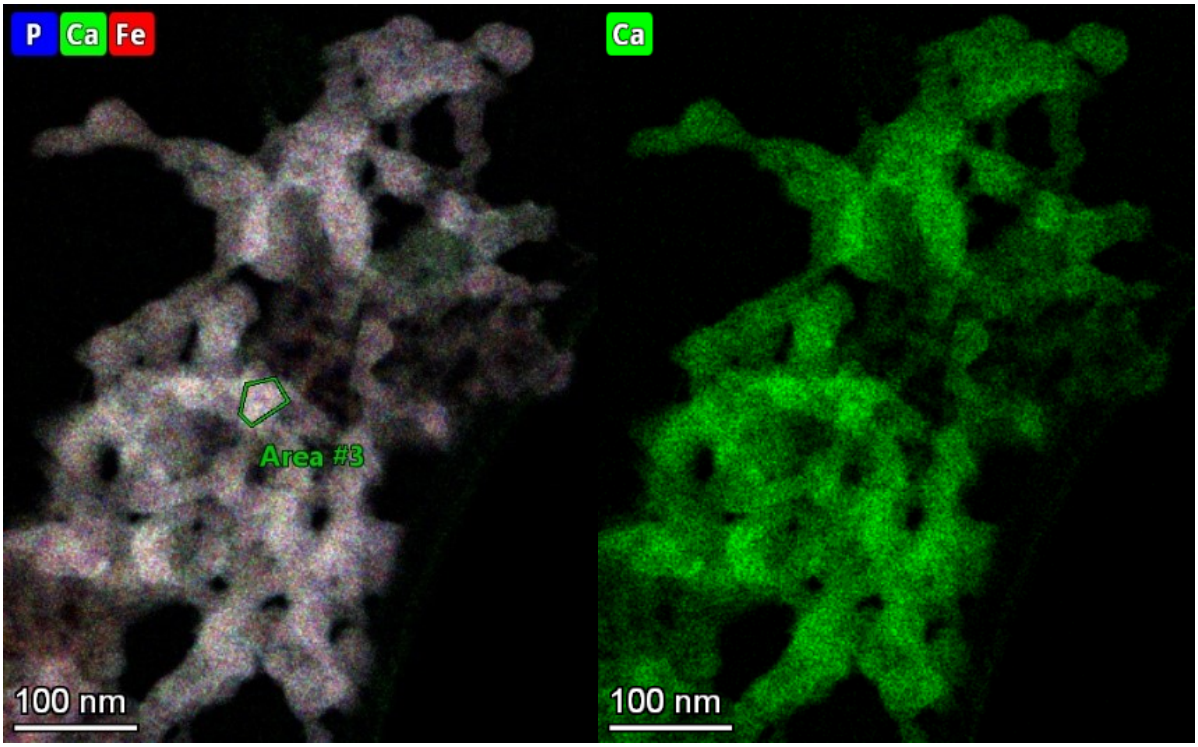

(a) (b)

Figure H.5: TEM images of the precipitates and EDX elemental maps from P7.

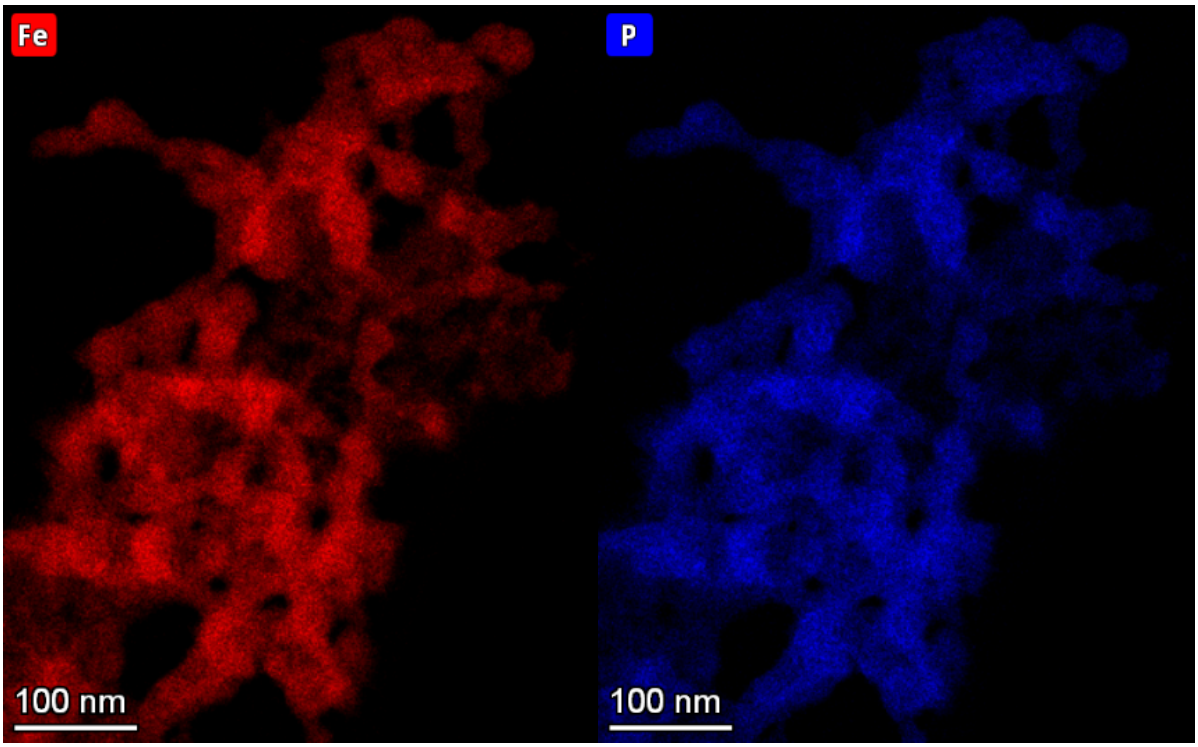

(a) (b)

Figure H.6: TEM images of the precipitates and EDX elemental maps from P7.

Discussion

The fact that the DOC in P7 is the same on day 0 and on day 92 indicates that there is no degradation od DOC and that it is recalcitrant organic matter that is very hard to degrade. Below the clay layer there is almost no iron and therefore no P removal. The differences in Br and in background elements indicate that the sand

layer above and below the clay are not connected. The same was observed in the groundwater profiles made with the GVP. The initial P/Fe dissolved concentrations on this area very high compared to other studies, nevertheless, the P/Fe ratio on the precipitates are in the expected range (Van der Grift et al., 2016). The oxidation of the groundwater at the beginning of the field, 60 m from the ditch, takes about 3 weeks. This reaction times should be considered with the water transport times from the field to the ditch. The iron content in P1 is high but is not enough to remove all the P from the solution. The soil lacks sorption capacity to adsorb the high P concentrations. In the sandy soil extraction, we obtained that the phosphorus saturation degree was above 0.25, indicating that is possible that the P forms precipitates with the iron instead of being adsorbed. In the extractions we found more iron in the first 20-30 cm than in the 40-60 cm layer. The manure is not a source of iron. Probably before the drains were installed the groundwater level reached the top soil and iron was oxidized and accumulated. The oxidation process of the water in P7 had probably already started when the samples were taken. This goes in line with the hypothesis that the oxygen rich ditch water penetrates the field and oxidizes the iron and removes some of the P. The final P contraptions in P7 were similar to the P concentrations in the drain outflow during dry weather. The Br concentrations indicate dilution from P1 to P7. After dilution and oxidation, the P concentration is 2.6 ± 0.2 mg/L for this field in the surface water. This concertation is very high for natural surface waters , however, concentrations are reduced about 2/3 when compared with the dissolved P in the groundwater at P1. The water management of the field helps to keep the P as low as possible. To decrease the P further P retention measures are needed. It is important to know from what depth is the water draining from, how far into the field is the ditch water infiltrating in winter and in summer, how much water is transported through the drains, and the transport times. The answer to these questions can help manage this fields with very high P concentrations and decide on the best mitigation measures.

References

Van der Grift, B. et al. (2016) 'Fe hydroxyphosphate precipitation and Fe(II) oxidation kinetics upon aeration of Fe(II) and phosphate-containing synthetic and natural solutions', Geochimica et Cosmochimica Acta, 186, pp. 71–90. doi: 10.1016/j.gca.2016.04.035. Senn, A. C. et al. (2017) 'Effect of aging on the structure and phosphate retention of Fe(III)-precipitates formed by Fe(II) oxidation in water', Geochimica et Cosmochimica Acta. Elsevier Ltd, 202, pp. 341–360. doi: 10.1016/j.gca.2016.12.033.

Location of Voorhout (Buijert et al. [1]), Noordwijkerhout (JUB and Hogervorst), Vogelenzang (HUB)

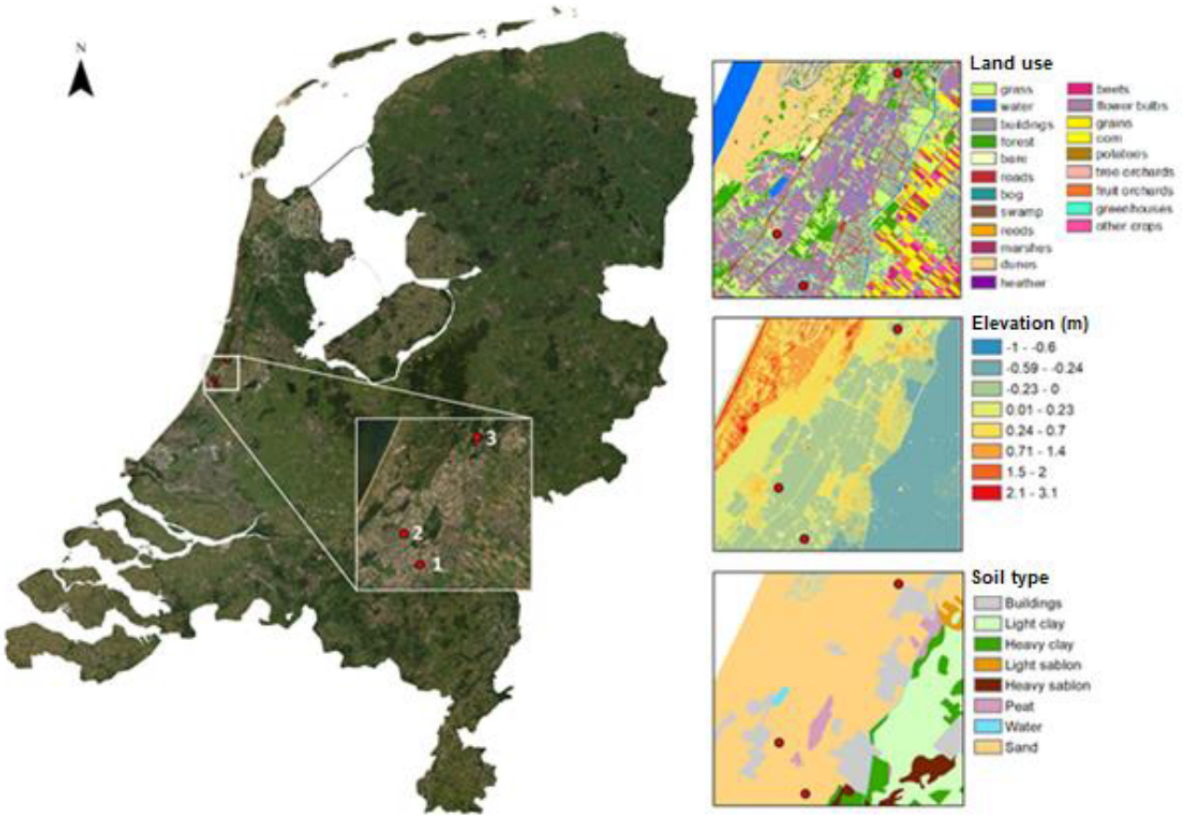

Figure I.1: Overview map of the area. 1 = location Voorhout [1], 2 = location Noordwijkerhout, field Hogervorst and JUB, 3= location Vogelenzang (HUB)